

Electronic Thesis and Dissertation Repository

7-16-2020 10:30 AM

Development Of Hybrid Coating Materials To Improve The Success Of Titanium Implants

Zach Gouveia, *The University of Western Ontario*

Supervisor: Zhu, Jesse, *The University of Western Ontario*

A thesis submitted in partial fulfillment of the requirements for the Master of Engineering Science degree in Biomedical Engineering

© Zach Gouveia 2020

Follow this and additional works at: <https://ir.lib.uwo.ca/etd>



Part of the [Biomaterials Commons](#)

Recommended Citation

Gouveia, Zach, "Development Of Hybrid Coating Materials To Improve The Success Of Titanium Implants" (2020). *Electronic Thesis and Dissertation Repository*. 7088.

<https://ir.lib.uwo.ca/etd/7088>

This Dissertation/Thesis is brought to you for free and open access by Scholarship@Western. It has been accepted for inclusion in Electronic Thesis and Dissertation Repository by an authorized administrator of Scholarship@Western. For more information, please contact wlsadmin@uwo.ca.

Abstract

While titanium (Ti) and its alloys have become ubiquitous within implantology as materials to restore or augment the function of human tissues, their success is plagued by complications associated with infection and aseptic implant loosening. These two risks account for the majority of implant failures in the clinic and limit the long-term success of titanium implants *in vivo*. Therefore, this thesis describes the development of robust multifunctional class II organic-inorganic hybrid coating materials for titanium implants that could be used to effectively target both complications, concurrently. During this master's work, two different coating systems were examined. First, class II hybrid coating materials composed of chitosan and silica loaded with silver nanoparticles were investigated. These coatings displayed a high resistance to fracture, great substrate adhesion and inhibited the growth of two clinically relevant pathogenic bacteria (*E. coli* and *S. aureus*) in both biofilm and planktonic cultures. Secondly, a novel class II hybrid coating material was developed that was composed of polyethylene glycol, calcium, and silica and loaded with silver nanoparticles. This hybrid bioactive glass material possessed similar mechanical and antimicrobial properties to the chitosan-silica coatings and displayed an increased bioactive response. From this study, a better understanding of the feasibility of class II hybrid materials as implant coatings was developed. The work presented in this work may afford a novel strategy in improving the success of implants for biomedical applications.

Keywords

Orthopedic implants; Dental implants; Titanium; Coatings; Antibacterial; Osseointegration; Class II hybrid; Sol-gel

Summary for Lay Audience

The use of titanium implant materials has become ubiquitous in the field of implantology. While titanium-based implant materials possess adequate mechanical properties to meet the demanding loading conditions of the human body, their interfaces fail to illicit positive physiological responses. For this reason, implant surfaces become targeted sites for microbial colonization (leading to infections) and are unable to promote the fixation of protheses (leading to loosening) in the body. These phenomena (implant associated infection and aseptic loosening, respectively) are the two major complications that affect the continued success of hard tissue restorations today.

In consideration of these complications, this study provides a potential coating solution that can synergistically prevent infection and promote the fixation of implantable materials. Using a coating framework composed of similar inorganic contents to that of bone, positive physiological responses can be promoted that encourage the fixation of the implantable devices within hard tissues. By imbedding coating networks with antimicrobial silver nanoparticles, implant surfaces could be afforded with infection-resistant properties.

This study also considered the factors attributed to the clinical translatability of developed “multifunctional” implant coatings. Coating materials developed for hard tissue implants should be robust. This means they remain adhered to the implant surface throughout its lifetime within the body and are resistant to the impacts of various surgical tools and bony protrusions upon implantation. Additionally, such coating materials should avoid the use of toxic chemicals or network forming agents. This ensures that during the lifetime of the implant potential coating degradation does not induce a toxic effect in the host.

Co-authorship Statement

Chapters 1 and 2 entitled “Introduction” and “Literature Review and Background” were written by Z. Gouveia. Dr. J. Zhu reviewed and edited these chapters.

Chapter 3 entitled “Development of robust chitosan–silica class II hybrid coatings with antimicrobial properties for titanium implants” was adapted from Gouveia et al., *Coatings* **2020**, *10*, 1–20. This publication was written by Z. Gouveia, Dr. H. Perinpanayagam and Dr. J. Zhu. All experiments were performed by Z. Gouveia in the laboratories of Dr. J. Zhu.

Chapter 4 entitled “Development of multifunctional bioactive implant coatings using a novel calcium precursor to improve osseointegration and antimicrobial effectiveness” was written by Z. Gouveia, Dr. H. Perinpanayagam, and Dr. J. Zhu. Experiments were performed by Z. Gouveia in the laboratories of Dr. J. Zhu.

Chapter 5 entitled “General Discussion” was written by Z. Gouveia. Dr. J. Zhu reviewed and edited this chapter.

Acknowledgements

First, I would like to sincerely thank my supervisor Dr. Jesse Zhu, for his patience, encouragement, guidance throughout my master's studies. Through our time working together, I have gained valuable knowledge on all levels from independence to critical thinking. This achievement would not have been possible without Dr. Zhu's support, for which I am truly grateful.

I would also like to extend my great appreciation to Dr. Hiran Perinpanayagam for his mentorship and support throughout my academic journey. I appreciate the time and effort he put towards this work and towards my development as a researcher. Thanks to his involvement and encouragement we were able to better elucidate some important aspects of our research and prepare it for publication.

From our group, I would also like to thank Ying Ma for her guidance throughout my research journey. My lab mates Dr. Zhehao Jing and Yuqing Ye have been great friends during my time at Western and their continued support has been invaluable.

Also, from our group, I would like to sincerely thank Jinbao Huang and Marshall Yang for their help with gathering SEM and EDX data for this work. I really appreciate the time spent after-hours to help me progress this study.

I would also like to thank my advisory committee members Dr. Elizabeth Gillies and Dr. Hui Zhang for their continuous advice and encouragement.

Lastly, I would like to sincerely thank my sources of support outside of the laboratory. Claire, your love and support throughout this process has been invaluable. I could not thank you enough for your assistance in improving my writing style throughout my studies. Trent, thank you for being an extremely supportive friend; it has been an absolute pleasure sharing this journey with you.

Table of Contents

Abstract.....	i
Summary for Lay Audience.....	ii
Co-authorship Statement.....	iii
Acknowledgements.....	iv
Table of Contents.....	v
List of Tables.....	viii
Table of Figures.....	ix
List of Abbreviations.....	xiii
Chapter 1: Introduction.....	1
1.1 Overview.....	1
1.2 Thesis Objectives.....	2
1.3 Hypothesis.....	2
1.4 Thesis Outline.....	2
1.5 References.....	2
Chapter 2: Literature Review and Background.....	4
2.1 Hard Tissue Implants.....	4
2.1.1 Titanium Implants.....	6
2.1.2 Implant Complications.....	9
2.1.2.1 Implant Associated Infections.....	9
2.1.2.2 Aseptic Loosening.....	11
2.2 Implant Surface Modifications.....	13
2.2.1 Antibacterial Surfaces.....	13
2.2.1.1 Non-Eluting/Static/Passive Antibacterial Strategies.....	13
2.2.1.2 Elution-based/Active Antibacterial Strategies.....	18
2.2.2 Osteoconductive Surfaces.....	24
2.2.2.1 Topographical Strategies / Bioactive Topographies.....	25
2.2.2.2 Bioactive Coatings.....	26
2.3 Rationale of the Study.....	33
2.4 References.....	33
Chapter 3: Development of robust chitosan–silica class II hybrid coatings with antimicrobial properties for titanium implants.....	49
3.1 Introduction.....	49

3.2 Materials and Methods.....	52
3.2.1 Synthesis of Coating Materials	52
3.2.2 Deposition of Hybrid Coatings	53
3.2.3 Characterization of Coating Surfaces	54
3.2.4 Evaluation of Mechanical Properties	55
3.2.5 Evaluation of Antimicrobial Properties	56
3.2.6 Statistical Analysis.....	57
3.3 Results and Discussion	57
3.3.1 Characterization of Coating Materials	57
3.3.2 Material Properties.....	63
3.3.3 Antimicrobial Properties	67
3.4 Conclusions.....	70
3.5 References.....	71
Chapter 4: Development of multifunctional bioactive implant coatings using a novel calcium precursor to improve osseointegration and antimicrobial effectiveness.....	79
4.1 Introduction.....	79
4.2 Materials and Methods.....	81
4.2.1 Synthesis of Coating Materials	82
4.2.2 Characterization of Coating Materials	83
4.2.3 Evaluation of Mechanical Properties	85
4.2.4 Evaluation of Biological Properties	85
4.2.5 Statistical Analysis.....	87
4.3 Results and Discussion	87
4.3.1 Characterization of Coating Materials	87
4.3.2 In Vitro Bioactivity	93
4.3.3 Antimicrobial Properties	94
4.4 Conclusions.....	97
4.5 References.....	98
Chapter 5: General Discussion.....	103
5.1 Summary	103
5.2 Contributions to current knowledge.....	104
5.3 Limitations and Suggestions for Future Work.....	105
5.4 References.....	106

5.5 Curriculum Vitae 107

List of Tables

Table 3.1 Composition of hybrid coatings 52

Table 4.1 Composition of Si-Ca-PEG based coatings 83

Table 4.2 Ionic composition of simulated body fluid and human blood plasma 85

Table of Figures

Figure 2.1 Examples of implant forms used for hard tissue implantation in orthopedics. Adapted from Rony et al. ⁶	5
Figure 2.2 Screw-abutment-crown dental implant design. Adapted from www.1888implant.com ¹⁴	6
Figure 2.3 Modulus of elasticity of commonly used implant metallics. Adapted from Geetha et al. ²⁴	8
Figure 2.4 Stages of biofilm formation on implant surfaces. Adapted from Chung et al. ⁴⁹	10
Figure 2.5 Concept of contact-killing membrane-active biocides surface-coupled via a polymeric spacer. Adapted from: Börner et al. ¹⁰²	17
Figure 3.1 Adhesive tensile testing of hybrid coatings on titanium (Ti6Al4V) substrates. The coating (black line) and Ti6Al4V substrate (red line) are forced apart (yellow arrows) in an Adelaide TCC universal testing machine	56
Figure 3.2 Chemical synthesis of chitosan–silica Class II hybrids and imbedding of silver nanoparticles (AgNPs). (A) Coupling of chitosan and 3-glycidyloxypropyltrimethoxysilane (GPTMS) in mildly acidic conditions; (B) polycondensation of coupled chitosan and hydrolyzed tetraethoxysilane (TEOS); (C) imbedding AgNPs into the hybrid sol network.....	58
Figure 3.3 Characterization of covalent coupling in hybrid materials. ¹³ C Magic-angle spinning nuclear magnetic resonance (MAS-NMR) spectra of the hybrid material. Covalent coupling was confirmed by peak “6”, which was from a nucleophilic attack of the primary amine in chitosan on the epoxide of 3-glycidyloxypropyltrimethoxysilane (GPTMS). The absence of other peaks associated with coupling of these species indicated that the amine in chitosan was the sole site of coupling.	59
Figure 3.4 Quantitative analysis of covalent coupling between chitosan and 3-glycidyloxypropyltrimethoxysilane (GPTMS) by ninhydrin assay. In finely ground aqueous suspensions of coupled material (Ch+GPTMS) and uncoupled chitosan (MMW Chitosan), ninhydrin reagents selectivity for primary amines was measured by optical absorbance at 590 nm. The degree of covalent coupling between chitosan and GPTMS was measured to be 91% and maintained throughout the study.	60
Figure 3.5 Scanning electron microscopy (SEM) and elemental (EDX) analysis of the 40% ChSi-nAg hybrid coating. SEM showed smooth undulating contours and microtopographies (A). EDX mapping detected a homogenous distribution of silicon (B), oxygen (C), nitrogen (D), carbon (E) and silver (F). The SEM/EDX analyses were representative and consistent across all coatings. Scale bar: 100 μm.	61

- Figure 3.6** Evaluation of synthesized AgNPs. (A) Transmission electron microscopy (TEM) confirmed nanoscale particle sizes. (B) UV spectroscopy of AgNP suspensions verified their consistency. 62
- Figure 3.7** Infrared analyses of chemical structures in hybrid materials. Total reflectance Fourier transform infrared (ATR-FTIR) spectra of chitosan, chitosan coupled with 3-glycidyloxypropyltrimethoxysilane (Ch+GPTMS), hybrid materials (80%–20% ChSi) and pure inorganic siloxane (condensed TEOS). There were more peaks attributed to chitosan and GPTMS (-NH, -NH₂, Epox) for hybrid materials with higher organic content. Their chemical characteristics were more similar to a purely inorganic siloxane network (Si–O–Si, Si–OH), as the organic fraction decreased. . 63
- Figure 3.8** Water contact angles for coatings and titanium (Ti6Al4V) substrates. Static water contact angles (n = 5/surface) for all coatings and polished Ti6Al4V were similar with an intermediate degree of hydrophilicity. Contact angles for acid-etched Ti6Al4V were significantly (*p* < 0.05) lower and more hydrophilic. ns—not significantly different; *—statistically significant difference. 64
- Figure 3.9** Scanning electron microscopy (SEM) of titanium (Ti6Al4V) substrates and coated surfaces. (A) Polished Ti6Al4V was flat with smoothly scalloped surfaces; (B) acid-etched Ti6Al4V had extensive surface fissures that created microscale roughness; (C) hybrid coating (60% ChSi) films on acid-etched Ti6Al4V substrates retained microtopographical features and surface roughness. SEM analyses were representative and consistent across all coatings. 65
- Figure 3.10** Microscopic examination of coatings in cross-hatch tests of adhesion. (A,B) Coating (60% ChSi) surfaces were unblemished by full-depth incisions in the standardized cross-hatch adhesion protocol; (C,D) inorganic siloxane material (control) developed extensive arrays of surface cracks and fissures from the same cross-hatch testing protocol. Adhesion of the 60% ChSi coating blend was representative and consistent across all hybrid coatings. 66
- Figure 3.11** Adhesive tensile strengths of coatings and chitosan on titanium (Ti6Al4V) substrates. All hybrid coatings (n = 3/surface) had significantly (*p* < 0.05) more adhesion to acid-etched than to polished Ti6Al4V substrates. All hybrid coatings were more adhesive than pure chitosan to both polished and acid-etched Ti6Al4V. *—statistically significant difference 67
- Figure 3.12** Inhibition of bacterial growth in planktonic cultures. There was a (A) marked reduction in *E. coli* growth and (B) complete inhibition of *S. aureus* grown in the presence of 80% ChSi-nAg compared to 80% ChSi. This inhibition of bacterial growth by 80% ChSi-nAg was representative and consistent for all hybrid coatings that contained AgNPs..... 68
- Figure 3.13** Inhibition of bacterial cultures by hybrid coatings with (+) and without (–) AgNPs. (A) *E. coli* and (B) *S. aureus* cultures were inhibited by incubation (24 hours) with all hybrid coatings, compared to uncoated titanium (Ti6Al4V) controls. There was

little inhibition from base coatings without AgNPs, but significantly ($p < 0.05$) more and almost total inhibition for coatings loaded with AgNPs.	69
Figure 3.14 Inhibition of bacterial biofilm formation on hybrid coatings with (+) and without (-) AgNPs. (A) <i>E. coli</i> and (B) <i>S. aureus</i> biofilm formation (24 h) were inhibited on all hybrid coatings, compared to uncoated titanium (Ti6Al4V) controls. Inhibition of biofilm formation was greater on coatings that contained AgNPs and was generally more on coatings with higher organic content. There was near complete inhibition of <i>S. aureus</i> biofilms on all hybrid coatings that contained AgNPs.....	70
Figure 4.1 ¹³ C NMR of synthesized calcium-2-ethoxyethoxide (Ca2EE)	88
Figure 4.2 ¹ H NMR of synthesized PEG-diamine (2K).....	89
Figure 4.3 Chemical synthesis of PEG–Ca-silica Class II hybrids and imbedding of silver nanoparticles (AgNPs). (1) Coupling of PEG-amine and 3-glycidyloxypropyltrimethoxysilane (GPTMS) in mildly acidic conditions; (2) polycondensation of coupled PEG-amine, calcium 2-ethoxyethoxide, and hydrolyzed tetraethoxysilane (TEOS); (3) imbedding AgNPs into the hybrid sol network.....	90
Figure 4.4 Infrared analyses of chemical structures in Si-Ca coating materials. Total reflectance Fourier transform infrared (ATR-FTIR) spectra of PEG-diamine, PEG-diamine coupled with 3-glycidyloxypropyltrimethoxysilane (PEG+GPTMS), hybrid coating material (Si- Ca-PEG), inorganic bioactive glass material (Si-Ca), and pure inorganic siloxane (condensed TEOS). Peaks attributed to PEG-diamine (-NH ₂ , -CH) were apparent for the hybrid coating material and absent in purely inorganic coating materials. The chemical characteristics of the inorganic bioactive glass coating materials was similar to that of the pure siloxane network with prominent Si-O-Si and Si-OH peaks.....	91
Figure 4.5 Scanning electron microscopy (SEM) of titanium (Ti6Al4V) substrates and coated surfaces. Polished Ti6Al4V was flat with smoothly scalloped surfaces (A). Acid-etched Ti6Al4V had extensive surface fissures that created micro-scale roughness (B). Hybrid bioactive glass coating (Si-Ca-PEG) films on acid-etched Ti6Al4V substrates retained micro-topographical features and surface roughness (C).....	92
Figure 4.6 Adhesive tensile strengths of coatings and chitosan on titanium (Ti6Al4V) substrates. Hybrid bioactive glass (Si-Ca-PEG) coatings (n=3/surface) were significantly ($p < 0.05$) more adherent to acid-etched Ti6Al4V substrates than they were to polished Ti6Al4V.* - statistically significant difference.....	93
Figure 4.7 Elemental EDX mapping analysis of the hybrid coating material (Si-Ca-PEG) after 72 hours immersion in SBF: (a) selected microscopic SEM field; (b) Si; (c) C; (d) Ag; (e) Ca, and (f) P. SEM micrographs display the presence of apatite globules on the surface of Si-Ca-PEG monoliths following immersion in SBF. Elemental analysis confirms the presence of apatite. Scale bar: 100 μ m.	94

Figure 4.8 Inhibition of bacterial cultures by Si-Ca-PEG coatings with (+) and without (-) AgNPs. *E. coli* and *S. aureus* cultures were inhibited by incubation (24 hours) with AgNP-loaded hybrid coatings, compared to uncoated titanium (Ti6Al4V) controls. There was little inhibition from base coatings without AgNPs, but significantly ($p < 0.05$) more and almost total inhibition for coatings loaded with AgNPs..... 96

Figure 4.9 Inhibition of bacterial biofilm formation on hybrid coatings with (+) and without (-) AgNPs. *E. coli* and *S. aureus* biofilm formation (24 hours) were inhibited on hybrid coatings, compared to uncoated titanium (Ti6Al4V) controls. Inhibition of biofilm formation was significantly greater ($p < 0.05$) on coatings that contained AgNPs. Hybrid bioactive glass coatings were generally more effective than purely inorganic bioactive glass coatings at inhibiting the formation of biofilms. The highest degree of biofilm inhibition was observed for *S. aureus* biofilms on for both coatings that contained AgNPs..... 97

List of Abbreviations

ACP	Amorphous calcium phosphate
Ag ⁺	Silver ions
Ag ⁰	Metallic silver
AgNO ₃	Silver nitrate
AgNPs	Silver nanoparticles
AMP	Antimicrobial peptide
ATR-FTIR	Attenuated total reflectance Fourier transform infrared spectroscopy
BMP-2	Bone morphogenetic protein 2
BSA	Bovine serum albumin
Ca	Calcium
Ca ₂ EE	Calcium 2-ethoxyethoxide
CaCl ₂	Calcium chloride
CaNO ₃	Calcium nitrate
CaO	Calcium oxide
CaP	Calcium phosphate
CFU	Colony forming units
Ch	Chitosan
CM	Calcium methoxide
CME	Calcium methoxyethoxide
CoCr	Cobalt-chromium
DDA	Degree of deacetylation
E. Coli	Escherichia coli
EDX	Energy-dispersive X-ray spectroscopy
EPS	Extracellular polymeric substances
FDA	United States Food and Drug Administration
GPTMS	3-glycydoxytrimethoxysilane
H ₂ SO ₄	Sulphuric acid
HA	Hydroxyapatite
HCl	Hydrochloric acid
IAI	Implant associated infection
ICP-MS	Inductively coupled plasma mass spectroscopy
LB	Luria Bertani
MAS-NMR	Magic-angle spinning nuclear magnetic resonance
Mg	Magnesium
MIH	Minimum inhibitory concentration
MRSA	Methicillin-resistant staphylococcus aureus

NaBH ₄	Sodium borohydride
NMR	Nuclear magnetic resonance
P	Phosphorus
<i>P. aeruginosa</i>	<i>Pseudomonas aeruginosa</i>
PBS	Phosphate buffered saline
PCL	Poly(ϵ -caprolactone)
PEG	Poly(ethylene) glycol
PEG-diamine	Poly(ethylene) glycol diamine
PEO	Poly(ethylene oxide)
PI	Peri-implantitis
PIM	Peri-implant mucositis
PLGA	Poly(lactic-co-glycolic acid)
PMMA	Poly(methyl methacrylate)
PVA	Poly(vinyl alcohol)
PVP	Polyvinylpyrrolidone
QACs	Quaternary ammonium compounds
RGD	Arginine-glycine-aspartic acid
<i>S. Aureus</i>	<i>Staphylococcus aureus</i>
<i>S. epidermidis</i>	<i>Staphylococcus epidermidis</i>
<i>S. mutans</i>	<i>Streptococcus mutans</i>
SBF	Simulated body fluid
SEM	Scanning electron microscopy
Si	Silicon
Si-OH	Silanol group
Si-O-Si	Siloxane group
SS	Stainless steel
TEM	Transmission electron microscopy
TEOS	Tetraethoxysilane
THA	Total hip arthroplasty
Ti	Titanium
TiO ₂	Titanium dioxide
TKA	Total knee arthroplasty
TMOS	Tetramethylorthosilane
TTCP	Tetracalcium phosphate

Chapter 1: Introduction

1.1 Overview

An implantable material (or biomaterial) is a biomedical device used to augment or restore the function of human tissues. Over the past fifty years, the popularity of biomaterial-based treatments has increased dramatically with more than 13 million devices implanted annually in the United States alone¹. Through advances in material science, biomaterials have become increasingly tailorable to human physiology. This has led to a considerable increase in the success of such materials in the replacement of damaged bone tissues.

Throughout this past half century, titanium (Ti) and its alloys have become the material of choice for biomedical implants^{2,3}. Their low specific weight, high strength to weight ratio, and resistance to corrosion are features that make titanium the ideal bulk material for numerous clinical applications^{4,5}. These include orthopaedic and dental implants where their resistance to chipping and capacity to endure repetitive high loading conditions are an advantage over non-metallic substrates^{4,6,7}. Furthermore, the titanium dioxide layer that forms on their surfaces are highly inert and biocompatible to the cells and extracellular matrix of surrounding tissues. However, along with the bio-inertia of titanium surfaces, is the lack of significant osteoinductive or antimicrobial properties.

Currently, the surface modifications on titanium implants are limited commercially to surface treatments (physical roughening, anodizing, chemical etching etc.), and inorganic ceramic coatings that typically incorporate hydroxyapatite (HA) as a bioactive layer. However, the application of ceramic coatings involves numerous disadvantages such as slow processes, high temperatures (biomimetism, plasma spraying), overly thick or weak film deposition, brittle substrates, and their inability to be loaded with temperature sensitive antimicrobials⁸⁻¹⁰.

Therefore, there has been significant interest in using alternative coating materials that consist of a larger organic content, which would improve their material properties while retaining an adequate level of bioactivity in tissues.

Given the limited success of commercially available coating materials, the development of multifunctional implant coatings, capable of providing osteoconductive interactions with native interfaces while also providing antimicrobial activity have been increasingly sought after. To this

end, the development of class II organic-inorganic hybrid materials that retain the biological benefits of polymers such as chitosan and PEG, while enhancing their physical properties, has been proposed¹¹⁻¹³. The covalent coupling of biopolymers to inorganic precursors is the focus of this thesis and is the framework of multifunctional coating materials evaluated in this study.

1.2 Thesis Objectives

Considering the limited success of bare and plasma coated titanium implant materials, the overall focus of this study was to synthesize robust coating materials on titanium substrates to improve on their overall success *in vivo*. Coatings developed in this work should greatly improve on the shortcomings of current bare and plasma coated titanium implant materials.

1.3 Hypothesis

It is hypothesized that the integration of silicon (Si) and calcium (Ca) into the coating network will act to improve the overall robustness of coating materials, and, will promote factors associated with osseointegration. Additionally, it is hypothesized that the addition of silver nanoparticles (AgNP) into the coating network will provide an antimicrobial effect against sessile and biofilm colonies of clinically relevant pathogenic bacteria.

1.4 Thesis Outline

As highlighted above, the objectives and hypothesis of this study focuses on the development of robust bioactive and antibacterial coating materials for titanium implantable devices. Chapter 2 provides a comprehensive review of the relevant literature in this area. Chapter 3 includes the synthesis and discussion of a robust chitosan-silicon class II hybrid coating materials to improve the antimicrobial efficacy of titanium implants. Chapter 4 includes the synthesis and relevant discussions related to the development of a robust PEG-Si-Ca class II hybrid coating to promote osseointegration while providing an antimicrobial effect. Chapter 5 provides a discussion on the relevant conclusions to this study and suggestions for future work.

1.5 References

- (1) Wang, X. Overview on Biocompatibilities of Implantable Biomaterials. In *Advances in Biomaterials Science and Biomedical Applications*; InTech, 2013.
- (2) Saini, M. Implant Biomaterials: A Comprehensive Review. *World J. Clin. Cases* **2015**, 3 (1), 52.
- (3) Van Noort, R. Titanium: The Implant Material of Today. *J. Mater. Sci.* **1987**, 22 (11),

3801–3811.

- (4) Özcan, M.; Hämmerle, C. Titanium as a Reconstruction and Implant Material in Dentistry: Advantages and Pitfalls. *Materials (Basel)*. **2012**, *5* (9), 1528–1545.
- (5) Greger, M.; Widomská, M.; Snášel, V. Structure and Properties of Dental Implants. In *METAL 2012 - Conference Proceedings, 21st International Conference on Metallurgy and Materials*; 2012; Vol. 120, pp 434–439.
- (6) Raigrodski, A. J.; Hillstead, M. B.; Meng, G. K.; Chung, K. H. Survival and Complications of Zirconia-Based Fixed Dental Prostheses: A Systematic Review. *J. Prosthet. Dent.* **2012**, *107* (3), 170–177.
- (7) Niinomi, M. Mechanical Biocompatibilities of Titanium Alloys for Biomedical Applications. *J. Mech. Behav. Biomed. Mater.* **2008**, *1* (1), 30–42.
- (8) Ong, J. L.; Lucas, L. C. Post-Deposition Heat Treatments for Ion Beam Sputter Deposited Calcium Phosphate Coatings. *Biomaterials* **1994**, *15* (5), 337–341.
- (9) Li, T.; Lee, J.; Kobayashi, T.; Aoki, H. Hydroxyapatite Coating by Dipping Method, and Bone Bonding Strength. *J. Mater. Sci. Mater. Med.* **1996**, *7* (6), 355–357.
- (10) Wang, B. C.; Lee, T. M.; Chang, E.; Yang, C. Y. The Shear Strength and the Failure Mode of Plasma-Sprayed Hydroxyapatite Coating to Bone: The Effect of Coating Thickness. *J. Biomed. Mater. Res.* **1993**, *27* (10), 1315–1327.
- (11) Tian, D.; Dubois, P.; Jérôme, R. Biodegradable and Biocompatible Inorganic-Organic Hybrid Materials. I. Synthesis and Characterization. *J. Polym. Sci. Part A Polym. Chem.* **1997**, *35* (11), 2295–2309.
- (12) Valliant, E. M.; Jones, J. R. Softening Bioactive Glass for Bone Regeneration: Sol-Gel Hybrid Materials. *Soft Matter* **2011**, *7* (11), 5083–5095.
- (13) Sachot, N.; Castaño, O.; Mateos-Timoneda, M. A.; Engel, E.; Planell, J. A. Hierarchically Engineered Fibrous Scaffolds for Bone Regeneration. *J. R. Soc. Interface* **2013**, *10* (88), 2–6.

Chapter 2: Literature Review and Background

While established as a field of scientific study in the 1960s, the use of biomaterials pre-dates ancient times. Evidence of foreign material usage as implants or prostheses has been found in the excavation of ancient burial sites of ancient Egyptian, Roman, Greek and Etruscan civilizations¹. Since these primitive designs, biomaterial implementation has been improved through industrialization, advances in material and polymer chemistry, and an increased understanding of the foreign body response to biomaterials.

2.1 Hard Tissue Implants

Since antiquity, hard tissue implants have found great use in the restoration and augmentation of diseased or damaged tissues. In general, hard tissue implants are prosthesis that are integrated with hard tissue systems in the body such as bones, joints, and teeth. In present day, these prostheses are predominantly made of metallic or ceramic materials that have sufficient chemical and mechanical stability to achieve successful integration and long-term stability with host tissues. The application of hard tissue implant materials finds greatest use in the fields of orthopedics and prosthodontics.

Orthopedic implants exist in many physical forms and can be used in a variety of restorations such as joint arthroplasty (hip, knee, and shoulder) and the repair of fractures to other osseous tissues (some shown in Figure 2.1)². Surgical interventions and implantations have become increasingly more common in this area due to the increased rates of osteoporosis and arthritis among older populations^{2,3}. Often large orthopedic restorative surgeries, such as total hip replacements, require special attention to the type of implant materials used. Consideration for material properties such as elastic modulus, hardness, and fatigue resistance have been shown to prevent long term complications associated with these load bearing implants such as stress shielding and wear^{3,4}. Other devices used in orthopedics include small, and non- or low-load bearing implant materials that include screws, pins, plates and meshes. These materials are often used as internal or external fixation devices which can maintain the alignment of bone fragments or material substitutes during the healing process⁵. During the application of these fixation devices, compressive force is often used to lower stresses placed on the implant and increase the contact area at repair sites⁵. Given that these devices are under significantly lower stresses than

larger orthopedic implants, procedural complications are more frequently associated with infection rather than stress shielding and wear.



Figure 2.1 Examples of implant forms used for hard tissue implantation in orthopedics. Adapted from Rony et al.⁶

In prosthodontics, dental implants are most commonly used as supports for artificial tooth replacements. The use of dental implants has increased dramatically in the past 30 years, limiting the need for non-fixed dentures and bridges to replace lost teeth in many cases⁷. Implants in this field exist in a variety of physical forms such as screws, cylinders and blades, with the most common structure of complete dental prosthesis following a screw-abutment-crown design (Figure 2.2)⁸. Here, screw-like devices are directly implanted into the maxilla or mandible which acts as an anchor for artificial teeth (crowns). Abutments are then used to connect the crown to the screw anchored in the patient's jawbone^{9,10}. Similar to the field of orthopedics, dental implants are used for both load bearing and low-load bearing applications which are determined by their placement in the oral cavity¹¹. The success of these implants is determined by the successful fixation of screw supports implanted within the jawbone and their ability to resist infection. Failure modes of these implants have been attributed to low bone density in the maxillofacial region and implant sepsis due to the contaminated surgical field within the oral cavity^{12,13}.



Figure 2.2 Screw-abutment-crown dental implant design. Adapted from www.1888implant.com¹⁴

In both orthopedic and prosthodontic implant interventions, the choice of material is a critical determinant to the overall success of the restoration. Titanium represents a large portion of these bone-interfacing biomaterials given its superior mechanical properties and proven ability to interface well with human tissues.

2.1.1 Titanium Implants

Metals have been the choice implant material since the advent of aseptic surgical techniques¹⁵. Since then, metals have found many uses as orthopedic and prosthodontic implant materials. Commonly used metals in these areas include stainless steel (SS), cobalt-chromium alloys (CoCr), and titanium alloys (Ti). Of which, SS and CoCr have lost favour in many applications due to their lack of performance in comparison to titanium alloys. Titanium based implants possess advantages over these metals in terms of their rate of corrosion, modulus value, and biocompatibility.

The corrosion of metallic implants leads to the release of metallic ions from the bulk material. The release of these cationic species affects surrounding tissues by modifying their electrical and chemical environment which can produce a degree of cytotoxicity^{16,17}. While all metals corrode to some extent *in vivo*, choice materials are those that corrode in a slow and controlled fashion¹⁸. For this reason, SS and CoCr implant materials have lost favour in many applications as they readily corrode in physiological environments. The corrosion of SS and CoCr, along with modifying the surrounding physiological environment, leads to a cytotoxic effect attributed to

the leaching of cytotoxic elements such as nickel, chromium and cobalt¹⁹. Titanium based materials, however, exhibit a high resistance to corrosion. Additionally, when alloyed, titanium based materials can contain relatively non-toxic elements such as magnesium niobium, tantalum, and zirconium leading to minimal cytotoxicity during corrosion^{20,21}. Titanium and titanium alloys display increased resilience to corrosion due to the formation of an oxide layer in the form of TiO₂, Ti₂O₃, TiO and TiO₂^{22,23}. This film, while robust, also possesses self healing properties *in vivo* due to the reactive nature of titanium. Any disruptions or damages to the outer oxide layer are repaired immediately in environments with air or oxidizing media such as physiological fluids.

Additionally, SS and CoCr based implant materials have relatively high modulus values compared to that of bone (Figure 2.3)²⁴. High modulus mismatches between implant materials and host bony tissues have been shown to cause a condition known as stress shielding. Stress shielding is a process in which high modulus implant materials prevent host tissues from being exposed to normal levels of mechanical loading²⁵. In cases where stress shielding occurs, host bony tissues around the implant are remodeled, leading to a decrease in bone strength, cell death, and subsequent implant loosening^{26,27}. Unlike SS and CoCr materials, titanium alloys can possess similar moduli to that of bone, leading to a decrease in the severity of stress shielding. The decreased effect of stress shielding becomes quite relevant in the comparison of different metallics used as high load bearing implant materials. In the case of total hip replacements, studies have shown that femoral stem materials made of titanium alloys, as opposed to higher modulus materials such as CoCr and SS, led to less femoral bone loss and better integration with host tissues²⁸⁻³⁰.

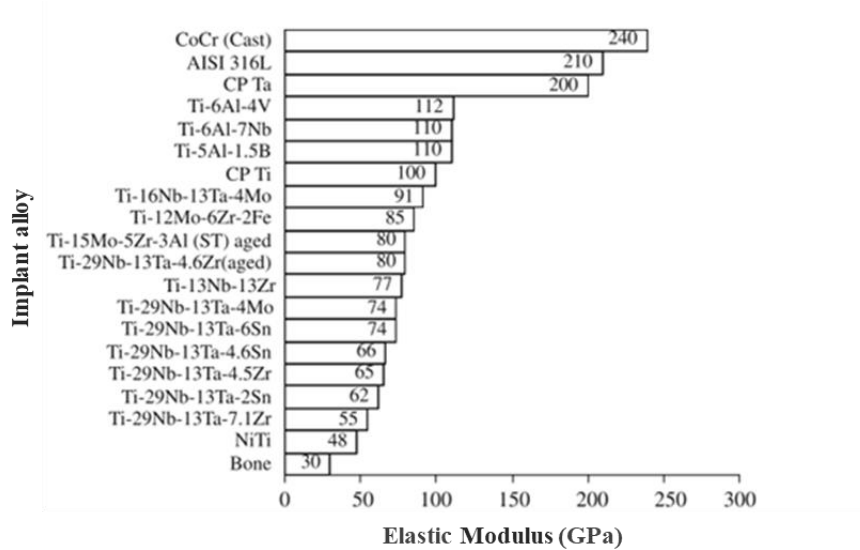


Figure 2.3 Modulus of elasticity of commonly used implant metallics. Adapted from Geetha et al.²⁴

In addition to being more resistant to corrosion and possessing improved mechanical properties to other metallics, titanium materials are also more biocompatible. While no surgical study of metallic implants is completely free of adverse reactions, titanium implant materials have been shown to be well tolerated as an inert material in the human body. When compared to SS and CoCr alloys, titanium implant materials exhibit superior biocompatibility, akin to their decreased cytotoxicity and decreased levels of fibrosis upon implantation^{20,24,31}. The increase in relative cytotoxicity and fibrosis of SS and CoCr implant materials have been owed to the release of metal ions upon corrosion and their lack of relevant topographical cues^{32,33}.

Despite the superior performance of titanium-based implant materials relative to other metallics, they are still continuously subjected to various surface modifications in order to better function with the human body. The development of appropriate surface topographies and coating materials has represented a large portion of research in implantology in recent years and has been a challenging problem in the field of metallics in general. The interface of implant materials has become a key factor to combat the complications faced in this field and, overall, increase the longevity and fixation of implants in the human body^{32,34–36}.

2.1.2 Implant Complications

2.1.2.1 Implant Associated Infections

One of the main problems that continues to limit the success of hard tissue implant interventions is implant associated infection (IAI). Orthopedic fixation devices, particularly external fixation devices, have notoriously high rates of post-operative infection, occurring in 5 and 30% of all internal and external interventions respectively^{37,38}. The infections of dental implants are also significant with IAI occurring in 5-10% of all implant procedures³⁹. While virtually all bacteria and fungi can cause IAI, the most common bacteria responsible are the staphylococci species including *Staphylococcus aureus* (*S. Aureus*) and *Staphylococcus epidermidis* (*S. epidermidis*)^{40,41}. The prevalence of such species can be owed to their natural residence within the skin flora and their ability to form pathogenic biofilms on implant surfaces⁴².

Biofilms are highly adherent colonies of bacteria that are encased within a bacterial-excreted polysaccharide matrix. The formation of biofilms occurs through several stages explained visually through Figure 2.4. In this process, planktonic species of bacteria adhere to a surface and then begin to proliferate and adhere to adjacent colonies through the release of extracellular polymeric substances (EPS). Mature biofilms encased in EPS subsequently release planktonic colonies within their matrix to continue the cycle. Additionally, mature biofilms present a favourable environment for symbiotic microbes such as *Escherichia coli* and *Pseudomonas aeruginosa* in the development of polymicrobial biofilms⁴³. The formation of biofilms presents major problems in combating IAI. First, the release of planktonic colonies from mature biofilms leads to a chronic inflammatory state at the implant site, and, can lead to infection in other parts of the body. Second, the bacteria within biofilms may be up to 1000 times more resistant to antibiotics than bacteria that are suspended in a planktonic state^{44,45}. In the antibiotic therapy of biofilm infections, the high doses of antibiotics required to combat biofilms result in systemic toxicity with associated renal and liver complications^{46,47}. When low dose treatments are used, therapeutic agents are often below the minimum inhibitory concentration (MIC) of biofilm bound bacteria which increases the risk of developing antibiotic resistance pathogens⁴⁸.

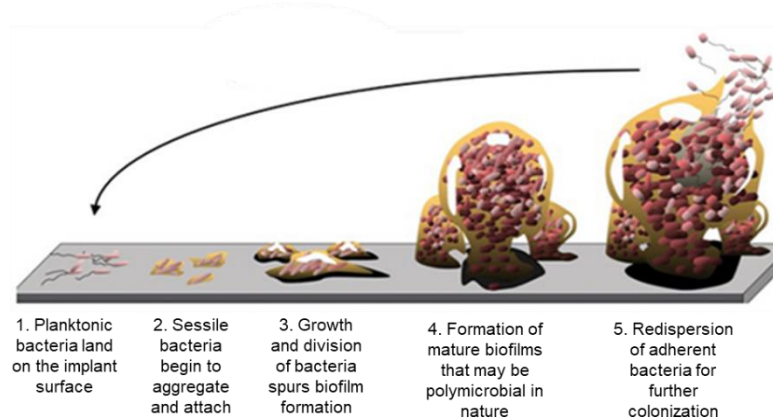


Figure 2.4 Stages of biofilm formation on implant surfaces. Adapted from Chung et al.⁴⁹

Due to the resistant nature of biofilms, the gold standard treatment of IAIs in orthopedics has been two-stage septic revisions⁵⁰. In this revision technique, the first stage involves the removal of the prosthesis, followed by extensive debridement of all damaged or infected tissues. At this stage, antibiotics are administered to patients and reimplantation is delayed until the completion of an antibiotic regimen. In conjunction with this regimen, antibiotic-loaded beads or spacers are typically inserted into the sites of larger infected prosthesis such as those used in total hip and knee replacements⁵¹. Reimplantation in these cases includes the removal of antibiotic-loaded beads or spacers before the placement of the new prosthesis. Septic revisions are technically complex and require significantly more resources than initial prosthesis placements⁴. The duration of these surgeries are longer, patient hospital stays are extended, and there are often more complications related to these interventions. Despite this rigorous procedure, the initial infection is not always completely eradicated which increases the chance of reinfection at the site of reimplantation⁵². For example, in the case of total hip arthroplasty (THA), there is typically a 1-2% risk of infection for primary THA, whereas secondary septic revisions of THA carry risks of infections as high as 17%^{51,53,54}.

In the field of prosthodontics, IAIs are typically caused by the colonization of pathogenic biofilms on the collar of dental implants. Biofilm formation on dental implant materials can initially lead to infections of the peri-implant mucosa in a condition known as peri-implant mucositis (PIM)⁵⁵. PIM, which causes inflammation and damage of the peri-implant mucosa, ultimately leads to the formation of soft tissue gaps around the implant. The formation of these

gaps allows for bacteria to spread to regions where hard tissues are exposed. The exposure of pathogenic bacteria to surrounding bone causes characteristic bone loss around the implant in a condition known as peri-implantitis (PI)⁵⁶. PI has been shown to be one of the main reasons for the loosening and failure of dental implants⁵⁷. Due to the placement of dental implants in endosseous tissues and the prevalence of biofilm occurring mainly at the collar of dental abutments, treatment methods typically do not follow the same septic two-stage revisions seen in the field of orthopedics. In the treatment of dental implant infections a variety of surgical (resective therapy, bone regeneration therapy) and non-surgical methods (abrasive cleaning, ultrasonic decontamination) are employed on a case to case basis^{58,59}. The efficacy of different treatment methods is debated frequently, with their success remaining variable over long-term studies⁶⁰. One of the main reasons for this variability is the difficulty in managing PIM. The continuation of PIM, as described above, leads to PI which is typically not responsive to non-surgical interventions^{56,61,62}. The failure to effectively treat infected dental implants and their environment have led to increased rates of reinfection. While the risk of initial post-periodontal infection is ~4%, the risk of reinfection or continued peri-implantitis 3-7 years after revision treatments ranges from 16-25%⁶³⁻⁶⁵.

Due to the resistant nature of biofilms, IAIs have become one of the most common causes of revisited surgeries and implant removal^{40,66,67}. Efforts to mitigate the prevalence of biofilms on implant surfaces have, to this point, showed mild effectiveness at eliminating the risks of post-operative infection. More specifically, the use of prophylactic antibiotic regimens has remained minimally effective at targeting developed biofilms and fails to accommodate the continued risks of infection throughout the lifetime of integrated implants. Therefore, the use of site-specific antimicrobial action that can retard the formation of biofilms, or, provide a localized release of biocidal components provides an attractive alternative in the treatment and mitigation of IAI.

2.1.2.2 Aseptic Loosening

While IAI remains the primary reason for the failure of most hard tissue implants, the loosening of implants without the presence of microbial infection presents another clinically relevant issue. Aseptic loosening is a result of the inability of an implant surface to bond to adjacent bone and other tissues⁶⁸. This lack of fixation leads to micromotions of the prosthesis which causes the

formation of fibrous tissues arounds the implant, and subsequent loosening from the site of implantation.

In the field of orthopedics, aseptic loosening is a major complication and is the cause of more than 52% of hip arthroplasty revisions in the US annually⁶⁹. Here, aseptic loosening typically occurs following the release of particulate debris around the site of implantation. Particulate debris can develop around the implant site from a variety of origins such as: poor surgical technique, the loss of mechanically fixed bone cement, or wear at polymer-metal interfaces^{3,68}. The formation of wear debris leads to an elevated inflammatory response, bone resorption, and osteolysis, leading to loosening and subsequent implant loss⁷⁰. Unsurprisingly, aseptic failures often require surgical revisions which include the complete removal and replacement of the initial prosthesis with site re-debridement leading to significant losses in surrounding tissues. Surgical revisions, in addition to increased hospital times for patients, carry increased risks for additional failures following replacements. In a study following aseptic total knee arthroplasty (TKA) revisions, 10% of revisions failed with majority of the causes being attributed to a continued state of instability and IAI⁷¹.

Due to the lack of articulation between implant features and their decreased loads, the modes of aseptic failure in the field of prosthodontics are not often attributed to the presence of particulate debris. Instead, aseptic failures of dental implants are often attributed to poor bone quantity, poor bone quality, and/or a lack of primary stability⁷². These factors can lead to excessive micro- and macro-motion at the bone-implant interface which promotes the development of a fibrous tissue membrane around the implant, subsequently leading to aseptic loosening and eventual failure⁷³. The absence of bone in these cases is often described by clinicians as marginal bone loss and is frequently monitored throughout the lifetime of dental implants using radiographs. While this method does allow for implant stability to be monitored over time, lack of patient compliance, radiographic accuracy, and non-surgical interventions limit treatment efficacy^{73,74}. Dental implants that fail through aseptic modes are often replaced through the complete removal of the initial implant, followed by either a 1 year wait period for the replacement of a similar screw fixture, or, immediate replacement of a larger diameter screw fixture that removes the threading and tissues surrounding the initial site⁷². In either case, these revisions in sites of aseptic failure have show mild success with risks of failure up to 30%^{75,76}.

As with IAI, aseptic loosening remains a clinical concern where often invasive treatment methods must be used at the burden of patient comfort and economic efficiency. Similarly, to mitigate the potential for aseptic loosening events, surface systems that are targeted to improve the fixation of hard tissue implants can afford a variety of advantages. Details of these systems, as well as the interrelation of coating systems to target both complications will be highlighted in the following sections of this literature review.

2.2 Implant Surface Modifications

Current strategies to mitigate the complications associated with IAI and aseptic loosening have relied mainly on implant surface modifications. Although titanium possesses a robust and stable film, its inert nature limits its ability to battle infections or promote long-term bonds with bone. Herein, surface modifications to mitigate IAIs and aseptic loosening will be discussed.

2.2.1 Antibacterial Surfaces

As previously discussed, the treatment of IAIs and the formation of biofilms on implant surfaces have shown minimal success and often present increased risks of continued infection. Given the increased resistance of biofilms to systemic antibiotic regimens, surface modifications have emerged as popular method to provide hard tissue implant materials with antibacterial properties. Antibacterial surface treatments often act by preventing the primary adhesion of planktonic bacteria to implant surfaces, or, by killing approaching bacteria. These two major approaches can be summarized within non-eluting, eluting, and combination antibacterial strategies.

2.2.1.1 Non-Eluting/Static/Passive Antibacterial Strategies

Static antimicrobial surface modifications are currently one of the most common coating strategies to target medical device related infections⁷⁷. Such strategies are currently utilized in to develop coatings for catheters, infusion lines, vascular stents and grafts, and sutures to prevent biofilm formation and infection⁷⁸. Many of the static antibacterial surface modifications employed to date act either by preventing initial microbial adhesion (anti-adhesive action), or, by killing microbes on contact with implant surfaces (contact-active action).

Anti-Adhesive Surfaces

Anti-adhesive or anti-fouling surface modifications passively target the initial adhesion of planktonic bacteria to the surface of implant materials. Due to their passive nature, these surface modifications are typically effective for long periods of time, leading to their popularity as

coatings for a variety of medical devices. In the clinic, most of these coatings are currently designed to be superhydrophobic to reduce bacterial adhesion and enable easy cleaning of various medical instruments⁷⁹. Typically, the chemical composition and roughness of material surfaces are manipulated in conjunction to modify material wetting. In chemical modifications, low surface energy materials, such as fluorinated compounds, are utilized to increase hydrophobicity⁸⁰. Once surfaces are hydrophobic, roughening in the micro and nano domain can increase the hydrophobicity of materials further in a process described by Wenzel⁸¹. For titanium materials, this process of roughening in conjunction with hydrophobic chemical treatments has shown effectiveness against clinically relevant pathogens in a variety of studies. Tang et al. was able to show a reduction in *S. aureus* colonization by roughening titanium surfaces with TiO₂ nanotubes, followed by surface functionalization with a fluoroalkyl silane⁸². Privett et al., through similar methods, was able to show the reduction in *S. aureus* and *P. aeruginosa* adhesion to roughened fluoroalkyl silane coatings compared to untreated titanium surfaces⁸³. This strategy, while abundant in work, has seen little clinical translation for titanium and other hard tissue implant materials. One reason for this lies in the differences between current commercial applications of these coatings and their hard tissue target area.

Current applications of these coating technologies find greatest use as coatings for urinary catheters lines⁸⁴⁻⁸⁶. These devices have a placement period of under 30 days and are not intended to be integrated with host tissues, or, interface with protein-rich fluids such as blood and serum. For hard tissue implants, materials directly interface with protein-rich physiological fluids and nearly instantly develop a protein-rich conditioning film which dictates the foreign body response to the implant⁸⁷. This conditioning film may contain a wide range of proteins such as: fibronectin, laminin, fibrin, collagen and immunoglobulins, which act as receptors to promote surface colonization^{88,89}. Potential colonizers of the conditioning film include tissue cells and microorganisms which participate in a well established “race to (colonize)” the surface of the material⁴³. Through the colonization of a strong monolayer of tissue cells, the implant surface can become resistant to colonization by microorganisms due to their viability, intact cell surface, and regular host defences⁸⁷. In contrast, the colonization of the surface by adherent microbes leads to poor interactions with host tissue cells and potential implant failure. Anti-adhesive coatings that employ superhydrophobicity limit the binding of host proteins. This in turn inhibits

the adhesion of both bacterial and tissue cell adhesion, which leads to limitations for osteogenesis and implant fixation⁹⁰.

Given the importance of protein-tissue cell interactions for the successful fixation, integration and biofilm prevention, mild and more specific anti-fouling coatings are currently under investigation. Some of the most recent strategies in this area include pre-grafting specific ligands and proteins to titanium implant materials to yield selective anti-fouling properties. An et al. have shown that titanium implants materials grafted with bovine serum albumin (BSA) can provide reduced rates of infection by *S. epidermidis* in rabbit models⁹¹. While this study utilized albumin to specifically target the adhesion of host tissue cells, they did not directly assess its interactions with osteoblasts. In another study an anti-fouling grafted PEG brush coating was modified with the cell-adhesive arginine-glycine-aspartic acid (RGD) ligand to retain interactions with osteoblasts⁹². In this study, the coating provided a reduction in the adhesion of *S. aureus* to implant surfaces, while the RGD ligand-maintained interactions with osteoblasts. Dextran, commonly used to decrease thrombosis, has also been used as a specific anti-fouling coating material as it has been shown to provide specific tethering sites for bone stimulating proteins such as bone morphogenetic protein 2 (BMP-2). A study by Shi et al., illustrated that the adhesion of *S. aureus* and *S. epidermidis* can be reduced by 50% compared to control titanium substrates⁹³.

While mild and selective anti-fouling coatings have shown moderate success experimentally, lack of tissue culture and *in vivo* data limits the consensus that they possess the features required for bone implant usage. Other limitations include a lack of analysis relating to the fixation and stability of selective antifouling coatings^{89,94}. Despite the lack of clinically relevant data, selective anti-adhesive surfaces present an interesting opportunity in the development of inert implant surfaces to reduce the risk of IAI.

Contact-active Antimicrobial Surfaces

Similarly to anti-fouling surfaces, contact-active surfaces have the potential to provide medical implants with antimicrobial properties without the release of biocidal agents. In contrast to anti-fouling surfaces, contact-active coatings often contain immobilized biocidal agents which are designed to kill bacteria upon contact with implant surfaces. These immobilized biocidal agents include components such as: antibacterial elements, antibiotics, and anti-microbial polymers and

peptides. Most contact-active strategies currently employ some combination of these components which have shown promising results.

The contact killing effects of antibacterial metallic elements has been known for hundreds of years. Oligodynamic effects, or the biocidal effect of metallic elements, were formally recognized in the late 19th century, although the usage of such techniques predates ancient times⁹⁵. Although the antibacterial effects of antimicrobial elements are well established, their mode contact-killing action is widely debated. Until recently, their antibacterial action has been mainly attributed to the release of metallic ions from bulk materials as a method to penetrate cell membranes. This theory, however, has been proven to occur in conjunction with the direct antimicrobial action of contact with metallic elements, where sophisticated protocols were established to limit and monitor the release of metallic ions^{96,97}. While the contact-killing action of antimicrobial elements has not been fully elucidated, they have shown success in providing an antibacterial effect in a variety of studies. Zeiger et al. showed that copper surfaces could be used to successfully inhibit the growth of *E. coli* in a contact-based system to mitigate nosocomial infections attribute to metallic devices⁹⁸. More recently, Mauter et al. reported that grafting polyethyleneimine-coated silver nanoparticles to the surface of polysulfone membranes can provide excellent contact-active resistance to colonization of *E. coli*⁹⁹. While metallic elements are most prevalent in this research area, recent work has also investigated the use of non-metallic antibacterial elements as well, such as selenium. Holinka et al. reported that selenium materials have potential as orthopedic implant coatings as they provided reduced attachment of *S. aureus* and *S. epidermidis* when compared to control titanium surfaces without affecting osteoblast viability¹⁰⁰.

Antibiotics and anti-microbial polymers and peptides function through damaging cell walls and inhibiting protein synthesis in microbes¹⁰¹. Most of these active components are designed to be contact-active through the use of polymeric spacers. These polymeric spacers are utilized to allow grafted antimicrobial components to penetrate the cell wall of an adhered bacteria (Figure 2.5)¹⁰². Ketonis et al. utilized this strategy to covalently tether vancomycin to allograft bone which showed significant reduction in *S. aureus* related surface colonization and stability over 60 days¹⁰³. Given the emergence of antibiotic resistant strains of pathogens, such as methicillin resistant *S. aureus* (MRSA), antimicrobial polymers and peptides have become significantly

more popular as antimicrobial grafting agents. While antimicrobial polymers can be developed synthetically with processes such as amine quarternization, emphasis has been placed on natural antimicrobial polymers due to their inherent biocompatibility and decreased toxicity concerns^{104,105}. Chitosan, known to possess natural antimicrobial properties, has been extensively studied as a natural polymer additive in contact-active antimicrobial systems. Chua et al. reported that coatings consisting of polyelectrolyte multilayers of hyaluronic acid and chitosan were significantly effective at reducing the adhesion of *S. aureus* on titanium implant materials¹⁰⁶. Cao et al. developed a modified chitosan surface which introduced N-halamine structures that was effective at reducing the colonization of both *S. aureus* and *E. coli* compared to control surface films¹⁰⁷. Work with grafting antibacterial peptides has been met with similar success. Kazemzadeh-Narbat et al. utilized a cationic antimicrobial peptide (AMP Tet213) in the development of an antimicrobial calcium phosphate titanium implant coating¹⁰⁸. The developed coatings possessed antimicrobial activity against both Gram-positive *S. aureus* and Gram-negative *Pseudomonas aeruginosa* while providing a non-cytotoxic surface for osteoblast-like cells. Similarly, Pfeufer et al, grafted a different cationic antimicrobial peptide (rHubD2) to titanium implant surfaces using self-assembled siloxane monolayers¹⁰⁹. Coatings developed in this study possessed increased antibacterial efficacy against *E. coli* compared to titanium controls.

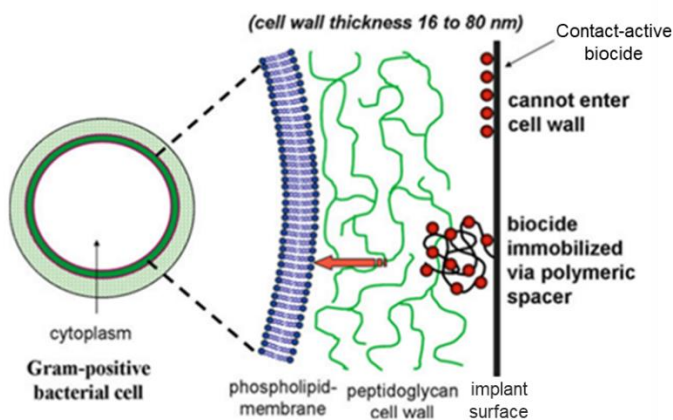


Figure 2.5 Concept of contact-killing membrane-active biocides surface-coupled via a polymeric spacer. Adapted from Börner et al.¹⁰²

While work on developing novel contact-active antimicrobial coating systems is emerging, there is still a high degree of skepticism with their possible translation as coatings for titanium implant materials. Similar to anti-adhesive coating systems, contact-active systems have shown little evidence of success in tissue culture and *in vivo* studies. This leads to a lack of conclusions related to the cytotoxicity, immunoreactivity, and genotoxicity of developed coatings in orthopedic and dental implant systems. In the case of contact-based coating solutions using antimicrobial elements, the release of toxic ions from coating matrices presents a relevant cytotoxic concern¹¹⁰⁻¹¹². In the case of coatings based on grafting antimicrobial polymers and peptides, the sensitivity and robustness of covalent coupling over time presents another clinically relevant toxicity issue¹¹³. Finally, while repelling and killing microbes on contact are obviously advantageous in an antimicrobial system, they can be easily deactivated through their contact with physiological fluids. Non-specific fouling of these surfaces can occur from dead cells and other physiological contaminants which deactivates these antibacterial systems and can allow microbes to colonize. In these cases, only systems that employ the release of biocides can retain their activity.

2.2.1.2 Elution-based/Active Antibacterial Strategies

Elution-based antibacterial strategies rely on the release of biocidal components to form a bacterial inhibition zone around the implant surface. The formation of this inhibition zone, attributed to the flux of biocides from eluting coating materials, has been shown to both reduce surface colonization *in vitro* and prevent the formation of biofilms *in vivo*¹¹⁴. Additionally, the elution from coating materials at the site of implantation enables the delivery of high local doses of biocidal components without exceeding systemic toxicity levels¹¹⁵. Since dead microbial cells cannot actively adhere to the substrate, they typically do not cover and deactivate the releasing coating material at high densities. Eluting coating systems may contain a single or combination of biocides such as: antibiotics, silver compounds, quaternary ammonium compounds (QACs), and nitric oxide. Many elution-based antibacterial coating systems rely on either a diffusion-controlled or a dissolution-controlled release method. These release methods can be further tuned to respond to certain biological cues, making the release of biocides stimuli responsive. Such triggered systems prevent the premature exhaustion of loaded biocidal components and mitigates the diminution of release that occurs in constant release systems¹⁰². In the area of antibacterial

coatings, each strategy affords different advantages and disadvantages in the localized delivery of biocides.

Diffusion-Controlled Coating Systems

Diffusion-controlled coating systems are non-erodible in physiological fluids and employ the delivery of biocides through reservoir or matrix delivery strategies. In a reservoir delivery system, biocides are dissolved or dispersed in a reservoir that is surrounded by a rate limiting, non-erodible membrane¹¹⁶. The release of biocides from the reservoirs of these systems are determined by their permeability and diffusion through a non-erodible membrane. In matrix delivery systems, biocides are dissolved or dispersed within the coating matrix without the presence of a rate controlling membrane. The release of biocides from these systems are determined by the concentration of biocide remaining within the permeable coating matrix. Both reservoir and matrix loading strategies have represented a large portion of work on antimicrobial implant coatings with a particular focus on the field of orthopedics.

Using a reservoir-loading strategy, Vasilev et al. incorporated the antibiotic lefloxacin between two non-erodible polymer layers¹¹⁷. They found that the release of lefloxacin could be effectively controlled by modifying the thickness of the outermost polymer layer, leading to a reduction of *S. aureus* colonization on implant materials. Other reservoir delivery strategies have involved the loading of biocides within porous reservoirs followed by the application of a non-erodible polymer coating membrane to control release. Michl et al. utilized this strategy to deliver nitric oxide from a porous reservoir in a controlled fashion to reduce the colonization of *S. epidermidis* on biomedical implant surfaces¹¹⁸. Kumeria et al., using a similar strategy, loaded titanium nanotubes with gentamicin and utilized a polylactic-co-glycolic acid film to control release¹¹⁹. Using this reservoir-release strategy the colonization of *S. epidermidis* was reduced while maintaining adequate osteoblast adhesion.

The most common use of matrix-bound biocide delivery systems has been in the field of orthopedics. Here, the use of vancomycin and gentamicin imbedded within non-erodible poly(methyl methacrylate) (PMMA) cement beads and coating materials has become a standard feature of two-stage revisions⁵⁰. The use of such materials has been shown to lower the rates of postoperative infections by 8-12% compared to the use of traditional systemic antibiotics^{120,121}. More recent studies have investigated the use of similar delivery methods using different matrix

materials. Kumar and Munstedt used a non-erodible polyamide coating material loaded with silver to provide an effective release of silver ions, which prevented the colonization of *E coli* and *S. Aureus* on hard material surfaces¹²². Thatiparti et al., utilized a swelling cyclodextrin-based coating matrix on titanium substrates to release vancomycin¹²³. These coatings were able to inhibit the growth of *S. aureus* for over 28 days and retained osteoblast cytocompatibility.

While diffusion-controlled systems have shown favourable results, there are significant limitations to their adoption as coating materials for orthopedic and dental implants. In non-erodible coating systems, the matrix or release-limiting membrane is often a non-biodegradable polymer material. This poses questions as the long-term robustness and retention of these membrane and matrix materials as well as their ability to promote the colonization of healthy tissues. Additionally, the release of biocides in diffusion-controlled antibacterial coatings diminishes with time until the quantities delivered lose efficacy and become subinhibitory⁸⁸. The release of subinhibitory concentrations of biocides over time not only limits the long-term effectiveness of these coating materials, but also leads to the development of biocide-resistant pathogens¹²⁴.

Dissolution-Controlled Coating Systems

Similar to diffusion controlled antibacterial coating systems, dissolution-controlled systems enable the continuous release of imbedded biocidal components. In contrast to diffusion-controlled systems, dissolution-based coating systems have release kinetics determined by the dissolution or erosion of their coating matrices in surrounding fluids. In these systems the release of imbedded biocides can be modified by changing the rate at which the coating matrix dissolves or erodes in the selected dissolution media. For this reason, the use of a variety of biodegradable organic and inorganic matrices have been explored as methods to develop antibacterial coatings that release biocides in the presence of physiological fluids. In the field of orthopedics, the controlled delivery of antibiotics based on these biodegradable or erodible coating matrices has become a popular area of research since the standardization of cementless prostheses¹²⁵.

Such systems have been developed using matrices composed of a variety of organic networks such as polylactic-co-glycolic acid copolymers (PLGA)^{126,127} and poly(D,L-lac- tide) (PDLLA)¹²⁸⁻¹³⁰ as well as inorganic networks derived from sol-gel precursors^{131,132}. For example, Kim et al. utilized a biodegradable PLA coating network loaded with chlorhexidine to

improve the antibacterial efficacy of dental implant materials¹³³. Through the degradation of the PLA coating network and release of chlorhexidine, the developed coating materials were able to effectively reduce the viability of *S. aureus* in culture. In a similar study, Metsemakers et al. developed a biodegradable PLGA coating matrix loaded with doxycycline to mitigate implant associate infection¹³⁴. This coating material provided protection for titanium alloy implant materials against clinically relevant methicillin-resistant *S. aureus* (MRSA) in a rabbit model. As for inorganic systems, sol-gel materials show significant promise in their applications within orthopedic and prosthodontic domains. Typically composed of siloxane networks, developed sol-gel films have notoriously high substrate adherence and possess natural osteoconductive dissolution products^{135,136}. In pioneering studies, Ducheyne et al. utilized this feature of siloxane networks to develop vancomycin loaded xerogel coatings to effectively inhibit the colonization of *S. aureus* on a variety of titanium implant materials^{131,137-139}. Other sol-gel based coating networks have been loaded with silver compounds¹⁴⁰⁻¹⁴², quaternary ammonium compounds^{143,144}, and nitric oxide^{145,146} that have shown great robustness and effectiveness against clinically relevant pathogenic bacteria such as *E. coli*, *S. aureus*, *S. Epidermidis*, and *S. mutans*.

While dissolution-based coating strategies certainly illustrate great potential for hard tissue implants, there are still some significant limitations to their adoption in the clinic. These erodible coating systems, especially those made of biodegradable polymers, have similar concerns related to their longevity and robustness within host tissues. Similar to diffusion-based systems, the release of biocides from the coating materials diminishes with time leads to the possibility of developing of biocide-resistant pathogens¹²⁴. However, unlike diffusion-based systems the release kinetics associated with degradation in dissolution-based systems are often difficult to control, with some coatings only providing an initial burst release of biocides during the first few hours of contact with physiologic fluids^{89,124}.

Stimuli-Responsive Systems

Materials that respond to external stimuli have been investigated in the biomedical field for decades with applications as biomedical sensors, actuators, and coating materials¹²⁴. In the development of elution-based coatings, these systems can eliminate some of the major limitations to the designs of both diffusion and dissolution coating systems. Unlike the later systems which liberate and exhaust their imbedded biocides quickly and continuously, stimuli-

responsive eluting coatings release imbedded biocides only in response to specific stimuli. Stimuli-responsive antibacterial coatings can rely on either the triggered degradation or swelling of the coating matrix to achieve controlled elution of imbedded biocides. The elution of biocides in both cases can be triggered by both physiological and exogenous stimuli.

Most stimuli-responsive antibacterial coating systems rely on biological triggers from surrounding bacteria. Through their metabolic cycle, bacteria produce a range of acidic substances, such as lactic and acetic acid, which lead to a pH drop in their immediate environment¹⁴⁷. For this reason, several antibacterial coating systems that respond to changes in pH have been investigated. Using a nano-valve reservoir equipped with a pH responsive membrane, Wang et al. successfully achieved the release of cinnamaldehyde and ampicillin in the presence of pathogenic bacteria¹⁴⁸. These coating materials provided a trigger active defence against *S. aureus*, *E. coli*, and MRSA. In another study, Zhuk et al. combined cationic gentamicin, tobramycin and polymyxin B, with polyanionic tannic acid in the development of antibacterial polyelectrolyte multilayer films¹⁴⁹. These films, responsive to changes in pH, strongly inhibited the growth of *S. epidermidis* and *E. coli* on surfaces and in surrounding media while maintaining osteoblast adhesion and viability. The pH change in the presence of bacteria can also be used to liberate grafted biocides in coating materials. Using this strategy, gentamicin was grafted to a PEO nanoparticle coating using pH-sensitive imine bonds¹⁵⁰. Coated titanium materials showed selected release at lower pH ranges and inhibited the growth of *S. aureus*. While stimuli from bacteria are most often utilized to activate these systems, other biological triggers which result from infection can also be used. For example, in the case of wound infections, the on-site production of the enzyme thrombin increases dramatically¹⁵¹. Using this trigger, Tanihara et al. developed a coating material consisting of crosslinked PVA with a thrombin-degradable crosslinker¹⁵². This coating material effectively released gentamicin only in the presence of thrombin, which actively inhibited the growth of *S. aureus* and *P. aeruginosa* bacteria.

Similar to biological stimuli, use of externally applied exogenous stimuli can afford a high degree of control over the release of biocidal components from stimuli-responsive coatings. Unlike biologically responsive coatings, exogenous stimuli can be applied in a prophylactic fashion, that may protect implant surfaces in the early stages of the “race to the surface” before

measurable chemical changes occur. Responsive coating materials can be triggered to release biocides from electrical, ultrasonic, photothermal, magnetic, and mechanical triggers¹⁵³. For example, Esrafilzadeh et al. utilized an electropolymerized polypyrrole coating to allow the electrically controlled release of ciprofloxacin¹⁵⁴. Coated conductive fibers were non-cytotoxic and displayed significant inhibition of both *S. pyogenes* and *E. coli* growth under electrical stimulus. In another system, Norris et al. developed a poly(2-hydroxyethyl methacrylate) hydrogel coating with ordered methylene chains as an ultrasound-responsive coating for indwelling prostheses¹⁵⁵. This system was able to retain loaded ciprofloxacin in the absence of ultrasound, and, provide controlled-release in the presence of low-intensity ultrasound. Triggered-release doses from this developed coating system provided significant inhibition to the growth of *P. aeruginosa* on material surfaces. Using a magnetic field, Aw et al. presented a coating system that can be used to release active drug components from a titanium nanotube reservoir upon application of magnetic stimulation¹⁵⁶. In this work titanium implant materials equipped with titanium nanotubes were loaded with drug-encapsulated micelles and were released only under the presence of magnetic stimuli. While this work did not explicitly use the release of biocides or perform experiments with bacterial cultures, the encapsulation of antibiotics in such a system is promising in this area.

While stimuli-responsive antibacterial systems provide “on-demand” therapeutic effects, there exist some limitations to their adoption in the clinic. For starters, there is a high degree of skepticism about how sensitive these systems are to their triggered stimuli *in vivo*. Given the dynamic nature of the body, systems that may promote release of biocides to changes in pH may not be suitably sensitive. Local pH changes associated the early stages of infection can be quite small are difficult to predict *in vivo*. Such pH changes can depend on the presence of different species of bacteria, the bacteria state (planktonic or biofilm) and the size and location of the implant. For this reason, many systems relying on release from biological stimuli may provide an effect too late as infections have been shown to occur as early as early as six hours of post-operatively from small quantities of pathogenic bacteria¹¹⁴. For systems that rely on external stimuli to release biocides, their application may be limited as they require the pre-identification of infection before their application. For this reason, their applications may be inappropriate in conditions where there is a sudden onset of inflammation or viral attack. This strategy is also significantly limited by patient compliance and access to the clinic.

2.2.2 Osteoconductive Surfaces

In the founding study by Brånemark, osseointegration was described as the direct anchorage of an implant material by the formation of bony tissue around the implant¹⁵⁷. Since then, many alternative definitions have been proposed to better describe the details of this phenomenon. More recent definitions identify osseointegration as a foreign body response, one in which interfacial bone may be formed as a defence to shield surrounding tissues from implant materials¹⁵⁸. Nevertheless, this integration originally identified by Brånemark remains a fundamental factor in promoting the bony attachment and fixation of hard tissue implant materials. A wonderful review by Albrektsson and Johansson breaks down the two major factors influencing osseointegration: osteoinduction and osteoconduction¹⁵⁹.

Osteoinduction describes the stimulation or promotion of undifferentiated pluripotent cells to differentiate into those within the bone-forming or pre-osteoblast cell lineage¹⁵⁸. This process occurs naturally in bone fracture healing and implant incorporation. In a traditional healing process, sensitized surviving cells release local biochemical and biophysical cues that help promote the differentiation of pre-osteoblast cells¹⁶⁰. BMP, a soluble bone growth factor known to be naturally released in response to bone trauma or remodeling, has been identified as one of the only known naturally inductive agents. Although the recruitment of pre-osteoblast cells is typically unobservable for several weeks, the process of osteoinduction begins immediately following implantation, making it a fundamental factor in the “race to the surface”.

Osteoconduction describes the action of differentiated bone cells to promote bone tissue growth around foreign surfaces. This process includes the release of growth factors which serve as signaling agents for bone cells in the production of bony tissues. In many ways the process of osteoconduction depends on the process of osteoinduction. Unlike osteoinduction, osteoconduction is strongly dependent on the biomaterial used for implantation. For this reason, materials, topographical cues, and eluting agents are most frequently investigated to optimize osteoconduction since the injury at placement is often sufficient to recruit the differentiation of pluripotent cells.

While initial osseointegration may be achieved through the strong osteoinductive and osteoconductive cues, the long-term stability and retained osseointegration remains a relevant issue. For this reason, surface strategies concerning the promotion tissue ingrowth and long-term

stability of hard tissue implants (osteoconduction and osseointegration) have been of primary focus of researchers. Many of such strategies promote these factors using topographical cues or bioactive coatings to ensure long term fixation of implant materials and prevent aseptic loosening.

2.2.2.1 Topographical Strategies / Bioactive Topographies

Surface topographies are important factors that influence the bioactivity of all biomaterials. Indeed, the effect of surface micro- and nanostructures are well established to determine cellular behaviors such as adhesion, proliferation and differentiation¹⁶¹. For this reason, altered topographies can influence osteoinduction, osteoconduction and, accordingly, improve osseointegration. To improve the bioactivity and osseointegration of titanium implant materials a variety of surface topographies have been developed that mimic the cellular microenvironment. Such surface strategies can be further separated into micro- and nanostructure templating which impart their own spatiotemporal cues to cells *in vivo*.

Surfaces roughened in the micro-domain are used to promote osteoblast adhesion, differentiation and to provide an appropriate surface for the mineralization of extracellular matrices¹⁶². Through the addition of a micro-pattern to Ti6Al4V substrates, Lu et al. was able to show increased apatite induction *in vitro* and increased bone growth and proliferation *in vivo*¹⁶³. In another study, Liao et al. investigated the role of surface microtopography on bone cell differentiation¹⁶⁴. Using a micro-pyramid design, they observed an increased differentiation of rat calvaria osteoblasts compared to smooth surfaces *in vitro*. Similarly, surfaces with nano-topographies have been used to promote implant fixation. These structures are more similar natural physiological orientation of native bone and play an important role in bone cell adhesion and integration¹⁶⁵. Many of the nanostructures developed on titanium surfaces are titania nanotubes due to their ease of tunability using traditional anodizing techniques¹⁶⁶. Nune et al. used this strategy of anodizing Ti6Al4V to develop surface titania nanotubes with a pore size of ~80 nm¹⁶⁷. Their structures promoted the nucleation of apatite globules *in vitro* and improved the proliferation and adhesion of mouse pre-osteoblast cells in culture. In another study, Wang et al. developed titanium implants with 70 nm titania nanotubes¹⁶⁸. Following a five-week implantation period in a pig model, nanotextured implant surfaces displayed increased bone-implant contact and osseointegration compared to control titanium surfaces. Brammer et al.,

using a smaller titania nanotube size (30 nm), also demonstrated increased osteoblast adhesion compared to control titanium surfaces in culture¹⁶⁹.

In general, topographical manipulation provides relatively simple and stable enhancement to the bioactivity of hard tissue implant surfaces. Additionally, the technologies to develop such topographies (anodizing, plasma spraying, acid-etching) are scalable, making them feasible as commercial solutions¹⁶⁶. There are, however, major limitations to these strategies being used solely as implant surface materials. By developing surfaces that promote cell adhesion and proliferation, there is often an added increase to the adhesion and proliferation of microbes. Studies have shown that some nanotopographies, such as nanotubular and nanotextured titanium, while providing a favourable environment for osteoblasts, indeed increase the adhesion of microbes to implant surfaces^{170,171}. For this reason, the implementation of such topographies may provide more of a risk to the success of intraosseous implants despite their promotion of osteoinductive and osteoconductive cues. Accordingly, other studies have investigated the use of such topographies in conjunction with bioactive coating materials to provide a more “cell tailored” surface.

2.2.2.2 Bioactive Coatings

While topographical roughening typically provides a non-specific influence on adhesion and proliferation, the effect of bioactive coating materials is often more specific to influencing bony ingrowth. Due to the release of naturally osteoconductive ions from these materials (such as Ca, P, Si, and Mg), they have the ability to stimulate osseointegration without providing factors to influence the adhesion or proliferation of microbes¹⁷². A wide range of such bioactive materials have been investigated for use as orthopedic and dental implants coatings. These include traditional calcium phosphate or hydroxyapatite coatings, bioactive glass coatings, and newly emerging bioactive hybrid coatings.

Hydroxyapatite-based Coatings

Calcium phosphates, and more specifically, hydroxyapatite (HA) coatings were among the first to be proposed to replace traditional cemented fixation of prosthesis¹⁷³. HA-based materials were identified as promising biomaterials due to their similar chemical and crystalline structure to the inorganic phase of human bone. The emergence of HA coatings in the clinic was further spurred by their early display of significant improvements to the fixation and lifetime of metallic

implants¹⁷⁴. This has been identified to occur due the formation of a carbonated-HA layer on the surface of HA coated materials shortly after implantation *in vivo*. This structure results from the elution of calcium and phosphate ions from HA coating materials which induces the deposition of relevant physiological proteins and provides an appropriate scaffold for osteoblasts in the formation of new bony tissue¹⁷⁴. Research in HA-based implant coatings spans decades and has been the study of many clinical trials¹⁷⁵⁻¹⁷⁸. For this reason, to date, HA-based plasma sprayed coatings remain the only orthopedic implant coating material approved by the FDA¹⁷⁹.

Despite thorough investigations into these materials, their clinical success and predictability remains controversial. Indeed, the integration of these materials *in vivo* compared to bare or textured titanium surfaces have been proven to be marginal, or in some cases, less effective¹⁸⁰⁻¹⁸³. Such studies have helped to better elucidate the shortcomings of plasma sprayed HA-based coatings which include phase inconsistency, coverage and topographical concerns, and coating delamination.

During the high temperature plasma spraying application of HA coatings to metallic substrates, HA can undergo phase changes, which in general, affect the crystallinity of the coating material. Such secondary phases include tricalcium phosphate, calcium oxide (CaO), tetracalcium phosphate (TTCP) along with amorphous calcium phosphate (ACP)^{184,185}. Difficulties exist in consistently controlling these phases within the processing conditions of plasma spraying which can greatly affect the bioactivity (or lack thereof) of plasma sprayed HA-based coatings.

Additionally, plasma spraying is a line-of-site technique which limits its ability to accommodate the fine contours or geometric complexities of some implant materials. This can lead to inconsistent coating thickness and heating of implant materials, affecting not only the phase of the coating material but also that of the metallic substrate¹⁷⁹. Along with an inability to accommodate fine geometries, the coating application of HA-based materials are often quite thick and dense leading to the coatings inability to match the topography of pretreated surfaces. Such surfaces are unable to provide the relevant topographical cues attributed to substrate pre-treatments (previously discussed) to improve the growth and proliferation of osteoblasts.

Lastly, and perhaps most importantly, some studies have addressed the potential for HA-based coatings to undergo delamination *in vivo*^{174,186,187}. As previously discussed, the delamination of

coating materials leads to the production of debris and micromotion of prosthesis, which can ultimately result in aseptic loosening.

Other coating methods that utilize sol-gel liquid techniques have been developed to aid in the control of HA coating properties¹⁸⁸. Despite their low temperature application, such coatings need to be cured at high temperatures to produce crystalline HA^{189,190}. Through this calcination process secondary phases of HA are developed, which leads to inconsistent dissolution properties and, due to differences between the thermal expansion coefficients of the coating and substrate, often cracking.

Although plasma sprayed HA-based coatings are the current standard and only FDA approved orthopedic and dental implant coating materials, there is a need for alternative materials that overcome their shortcomings. While the proposed bioactive conduction method through the release of osteoconductive ions remains a viable bioactive model, the lack of consistency in their material properties limit the application of these coatings in the clinic. Therefore, further studies have investigated coating materials with improved material properties while possessing similar osteoconductive strategies.

Bioactive Glass Coatings

Bioactive glasses consist of a variety of glass-ceramic materials (typically silicate based) that promote the bonding and mineralization of bone tissue. The first bioactive glass named “Bioglass” was invented by Larry Hench in 1969 and consisted of 46.1 mol.% SiO₂, 24.4 mol.% Na₂O, 26.9 mol.% CaO and 2.6 mol.% P₂O₅. The original Hench Bioglass has since been used in over a million patients in the repair of bone defects during oral and orthopedic surgeries^{191,192}. Such glasses can be synthesized using a traditional melt-quench methods or sol-gel techniques. Sol-gel derived bioactive glasses display higher surface areas, rates of bioactive ion release, HA formation and crystallinity compared to melt-derived glasses, and have thus been more frequently studied¹⁹³. Almost all synthesized bioactive glass materials contain Si and Ca species as these ions in specific concentrations are known to elicit positive bioactive responses such as the promotion of new bone tissue growth¹⁹¹. An excellent review by Jones delves in great detail into various bioactive glass compositions and their uses as bone-growth grafting materials¹⁹². As Jones highlights in his review, despite their ability to promote rapid bone growth, these materials pose some complications for applications as implant coatings.

Most feasible bioactive glass coatings are synthesized using the sol-gel technique. Sol-gel systems, briefly touched on in Chapter 2.2.1.2.2, are prepared through the hydrolysis and condensation of liquid ceramic precursors. Since sol-gel materials typically have higher surface areas and porosities compared to traditional melt-quench glasses, they often better promote cell adhesion and tissue ingrowth as coatings¹⁹⁴. Using a sol-gel synthesis, Köseoglu et al. developed a HA and bioactive glass dual coating for use on metallic implants¹⁹⁵. Their HA/bioactive glass coating material displayed significantly more apatite deposition during *in vitro* testing than HA coating materials. In another study, Hamadouche et al. used a sol-gel derived Bioglass formulation to coat alumina implants¹⁹⁶. These coatings increased the deposition of HA on implant surfaces *in vitro* and eliminated aluminum leaching compared to uncoated controls. Both of these coatings, however required the use of high curing temperatures (>600°C) to enable the inclusion of calcium into the coating network. This led to significant cracking and fissures of the inorganic coating materials, leaving in question their robustness and longevity of these coatings *in vivo*.

When form is of no concern, such in the case of powder development, processing bioactive glasses at high temperatures remains ideal from a processing perspective. For materials that assume the form of a mold or template, as in the case with scaffolds and coatings, developed materials are often too brittle to provide adequate support, or, crack and delaminate upon curing on metallic substrates. For implant coatings, this leads to many of the same issues associated with the sol-gel processing of HA-based materials, also prone to material separation and significant coating cracking. The reason for such cracking can be attributed to the large shrinkage that occurs during drying and the evaporation of the liquid by-products of the sol-gel synthesis¹⁹². Unlike HA-processing where crystallinity is the main objective, high temperatures for bioactive glass processing are used to ensure that all liquid components are included into the coating network. For example, it is common for bioactive glasses to include Ca into the coating network using sols containing CaNO₃ or CaCl₂¹⁹⁷. For Ca to be included into the cured network and to remove the potentially toxic salt by-products, these materials must be annealed at >400°C. This process is not always ideal, and often, due to the salts solubility in the pore liquor of the sol, can lead to an inhomogeneous surfaces distribution of elements¹⁹⁸.

Hybrid Material Coatings

To improve upon the mechanical properties and processability of bioactive glasses for use as coatings, several composite and hybrid systems have been developed to combine organic polymers with sol-gel ceramic materials. Through the simple blending of these organic and inorganic networks, sol-gel composite materials can be developed. This method, however, usually leads to inhomogeneous materials with mismatching degradation rates, which can cause instability and premature deterioration of composite materials^{192,199}. Alternatively, hybrid material systems, possessing nanoscale molecular interactions between the organic and inorganic phases, have shown significant improvements in stability over their composite counterparts. These hybrid materials are further characterized based on the molecular interactions between their organic and inorganic components. When weak molecular interactions (such as hydrogen and van der Waals bonding) are present between organic and inorganic components they are designated as class I hybrids. In the case where strong covalent interactions are present between both organic and inorganic components materials are deemed as class II hybrids. Highlighted below are examples of promising class I and class II hybrid materials for use as implant coatings as well as a discussion on integration of calcium.

Using class I hybrid materials, a variety of researchers have been able to improve the bioactivity of implant surfaces. For example, Catauro et al. has investigated the use of poly (ϵ -caprolactone) (PCL) and polyethylene glycol (PEG) to develop class I siloxane hybrid coatings²⁰⁰⁻²⁰². These coatings, when applied to Ti substrates, displayed superior bioactivity by promoting the vitality of mouse embryonic fibroblast cells compared to bare Ti substrates while displaying crack-free coatings with good adhesion properties. Other studies have investigated using natural polymers such as chitosan and gelatin as the organic components in their class I hybrids. Pebdeni et al. developed a nanofiber coating for use on orthopedic implants that consisted of chitosan, PEO, and silica²⁰³. Chitosan, in this study, acted to improve the flexibility of the developed nanofibers and increase the attachment and growth of fibroblasts. In another study, Jun et al. used chitosan to improve the material properties of a bioactive sol-gel coating composed of tetramethylorthosilane (TMOS), CaCl_2 and triethyl phosphate²⁰⁴. Hybrid coating materials were crack-free compared to their inorganic counterparts and displayed appropriate levels of cell attachment, bone forming ability, and mineralization.

Compared to the simple entanglement of organic and inorganic chains, class II hybrids act as single-phase materials exhibiting improved mechanical properties and material homogeneity compared to class I hybrids. This is particularly the case with dissolution characteristics of hybrid materials. Due to the lack of covalent coupling present between the two phases in class I hybrids, organic components can often be lost more rapidly than inorganic components in dissolution studies. This emphasizes the fact that class II hybrids may be more suitable for implant coatings where material properties, including degradation and dissolution rates, are often congruent throughout the material.

Class II hybrid materials has become an increasingly popular research area in the development of hard tissue implant coatings. Studies have investigated the use of a variety of organic, coupling, and inorganic agents in the development of these coatings. Many relevant studies have investigated class II systems consisting of chitosan as an organic component, coupled to inorganic siloxane networks using 3-glycydoxytrimethoxysilane (GPTMS). For example, Palla-Rubio et al. used such a system as a coating for Ti implant materials that facilitated the release of osteoconductive Si which promoted the proliferation of human fibroblasts in culture²⁰⁵. In other studies, Shirotsaki et al. showed how these coating materials could also promote the adhesion and proliferation of an osteoblastic cell line (MG63) compared to relevant controls and remain stable for up to 6 months in enzymatic solutions^{206,207}. Other materials have been developed using similar systems but with varying organic networks components such as gelatin, poly(γ -glutamic acid), and PEG²⁰⁸⁻²¹⁰.

These materials, owed to their low temperature processing, have also been able to manifest antimicrobial properties. For example, the coating materials involving chitosan above were able to provide a degree of antimicrobial efficacy against relevant pathogenic bacteria while providing a crack-free surface^{204,205}. Other examples include the work of Pebdeni et al. and Hernández-Escolano et al. where they used the low temperature synthesis of the hybrid coating materials to enable the loading of temperature-sensitive antimicrobial agents cefepime and procaine, respectively^{203,211}. These materials provided a significant antimicrobial effect along with displayed signs of bioactivity. The multifunctional nature of these materials has become particularly attractive to researchers as coatings that can promote osseointegration whilst

mitigating microbial proliferation can effectively eliminate both major failure modes effecting implantology today.

Most of the above-mentioned class II hybrid materials, and those reported in literature, consist of a polymer-siloxane system. The synthesis and integration of calcium into such materials remains challenging due to their low temperature synthesis and curing temperatures¹⁹². For this reason, more recently, calcium alkoxides have been investigated as precursors to incorporate calcium into the inorganic portion of sol-gel hybrid materials. These precursors participate in the same network forming hydrolysis and condensation reactions as traditional silica precursors, allowing their simple integration into these networks at room temperature

Accordingly, more advanced methods in the development of multifunctional hybrid coatings have utilized calcium alkoxides to allow low temperature Ca integration into sol-gel networks. For example, Li et al. developed PEG/SiO₂-CaO class II hybrid coating materials using calcium methoxyethoxide (CME)²¹². Hybrid materials developed in this study possessed a degradation-controlled release of calcium and promoted apatite deposition on all material monoliths. Coating materials were able to be cured at low temperatures and displayed enhanced apatite deposition while exhibiting good cell viability and proliferation. In another study, Poologasundarampillai et al. developed Poly(γ -glutamic acid)/SiO₂-CaO hybrids using the same CME precursor²¹³. Most of the calcium alkoxides used to date, however, have had a high sensitivity towards hydrolysis and condensation reactions in the presence of water. This instability in aqueous systems often leads to premature gelation of the inorganic network leading to poor and inhomogeneous integration of calcium into hybrid materials. Additionally, many of these calcium alkoxides, if not hydrolyzed completely, can leach toxic by-products *in vivo* (such as methanol for calcium methoxide and calcium methoxyethoxide).

Therefore, while bioactive class II hybrid materials present desirable characteristics, there is a need to improve their properties for use as hard tissue implant coatings. In an effort to better assess their potential to be clinically translatable, more rigorous delamination initiatives should be pursued to assess the adhesive properties of these coatings. Additionally, due to their low temperature synthesis, antimicrobial agents should be opportunistically added to material coatings to provide implant materials with an effective resistance against pathogenic bacteria. And lastly, there is a need to investigate new calcium alkoxide precursors that possesses less

toxic degradation products and increased resistance to water to enable the inclusion of calcium into coating networks at low temperatures. The above points will be the focus of the work presented in this thesis.

2.3 Rationale of the Study

Titanium implant materials, while ideal from a biomechanical standpoint, are plagued clinically by two major complications: IAI and aseptic loosening. While these issues seem distinct given their nomenclature, their interrelation and the “race to the surface” between native cells and pathogens is often attributed to the success or failure of implants in both domains⁴³. Various antimicrobial coating strategies have been developed to target a range of pathogenic bacteria which each afford their own advantages and disadvantages. Osteoconduction on the other hand, has been well established to be promoted by topographical stimuli and the dissolution of relevant inorganic ceramic materials. Both coating strategies, in addition to their relevant cues, need to be resistant fracture and delamination to be feasibly implemented in the clinic.

Therefore, the purpose of this study is to develop multifunctional coating materials that can:

1. Manifest antimicrobial properties that can be applied in a complementary manner (contact and release based)
2. Provide inherently osteoconductive/bioactive physiological cues
 - a. Through the use of hybrid bioactive glass networks
 - b. Using a new calcium alkoxide precursor
3. Possess a degree of mechanical robustness to promote clinical translatability

With this in mind, this study describes the synthesis of robust class II hybrid multifunctional coatings to improve success of titanium implant materials.

2.4 References

- (1) Migonney, V. History of Biomaterials. *Biomaterials* **2014**, 1–10.
- (2) Mantripragada, V. P.; Lecka-Czernik, B.; Ebraheim, N. A.; Jayasuriya, A. C. An Overview of Recent Advances in Designing Orthopedic and Craniofacial Implants. *J. Biomed. Mater. Res. Part A* **2012**, 176 (1), NA-NA.
- (3) Buechel, F. F.; Pappas, M. J. Properties of Materials Used in Orthopaedic Implant Systems. In *Principles of Human Joint Replacement*; Springer Berlin Heidelberg: Berlin, Heidelberg, 2011; Vol. 53, pp 1–35.
- (4) Mirza, S. B.; Dunlop, D. G.; Panesar, S. S.; Naqvi, S. G.; Gangoo, S.; Salih, S. Basic

- Science Considerations in Primary Total Hip Replacement Arthroplasty. *Open Orthop. J.* **2010**, *4* (1), 169–180.
- (5) Slone, R. M.; Heare, M. M.; Vander Griend, R. A.; Montgomery, W. J. Orthopedic Fixation Devices. *Radiographics* **1991**, *11* (5), 823–847.
 - (6) Rony, L.; Lancigu, R.; Hubert, L. Intraosseous Metal Implants in Orthopedics: A Review. *Morphologie* **2018**, *102* (339), 231–242.
 - (7) Jenny, G.; Jauernik, J.; Bierbaum, S.; Bigler, M.; Grätz, K. W.; Rücker, M.; Stadlinger, B. A Systematic Review and Meta-Analysis on the Influence of Biological Implant Surface Coatings on Periimplant Bone Formation. *J. Biomed. Mater. Res. - Part A* **2016**, *104* (11), 2898–2910.
 - (8) Hong, D. G. K.; Oh, J. Recent Advances in Dental Implants. *Maxillofac. Plast. Reconstr. Surg.* **2017**, *39* (1).
 - (9) Francisco, S. Surgical Guide for Dental Implant and Methods Therefor. US7905726B2, 2007.
 - (10) Becker, C. M.; Kaiser, D. A. Surgical Guide for Dental Implant Placement. *J. Prosthet. Dent.* **2000**, *83* (2), 248–251.
 - (11) Tacir, I. H.; Dirihan, R. S.; Polat, Z. S.; Salman, G. Ö.; Vallittu, P.; Lassila, L.; Ayna, E. Comparison of Load-Bearing Capacities of 3-Unit Fiber-Reinforced Composite Adhesive Bridges with Different Framework Designs. *Med. Sci. Monit.* **2018**, *24*, 4440–4448.
 - (12) Wang, B.; Sen, H. K.; Khin, N. T.; Cheng, A. C. Mini-Dental Implants for Definitive Prosthesis Retention — A Synopsis of the Current Evidence. *Singapore Dent. J.* **2019**, *39*, 1–9.
 - (13) Pye, A. D.; Lockhart, D. E. A.; Dawson, M. P.; Murray, C. A.; Smith, A. J. A Review of Dental Implants and Infection. *J. Hosp. Infect.* **2009**, *72* (2), 104–110.
 - (14) Dental Implants http://www.1888implant.com/mobile/dental_implants.html (accessed Apr 2, 2020).
 - (15) Park, J. B.; Bronzino, J. D. *Biomaterials - Principles and Applications*; 2003.
 - (16) Eliaz, N. Corrosion of Metallic Biomaterials: A Review. *Materials (Basel)*. **2019**, *12* (3).
 - (17) Nielsen, K. Corrosion of Metallic Implants. *Br. Corros. J.* **1987**, *22* (4), 272–278.
 - (18) BUNDY, K. Biomaterials and the Chemical Environment of the Body. In *Joint Replacement Technology*; Elsevier, 2008; pp 56–80.
 - (19) Okazaki, Y.; Gotoh, E. Comparison of Metal Release from Various Metallic Biomaterials in Vitro. *Biomaterials* **2005**, *26* (1), 11–21.
 - (20) Chen, Q.; Thouas, G. A. Metallic Implant Biomaterials. *Mater. Sci. Eng. R Reports* **2015**, *87*, 1–57.
 - (21) Sing, S. L.; Tey, C. F.; Tan, J. H. K.; Huang, S.; Yeong, W. Y. 3D Printing of Metals in Rapid Prototyping of Biomaterials: Techniques in Additive Manufacturing. In *Rapid*

Prototyping of Biomaterials; Elsevier, 2020; pp 17–40.

- (22) Brown, S. A.; Lemons, J. E. Medical Applications of Titanium and Its Alloys: The Material and Biological Issues. *Med. Appl. Titan. Its Alloy. Mater. Biol. Issues* **1996**.
- (23) Li, P. Y.; Liu, H. W.; Chen, T. H.; Chang, C. H.; Lu, Y. S.; Liu, D. S. Characterization of an Amorphous Titanium Oxide Film Deposited onto a Nano-Textured Fluorination Surface. *Materials (Basel)*. **2016**, *9* (6).
- (24) Geetha, M.; Singh, A. K.; Asokamani, R.; Gogia, A. K. Ti Based Biomaterials, the Ultimate Choice for Orthopaedic Implants - A Review. *Prog. Mater. Sci.* **2009**, *54* (3), 397–425.
- (25) Yamako, G.; Janssen, D.; Hanada, S.; Anijs, T.; Ochiai, K.; Totoribe, K.; Chosa, E.; Verdonschot, N. Improving Stress Shielding Following Total Hip Arthroplasty by Using a Femoral Stem Made of β Type Ti-33.6Nb-4Sn with a Young's Modulus Gradation. *J. Biomech.* **2017**, *63*, 135–143.
- (26) Oldani, C.; Dominguez, A. Titanium as a Biomaterial for Implants. *Recent Adv. Arthroplast.* **2012**.
- (27) Niinomi, M.; Liu, Y.; Nakai, M.; Liu, H.; Li, H. Biomedical Titanium Alloys with Young's Moduli Close to That of Cortical Bone. *Regen. Biomater.* **2016**, *3* (3), 173–185.
- (28) GRANT, P.; AAMODT, A.; FALCH, J.; NORDSLETTEN, L. Differences in Stability and Bone Remodeling between a Customized Uncemented Hydroxyapatite Coated and a Standard Cemented Femoral Stem A Randomized Study with Use of Radiostereometry and Bone Densitometry. *J. Orthop. Res.* **2005**, *23* (6), 1280–1285.
- (29) Karachalios, T.; Tsatsaronis, C.; Efraimis, G.; Papadelis, P.; Lyritis, G.; Diakoumopoulos, G. The Long-Term Clinical Relevance of Calcar Atrophy Caused by Stress Shielding in Total Hip Arthroplasty. *J. Arthroplasty* **2004**, *19* (4), 469–475.
- (30) KÄRRHOLM, J.; ANDERBERG, C.; SNORRASON, F.; THANNER, J.; LANGELAND, N.; MALCHAU, H.; HERBERTS, P. EVALUATION OF A FEMORAL STEM WITH REDUCED STIFFNESS. *J. Bone Jt. Surgery-American Vol.* **2002**, *84* (9), 1651–1658.
- (31) US FDA. Biological Responses to Metal Implants. *Food Drug Administration* **2019**, No. September.
- (32) Lee, M. H.; Park, I. S.; Min, K. S.; Ahn, S. G.; Park, J. M.; Song, K. Y.; Park, C. W. Evaluation of in Vitro and in Vivo Tests for Surface-Modified Titanium by H₂SO₄ and H₂O₂ Treatment. *Met. Mater. Int.* **2007**, *13* (2), 109–115.
- (33) Plecko, M.; Sievert, C.; Andermatt, D.; Frigg, R.; Kronen, P.; Klein, K.; Stübinger, S.; Nuss, K.; Bürki, A.; Ferguson, S.; et al. Osseointegration and Biocompatibility of Different Metal Implants - A Comparative Experimental Investigation in Sheep. *BMC Musculoskelet. Disord.* **2012**, *13*, 1–12.
- (34) Escobar, A.; Muzzio, N.; Coy, E.; Liu, H.; Bindini, E.; Andreozzi, P.; Wang, G.; Angelomé, P.; Delcea, M.; Grzelczak, M.; et al. Antibacterial Mesoporous Titania Films with Embedded Gentamicin and Surface Modified with Bone Morphogenetic Protein 2 to

- Promote Osseointegration in Bone Implants. *Adv. Mater. Interfaces* **2019**, 6 (9), 1–12.
- (35) Radin, S.; Ducheyne, P. Controlled Release of Vancomycin from Thin Sol-Gel Films on Titanium Alloy Fracture Plate Material. *Biomaterials* **2007**, 28 (9), 1721–1729.
- (36) Macák, J. M.; Tsuchiya, H.; Schmuki, P. High-Aspect-Ratio TiO₂ Nanotubes by Anodization of Titanium. *Angew. Chemie Int. Ed.* **2005**, 44 (14), 2100–2102.
- (37) Trampuz, A.; Zimmerli, W. Diagnosis and Treatment of Infections Associated with Fracture-Fixation Devices. *Injury* **2006**, 37 (2 SUPPL.), 59–66.
- (38) Steinmetz, S.; Wernly, D.; Moerenhout, K.; Trampuz, A.; Borens, O. Infection after Fracture Fixation. *EFORT Open Rev.* **2019**, 4 (7), 468–475.
- (39) Cooper, L. B. and I. R. *Biomaterials and Medical Device - Associated Infections*; Woodhead Publishing, 2014; Vol. 1.
- (40) Ribeiro, M.; Monteiro, F. J.; Ferraz, M. P. Infection of Orthopedic Implants with Emphasis on Bacterial Adhesion Process and Techniques Used in Studying Bacterial-Material Interactions. *Biomatter* **2012**, 2 (4), 176–194.
- (41) Encyclopedia. *Biofilm Infections*; Bjarnsholt, T., Jensen, P. Ø., Moser, C., Høiby, N., Eds.; Springer New York: New York, NY, 2011; Vol. 53.
- (42) Cogen, A. L.; Nizet, V.; Gallo, R. L. Skin Microbiota: A Source of Disease or Defence? *Br. J. Dermatol.* **2008**, 158 (3), 442–455.
- (43) Gristina, A. Biomaterial-Centered Infection: Microbial Adhesion versus Tissue Integration. *Science (80-.)*. **1987**, 237 (4822), 1588–1595.
- (44) Mah, T. F.; Pitts, B.; Pellock, B.; Walker, G. C.; Stewart, P. S.; O’Toole, G. A. A Genetic Basis for *Pseudomonas Aeruginosa* Biofilm Antibiotic Resistance. *Nature* **2003**, 426 (6964), 306–310.
- (45) Chourifa, H.; Bouloussa, H.; Migonney, V.; Falentin-daudré, C. Review of Titanium Surface Modification Techniques and Coatings for Antibacterial Applications. *Acta Biomater.* **2018**.
- (46) Price, J. S.; Tencer, A. F.; Arm, D. M.; Bohach, G. A. Controlled Release of Antibiotics from Coated Orthopedic Implants. *J. Biomed. Mater. Res.* **1996**, 30 (3), 281–286.
- (47) Ruszczak, Z. Collagen as a Carrier for On-Site Delivery of Antibacterial Drugs. *Adv. Drug Deliv. Rev.* **2003**, 55 (12), 1679–1698.
- (48) Costerton, J. W.; Montanaro, L.; Arciola, C. R. Biofilm in Implant Infections: Its Production and Regulation. *Int. J. Artif. Organs* **2005**, 28 (11), 1062–1068.
- (49) Chung, P. Y.; Toh, Y. S. Anti-Biofilm Agents: Recent Breakthrough against Multi-Drug Resistant *Staphylococcus Aureus*. *Pathog. Dis.* **2014**, 70 (3), 231–239.
- (50) Lee, Y. S.; Chen, A. F. Two-Stage Reimplantation in Infected Total Knee Arthroplasty. *Knee Surg. Relat. Res.* **2018**, 30 (2), 107–114.
- (51) Charette, R. S.; Melnic, C. M. Two-Stage Revision Arthroplasty for the Treatment of

- Prosthetic Joint Infection. *Curr. Rev. Musculoskelet. Med.* **2018**, *11* (3), 332–340.
- (52) Akgün, D.; Müller, M.; Perka, C.; Winkler, T. High Cure Rate of Periprosthetic Hip Joint Infection with Multidisciplinary Team Approach Using Standardized Two-Stage Exchange. *J. Orthop. Surg. Res.* **2019**, *14* (1), 1–8.
- (53) Kheir, M. M.; Tan, T. L.; Gomez, M. M.; Chen, A. F.; Parvizi, J. Patients With Failed Prior Two-Stage Exchange Have Poor Outcomes After Further Surgical Intervention. *J. Arthroplasty* **2017**, *32* (4), 1262–1265.
- (54) Tan, T. L.; Gomez, M. M.; Manrique, J.; Parvizi, J.; Chen, A. F. Positive Culture During Reimplantation Increases the Risk of Subsequent Failure in Two-Stage Exchange Arthroplasty. *J. Bone Jt. Surg.* **2016**, *98* (15), 1313–1319.
- (55) Renvert, S.; Persson, G. R.; Pirih, F. Q.; Camargo, P. M. Peri-Implant Health, Peri-Implant Mucositis, and Peri-Implantitis: Case Definitions and Diagnostic Considerations. *J. Clin. Periodontol.* **2018**, *45* (January), S278–S285.
- (56) Algraffee, H.; Borumandi, F.; Cascarini, L. Peri-Implantitis. *Br. J. Oral Maxillofac. Surg.* **2012**, *50* (8), 689–694.
- (57) Smeets, R.; Henningsen, A.; Jung, O.; Heiland, M.; Hammächer, C.; Stein, J. M. Definition, Etiology, Prevention and Treatment of Peri-Implantitis - a Review. *Head Face Med.* **2014**, *10* (1), 1–13.
- (58) Claffey, N.; Clarke, E.; Polyzois, I.; Renvert, S. Surgical Treatment of Peri-Implantitis. *J. Clin. Periodontol.* **2008**, *35*, 316–332.
- (59) Prathapachandran, J.; Suresh, N. Management of Peri-Implantitis. *Dent. Res. J. (Isfahan)*. **2012**, *9* (5), 516.
- (60) Renvert, S.; Roos-Jansåker, A.-M.; Claffey, N. Non-Surgical Treatment of Peri-Implant Mucositis and Peri-Implantitis: A Literature Review. *J. Clin. Periodontol.* **2008**, *35*, 305–315.
- (61) Jepsen, S.; Berglundh, T.; Genco, R.; Aass, A. M.; Demirel, K.; Derks, J.; Figuero, E.; Giovannoli, J. L.; Goldstein, M.; Lambert, F.; et al. Primary Prevention of Peri-Implantitis: Managing Peri-Implant Mucositis. *J. Clin. Periodontol.* **2015**, *42* (S16), S152–S157.
- (62) Kripal, K.; Chandrasekaran, K. Supportive Periodontal Therapy for Dental Implant Patients. In *Periodontology and Dental Implantology*; IntechOpen, 2019.
- (63) Abu-Ta'a, M.; Quirynen, M.; Teughels, W.; Van Steenberghe, D. Asepsis during Periodontal Surgery Involving Oral Implants and the Usefulness of Peri-Operative Antibiotics: A Prospective, Randomized, Controlled Clinical Trial. *J. Clin. Periodontol.* **2008**, *35* (1), 58–63.
- (64) Heitz-Mayfield, L. J. A.; Salvi, G. E.; Mombelli, A.; Loup, P. J.; Heitz, F.; Kruger, E.; Lang, N. P. Supportive Peri-Implant Therapy Following Anti-Infective Surgical Peri-Implantitis Treatment: 5-Year Survival and Success. *Clin. Oral Implants Res.* **2018**, *29* (1), 1–6.

- (65) Froum, S. J.; Froum, S. H.; Rosen, P. S. Successful Management of Peri-Implantitis with a Regenerative Approach: A Consecutive Series of 51 Treated Implants with 3- to 7.5-Year Follow-Up. *Int. J. Periodontics Restorative Dent.* **2012**, *32* (1), 11–20.
- (66) Trampuz, A.; Widmer, A. F. Infections Associated with Orthopedic Implants. *Curr. Opin. Infect. Dis.* **2006**, *19* (4), 349–356.
- (67) Hedrick, T. L.; Adams, J. D.; Sawyer, R. G. Implant-Associated Infections: An Overview. *J. Long. Term. Eff. Med. Implants* **2006**, *16* (1), 83–99.
- (68) Wooley, P. H.; Schwarz, E. M. Aseptic Loosening. *Gene Ther.* **2004**, *11* (4), 402–407.
- (69) Ulrich, S. D.; Seyler, T. M.; Bennett, D.; Delanois, R. E.; Saleh, K. J.; Thongtrangan, I.; Kuskowski, M.; Cheng, E. Y.; Sharkey, P. F.; Parvizi, J.; et al. Total Hip Arthroplasties: What Are the Reasons for Revision? *Int. Orthop.* **2008**, *32* (5), 597–604.
- (70) Maguire, J. K.; Coscia, M. F.; Lynch, M. H. Foreign Body Reaction to Polymeric Debris Following Total Hip Arthroplasty. *Clin. Orthop. Relat. Res.* **1987**, No. 216, 213–223.
- (71) Leta, T. H.; Lygre, S. H. L.; Skredderstuen, A.; Hallan, G.; Furnes, O. Failure of Aseptic Revision Total Knee Arthroplasties: 145 Revision Failures from the Norwegian Arthroplasty Register, 1994–2011. *Acta Orthop.* **2015**, *86* (1), 48–57.
- (72) Levin, L. Dealing with Dental Implant Failures. *J. Appl. Oral Sci.* **2008**, *16* (3), 171–175.
- (73) Geraets, W.; Zhang, L.; Liu, Y.; Wismeijer, D. Annual Bone Loss and Success Rates of Dental Implants Based on Radiographic Measurements. *Dentomaxillofacial Radiol.* **2014**, *43* (7), 3–5.
- (74) Duan, X. B.; Wu, T. X.; Guo, Y. C.; Zhou, X. D.; Lei, Y. L.; Xu, X.; Mo, A. C.; Wang, Y. Y.; Yuan, Q. Marginal Bone Loss around Non-Submerged Implants Is Associated with Salivary Microbiome during Bone Healing. *Int. J. Oral Sci.* **2017**, *9* (2), 95–103.
- (75) Alsaadi, Ghada; Quirynen, Marc; van Steenberghe, D. The Importance of Implant Surface Characteristics in the Replacement of Failed Implants. *Int. J. Oral Maxillofac. Implants* **2006**, *21* (2), 270–274.
- (76) Grossmann, Y.; Levin, L. Success and Survival of Single Dental Implants Placed in Sites of Previously Failed Implants. *J. Periodontol.* **2007**, *78* (9), 1670–1674.
- (77) Zhang, Z.; Wagner, V. E. *Antimicrobial Coatings and Modifications on Medical Devices*; 2017.
- (78) Harding, J. L.; Reynolds, M. M. Combating Medical Device Fouling. *Trends Biotechnol.* **2014**, *32* (3), 140–146.
- (79) Francolini, I.; Vuotto, C.; Piozzi, A.; Donelli, G. Antifouling and Antimicrobial Biomaterials: An Overview. *Apmis* **2017**, *125* (4), 392–417.
- (80) Leszczynski, R.; Gumula, T.; Stodolak-Zych, E.; Pawlicki, K.; Wieczorek, J.; Kajor, M.; Blazewicz, S. Histopathological Evaluation of a Hydrophobic Terpolymer (PTFE-PVD-PP) as an Implant Material for Nonpenetrating Very Deep Sclerectomy. *Investig. Ophthalmol. Vis. Sci.* **2015**, *56* (9), 5203–5209.

- (81) Wenzel, R. N. Resistance of Solid Surfaces to Wetting by Water. *Ind. Eng. Chem.* **1936**, 28 (8), 988–994.
- (82) Tang, P.; Zhang, W.; Wang, Y.; Zhang, B.; Wang, H.; Lin, C.; Zhang, L. Effect of Superhydrophobic Surface of Titanium on Staphylococcus Aureus Adhesion. *J. Nanomater.* **2011**, 2011, 1–8.
- (83) Privett, B. J.; Youn, J.; Hong, S. A.; Lee, J.; Han, J.; Shin, J. H.; Schoenfisch, M. H. Antibacterial Fluorinated Silica Colloid Superhydrophobic Surfaces. *Langmuir* **2011**, 27 (15), 9597–9601.
- (84) Kazmierska, K.; Szwast, M.; Ciach, T. Determination of Urethral Catheter Surface Lubricity. *J. Mater. Sci. Mater. Med.* **2008**, 19 (6), 2301–2306.
- (85) Connor, O. CATHETER HAVING HYDROPHOBIC PROPERTIES. **1996**, No. 19.
- (86) Lakes, F.; Finkel, S. Expandable Catheter Having Hydrophobic Surface. **1992**.
- (87) Pace, J. L.; Rupp, M. E.; Finch, R. G. *Biofilms, Infection, and Antimicrobial Therapy*; CRC Press, 2005.
- (88) Campoccia, D.; Montanaro, L.; Arciola, C. R. A Review of the Biomaterials Technologies for Infection-Resistant Surfaces. *Biomaterials* **2013**, 34 (34), 8533–8554.
- (89) Gallo, J.; Holinka, M.; Moucha, C. S. *Antibacterial Surface Treatment for Orthopaedic Implants*; 2014; Vol. 15.
- (90) Neoh, K. G.; Hu, X.; Zheng, D.; Kang, E. T. Balancing Osteoblast Functions and Bacterial Adhesion on Functionalized Titanium Surfaces. *Biomaterials* **2012**, 33 (10), 2813–2822.
- (91) An, Y. H.; Bradley, J.; Powers, D. L.; Friedman, R. J. The Prevention of Prosthetic Infection Using a Cross-Linked Albumin Coating in a Rabbit Model. *J. Bone Jt. Surg. - Ser. B* **1997**, 79 (5), 816–819.
- (92) Harris, L. G.; Tosatti, S.; Wieland, M.; Textor, M.; Richards, R. G. Staphylococcus Aureus Adhesion to Titanium Oxide Surfaces Coated with Non-Functionalized and Peptide-Functionalized Poly(l-Lysine)-Grafted-Poly(Ethylene Glycol) Copolymers. *Biomaterials* **2004**, 25 (18), 4135–4148.
- (93) Shi, Z.; Neoh, K. G.; Kang, E.-T.; Poh, C.; Wang, W. Titanium with Surface-Grafted Dextran and Immobilized Bone Morphogenetic Protein-2 for Inhibition of Bacterial Adhesion and Enhancement of Osteoblast Functions. *Tissue Eng. Part A* **2009**, 15 (2), 417–426.
- (94) Civantos, A.; Martínez-Campos, E.; Ramos, V.; Elvira, C.; Gallardo, A.; Abarrategi, A. Titanium Coatings and Surface Modifications: Toward Clinically Useful Bioactive Implants. *ACS Biomater. Sci. Eng.* **2017**, 3 (7), 1245–1261.
- (95) Cramer, C. E. *Über Oligodynamische Erscheinungen in Lebenden Zellen von C. von Nägeli*; 1893.
- (96) Mathews, S.; Hans, M.; Mücklich, F.; Solioz, M. Contact Killing of Bacteria on Copper Is Suppressed If Bacterial-Metal Contact Is Prevented and Is Induced on Iron by Copper

- Ions. *Appl. Environ. Microbiol.* **2013**, *79* (8), 2605–2611.
- (97) Gunawan, P.; Guan, C.; Song, X.; Zhang, Q.; Leong, S. S. J.; Tang, C.; Chen, Y.; Chan-Park, M. B.; Chang, M. W.; Wang, K.; et al. Hollow Fiber Membrane Decorated with Ag/MWNTs: Toward Effective Water Disinfection and Biofouling Control. *ACS Nano* **2011**, *5* (12), 10033–10040.
- (98) Zeiger, M.; Solioz, M.; Edongué, H.; Arzt, E.; Schneider, A. S. Surface Structure Influences Contact Killing of Bacteria by Copper. *Microbiologyopen* **2014**, *3* (3), 327–332.
- (99) Mauter, M. S.; Wang, Y.; Okemgbo, K. C.; Osuji, C. O.; Giannelis, E. P.; Elimelech, M. Antifouling Ultrafiltration Membranes via Post-Fabrication Grafting of Biocidal Nanomaterials. *ACS Appl. Mater. Interfaces* **2011**, *3* (8), 2861–2868.
- (100) Holinka, J.; Pilz, M.; Kubista, B.; Presterl, E.; Windhager, R. Effects of Selenium Coating of Orthopaedic Implant Surfaces on Bacterial Adherence and Osteoblastic Cell Growth. *Bone Jt. J.* **2013**, *95 B* (5), 678–682.
- (101) Fjell, C. D.; Hiss, J. A.; Hancock, R. E. W.; Schneider, G. Designing Antimicrobial Peptides: Form Follows Function. *Nat. Rev. Drug Discov.* **2012**, *11* (1), 37–51.
- (102) Börner, H. G.; Lutz, J.-F. *Bioactive Surfaces*; Börner, H. G., Lutz, J.-F., Eds.; Advances in Polymer Science; Springer Berlin Heidelberg: Berlin, Heidelberg, 2011; Vol. 240.
- (103) Ketonis, C.; Barr, S.; Adams, C. S.; Shapiro, I. M.; Parvizi, J.; Hickok, N. J. Vancomycin Bonded to Bone Grafts Prevents Bacterial Colonization. *Antimicrob. Agents Chemother.* **2011**, *55* (2), 487–494.
- (104) Huang, K. S.; Yang, C. H.; Huang, S. L.; Chen, C. Y.; Lu, Y. Y.; Lin, Y. S. Recent Advances in Antimicrobial Polymers: A Mini-Review. *Int. J. Mol. Sci.* **2016**, *17* (9).
- (105) Muñoz-Bonilla, A.; Echeverria, C.; Sonseca, Á.; Arrieta, M. P.; Fernández-García, M. Bio-Based Polymers with Antimicrobial Properties towards Sustainable Development. *Materials (Basel)*. **2019**, *12* (4), 1–50.
- (106) Chua, P. H.; Neoh, K. G.; Kang, E. T.; Wang, W. Surface Functionalization of Titanium with Hyaluronic Acid/Chitosan Polyelectrolyte Multilayers and RGD for Promoting Osteoblast Functions and Inhibiting Bacterial Adhesion. *Biomaterials* **2008**, *29* (10), 1412–1421.
- (107) Cao, Z.; Sun, Y. N-Halamine-Based Chitosan: Preparation, Characterization, and Antimicrobial Function. *J. Biomed. Mater. Res. - Part A* **2008**, *85* (1), 99–107.
- (108) Kazemzadeh-Narbat, M.; Kindrachuk, J.; Duan, K.; Jenssen, H.; Hancock, R. E. W.; Wang, R. Antimicrobial Peptides on Calcium Phosphate-Coated Titanium for the Prevention of Implant-Associated Infections. *Biomaterials* **2010**, *31* (36), 9519–9526.
- (109) Pfeufer, N. Y.; Hofmann-Peiker, K.; Mühle, M.; Warnke, P. H.; Weigel, M. C.; Kleine, M. Bioactive Coating of Titanium Surfaces with Recombinant Human β -Defensin-2 (RHu β D2) May Prevent Bacterial Colonization in Orthopaedic Surgery. *J. Bone Jt. Surg. - Ser. A* **2011**, *93* (9), 840–846.

- (110) Puleo, D. A.; Huh, W. W. Acute Toxicity of Metal Ions in Cultures of Osteogenic Cells Derived from Bone Marrow Stromal Cells. *J. Appl. Biomater.* **1995**, *6* (2), 109–116.
- (111) Sabella, S.; Carney, R. P.; Brunetti, V.; Malvindi, M. A.; Al-Juffali, N.; Vecchio, G.; Janes, S. M.; Bakr, O. M.; Cingolani, R.; Stellacci, F.; et al. A General Mechanism for Intracellular Toxicity of Metal-Containing Nanoparticles. *Nanoscale* **2014**, *6* (12), 7052.
- (112) Hahn, A.; Fuhlrott, J.; Loos, A.; Barcikowski, S. Cytotoxicity and Ion Release of Alloy Nanoparticles. *J. Nanoparticle Res.* **2012**, *14* (1), 686.
- (113) Shchukin, D.; Mohwald, H. A Coat of Many Functions. *Science* (80-.). **2013**, *341* (6153), 1458–1459.
- (114) Hetrick, E. M.; Schoenfisch, M. H. Reducing Implant-Related Infections: Active Release Strategies. *Chem. Soc. Rev.* **2006**, *35* (9), 780–789.
- (115) Pan, C.; Zhou, Z.; Yu, X. Coatings as the Useful Drug Delivery System for the Prevention of Implant-Related Infections. *J. Orthop. Surg. Res.* **2018**, *13* (1), 1–11.
- (116) Baker, R. W.; Sanders, L. M. Controlled Release Delivery Systems. In *Synthetic Membranes: Science, Engineering and Applications*; Springer Netherlands: Dordrecht, 1986; pp 581–624.
- (117) Vasilev, K.; Poulter, N.; Martinek, P.; Griesser, H. J. Controlled Release of Levofloxacin Sandwiched between Two Plasma Polymerized Layers on a Solid Carrier. *ACS Appl. Mater. Interfaces* **2011**, *3* (12), 4831–4836.
- (118) Michl, T. D.; Coad, B. R.; Doran, M.; Osiecki, M.; Kafshgari, M. H.; Voelcker, N. H.; Hüsler, A.; Vasilev, K.; Griesser, H. J. Nitric Oxide Releasing Plasma Polymer Coating with Bacteriostatic Properties and No Cytotoxic Side Effects. *Chem. Commun.* **2015**, *51* (32), 7058–7060.
- (119) Kumeria, T.; Mon, H.; Aw, M. S.; Gulati, K.; Santos, A.; Griesser, H. J.; Losic, D. Advanced Biopolymer-Coated Drug-Releasing Titania Nanotubes (TNTs) Implants with Simultaneously Enhanced Osteoblast Adhesion and Antibacterial Properties. *Colloids Surfaces B Biointerfaces* **2015**, *130* (October), 255–263.
- (120) Keating, J. F.; Blachut, P. A.; O'Brien, P. J.; Meek, R. N.; Broekhuysse, H. Reamed Nailing of Open Tibial Fractures: Does the Antibiotic Bead Pouch Reduce the Deep Infection Rate? *J. Orthop. Trauma* **1996**, *10* (5), 298–303.
- (121) Ostermann, P.; Seligson, D.; Henry, S. Local Antibiotic Therapy for Severe Open Fractures. A Review of 1085 Consecutive Cases. *J. Bone Joint Surg. Br.* **1995**, *77-B* (1), 93–97.
- (122) Kumar, R.; Münstedt, H. Silver Ion Release from Antimicrobial Polyamide/Silver Composites. *Biomaterials* **2005**, *26* (14), 2081–2088.
- (123) Thatiparti, T. R.; Shoffstall, A. J.; von Recum, H. A. Cyclodextrin-Based Device Coatings for Affinity-Based Release of Antibiotics. *Biomaterials* **2010**, *31* (8), 2335–2347.
- (124) Cloutier, M.; Mantovani, D.; Rosei, F. Antibacterial Coatings: Challenges, Perspectives,

- and Opportunities. *Trends Biotechnol.* **2015**, 33 (11), 637–652.
- (125) Pilliar, R. M. Cementless Implant Fixation—toward Improved Reliability. *Orthop. Clin. North Am.* **2005**, 36 (1), 113–119.
- (126) Aviv, M.; Berdicevsky, I.; Zilberman, M. Gentamicin-Loaded Bioresorbable Films for Prevention of Bacterial Infections Associated with Orthopedic Implants. *J. Biomed. Mater. Res. Part A* **2007**, 83A (1), 10–19.
- (127) McLaren, J.; White, L.; Cox, H.; Ashraf, W.; Rahman, C.; Blunn, G.; Goodship, A.; Quirk, R.; Shakesheff, K.; Bayston, R.; et al. A Biodegradable Antibiotic-Impregnated Scaffold to Prevent Osteomyelitis in a Contaminated in Vivo Bone Defect Model. *Eur. Cells Mater.* **2014**, 27, 332–349.
- (128) Gollwitzer, H. Antibacterial Poly(D,L-Lactic Acid) Coating of Medical Implants Using a Biodegradable Drug Delivery Technology. *J. Antimicrob. Chemother.* **2003**, 51 (3), 585–591.
- (129) Vester, H.; Wildemann, B.; Schmidmaier, G.; Stöckle, U.; Lucke, M. Gentamycin Delivered from a PDLA Coating of Metallic Implants. *Injury* **2010**, 41 (10), 1053–1059.
- (130) Strobel, C.; Schmidmaier, G.; Wildemann, B. Changing the Release Kinetics of Gentamicin from Poly(D, L-Lactide) Implant Coatings Using Only One Polymer. *Int. J. Artif. Organs* **2011**, 34 (3), 304–316.
- (131) Radin, S.; Falaize, S.; Lee, M. H.; Ducheyne, P. In Vitro Bioactivity and Degradation Behavior of Silica Xerogels Intended as Controlled Release Materials. *Biomaterials* **2002**, 23 (15), 3113–3122.
- (132) Qu, H.; Knabe, C.; Radin, S.; Garino, J.; Ducheyne, P. Percutaneous External Fixator Pins with Bactericidal Micron-Thin Sol-Gel Films for the Prevention of Pin Tract Infection. *Biomaterials* **2015**, 62, 95–105.
- (133) Kim, W.-H.; Lee, S.-B.; Oh, K.-T.; Moon, S.-K.; Kim, K.-M.; Kim, K.-N. The Release Behavior of CHX from Polymer-Coated Titanium Surfaces. **2008**.
- (134) Metsemakers, W. J.; Emanuel, N.; Cohen, O.; Reichart, M.; Potapova, I.; Schmid, T.; Segal, D.; Riool, M.; Kwakman, P. H. S.; De Boer, L.; et al. A Doxycycline-Loaded Polymer-Lipid Encapsulation Matrix Coating for the Prevention of Implant-Related Osteomyelitis Due to Doxycycline-Resistant Methicillin-Resistant Staphylococcus Aureus. *J. Control. Release* **2015**, 209, 47–56.
- (135) Juan-Díaz, M. J.; Martínez-Ibáñez, M.; Lara-Sáez, I.; da Silva, S.; Izquierdo, R.; Gurruchaga, M.; Goñi, I.; Suay, J. Development of Hybrid Sol–Gel Coatings for the Improvement of Metallic Biomaterials Performance. *Prog. Org. Coatings* **2015**, 96, 42–51.
- (136) Roest, R.; Latella, B. A.; Heness, G.; Ben-Nissan, B. Adhesion of Sol-Gel Derived Hydroxyapatite Nanocoatings on Anodised Pure Titanium and Titanium (Ti6Al4V) Alloy Substrates. *Surf. Coatings Technol.* **2011**, 205 (11), 3520–3529.
- (137) Adams, C. S.; Antoci, V.; Harrison, G.; Patal, P.; Freeman, T. A.; Shapiro, I. M.; Parvizi,

- J.; Hickok, N. J.; Radin, S.; Ducheyne, P. Controlled Release of Vancomycin from Thin Sol-Gel Films on Implant Surfaces Successfully Controls Osteomyelitis. *J. Orthop. Res.* **2009**, *27* (6), 701–709.
- (138) Qu, H.; Radin, S.; Ducheyne, P. Release Kinetics from Porous Xerogels Determined by Sol-Gel Synthesis, Porous Nanostructure and Immersion. **2014**, *1*, 11–17.
- (139) Qu, H.; Knabe, C.; Burke, M.; Radin, S.; Garino, J.; Schaer, T.; Ducheyne, P. Bactericidal Micron-Thin Sol–Gel Films Prevent Pin Tract and Periprosthetic Infection. *Mil. Med.* **2014**, *179* (8S), 29–33.
- (140) Babapour, A.; Akhavan, O.; Azimirad, R.; Moshfegh, A. Z. Physical Characteristics of Heat-Treated Nano-Silvers Dispersed in Sol-Gel Silica Matrix. *Nanotechnology* **2006**, *17* (3), 763–771.
- (141) Batebi, K.; Abbasi Khazaei, B.; Afshar, A. Characterization of Sol-Gel Derived Silver/Fluor-Hydroxyapatite Composite Coatings on Titanium Substrate. *Surf. Coatings Technol.* **2018**, *352* (August), 522–528.
- (142) Jaiswal, S.; Bhattacharya, K.; Sullivan, M.; Walsh, M.; Creaven, B. S.; Laffir, F.; Duffy, B.; McHale, P. Non-Cytotoxic Antibacterial Silver-Coumarin Complex Doped Sol-Gel Coatings. *Colloids Surfaces B Biointerfaces* **2013**, *102*, 412–419.
- (143) Saif, M. J.; Anwar, J.; Munawar, M. A. A Novel Application of Quaternary Ammonium Compounds as Antibacterial Hybrid Coating on Glass Surfaces. *Langmuir* **2009**, *25* (1), 377–379.
- (144) Gong, S.; Niu, L.; Kemp, L. K.; Yiu, C. K. Y.; Ryou, H.; Qi, Y.; Blizzard, J. D.; Nikonov, S.; Brackett, M. G.; Messer, R. L. W.; et al. Quaternary Ammonium Silane-Functionalized, Methacrylate Resin Composition with Antimicrobial Activities and Self-Repair Potential. *Acta Biomater.* **2012**, *8* (9), 3270–3282.
- (145) Nablo, B. J.; Rothrock, A. R.; Schoenfisch, M. H. Nitric Oxide-Releasing Sol–Gels as Antibacterial Coatings for Orthopedic Implants. *Biomaterials* **2005**, *26* (8), 917–924.
- (146) Park, K.; Jeong, H.; Tanum, J.; Yoo, J. chan; Hong, J. Developing Regulatory Property of Gelatin-Tannic Acid Multilayer Films for Coating-Based Nitric Oxide Gas Delivery System. *Sci. Rep.* **2019**, *9* (1), 1–8.
- (147) Rippke, F.; Berardesca, E.; Weber, T. M. PH and Microbial Infections. *Curr. Probl. Dermatology* **2018**, *54*, 87–94.
- (148) Wang, T.; Wang, C.; Zhou, S.; Xu, J.; Jiang, W.; Tan, L.; Fu, J. Nanovalves-Based Bacteria-Triggered, Self-Defensive Antibacterial Coating: Using Combination Therapy, Dual Stimuli-Responsiveness, and Multiple Release Modes for Treatment of Implant-Associated Infections. *Chem. Mater.* **2017**, *29* (19), 8325–8337.
- (149) Zhuk, I.; Jariwala, F.; Attygalle, A. B.; Wu, Y.; Libera, M. R.; Sukhishvili, S. A. Self-Defensive Layer-by-Layer Films with Bacteria-Triggered Antibiotic Release. *ACS Nano* **2014**, *8* (8), 7733–7745.
- (150) Pichavant, L.; Amador, G.; Jacqueline, C.; Brouillaud, B.; Héroguez, V.; Durrieu, M. C.

- PH-Controlled Delivery of Gentamicin Sulfate from Orthopedic Devices Preventing Nosocomial Infections. *J. Control. Release* **2012**, *162* (2), 373–381.
- (151) Wolberg, A. S.; Campbell, R. A. Thrombin Generation, Fibrin Clot Formation and Hemostasis. *Transfus. Apher. Sci.* **2008**, *38* (1), 15–23.
- (152) Tanihara, M.; Suzuki, Y.; Nishimura, Y.; Suzuki, K.; Kakimaru, Y.; Fukunishi, Y. A Novel Microbial Infection-responsive Drug Release System. *J. Pharm. Sci.* **1999**, *88* (5), 510–514.
- (153) Shchukin, D. G.; Möhwald, H. Self-Repairing Coatings Containing Active Nanoreservoirs. *Small* **2007**, *3* (6), 926–943.
- (154) Esrafilzadeh, D.; Razal, J. M.; Moulton, S. E.; Stewart, E. M.; Wallace, G. G. Multifunctional Conducting Fibres with Electrically Controlled Release of Ciprofloxacin. *J. Control. Release* **2013**, *169* (3), 313–320.
- (155) Norris, P.; Noble, M.; Francolini, I.; Vinogradov, A. M.; Stewart, P. S.; Ratner, B. D.; Costerton, J. W.; Stoodley, P. Ultrasonically Controlled Release of Ciprofloxacin from Self-Assembled Coatings on Poly(2-Hydroxyethyl Methacrylate) Hydrogels for *Pseudomonas Aeruginosa* Biofilm Prevention. *Antimicrob. Agents Chemother.* **2005**, *49* (10), 4272–4279.
- (156) Aw, M. S.; Addai-Mensah, J.; Losic, D. Magnetic-Responsive Delivery of Drug-Carriers Using Titania Nanotube Arrays. *J. Mater. Chem.* **2012**, *22* (14), 6561–6563.
- (157) Brånemark, P. I.; Hansson, B. O.; Adell, R.; Breine, U.; Lindström, J.; Hallén, O.; Ohman, A. Osseointegrated Implants in the Treatment of the Edentulous Jaw. Experience from a 10-Year Period. *Scand. J. Plast. Reconstr. Surg. Suppl.* **1977**, *16*, 1–132.
- (158) Albrektsson, T.; Chrcanovic, B.; Jacobsson, M.; Wennerberg, A. Osseointegration of Implants – A Biological and Clinical Overview. *JSM Dent Surg* **2017**, *2* (3), 1022.
- (159) Albrektsson, T.; Johansson, C. Osteoinduction, Osteoconduction and Osseointegration. *Eur. Spine J.* **2001**, *10*, S96–S101.
- (160) Frost, H. M. The Biology of Fracture Healing. An Overview for Clinicians. Part I. *Clin. Orthop. Relat. Res.* **1989**, No. 248, 283–293.
- (161) Chang, J.; Zhang, X.; Dai, and K. *Bioactive Materials for Bone Regeneration*; Elsevier, 2020.
- (162) Masaki, C.; Schneider, G. B.; Zaharias, R.; Seabold, D.; Stanford, C. Effects of Implant Surface Microtopography on Osteoblast Gene Expression. *Clin. Oral Implants Res.* **2005**, *16* (6), 650–656.
- (163) Lu, X.; Leng, Y.; Zhang, X.; Xu, J.; Qin, L.; Chan, C. W. Comparative Study of Osteoconduction on Micromachined and Alkali-Treated Titanium Alloy Surfaces in Vitro and in Vivo. *Biomaterials* **2005**, *26* (14), 1793–1801.
- (164) Liao, H.; Andersson, A. S.; Sutherland, D.; Petronis, S.; Kasemo, B.; Thomsen, P. Response of Rat Osteoblast-like Cells to Microstructured Model Surfaces in Vitro.

Biomaterials **2003**, 24 (4), 649–654.

- (165) Wang, T.; Wan, Y.; Kou, Z.; Cai, Y.; Wang, B.; Liu, Z. Construction of a Bioactive Surface with Micro/Nano-Topography on Titanium Alloy by Micro-Milling and Alkali-Hydrothermal Treatment. *Proc. Inst. Mech. Eng. Part H J. Eng. Med.* **2016**, 230 (12), 1086–1095.
- (166) Wang, G.; Moya, S.; Lu, Z.; Gregurec, D.; Zreiqat, H. Enhancing Orthopedic Implant Bioactivity: Refining the Nanotopography. *Nanomedicine* **2015**, 10 (8), 1327–1341.
- (167) Nune, K. C.; Misra, R. D. K.; Gai, X.; Li, S. J.; Hao, Y. L. Surface Nanotopography-Induced Favorable Modulation of Bioactivity and Osteoconductive Potential of Anodized 3D Printed Ti-6Al-4V Alloy Mesh Structure. *J. Biomater. Appl.* **2018**, 32 (8), 1032–1048.
- (168) Wang, N.; Li, H.; Lü, W.; Li, J.; Wang, J.; Zhang, Z.; Liu, Y. Effects of TiO₂ Nanotubes with Different Diameters on Gene Expression and Osseointegration of Implants in Minipigs. *Biomaterials* **2011**, 32 (29), 6900–6911.
- (169) Brammer, K. S.; Oh, S.; Cobb, C. J.; Bjursten, L. M.; Heyde, H. van der; Jin, S. Improved Bone-Forming Functionality on Diameter-Controlled TiO₂ Nanotube Surface. *Acta Biomater.* **2009**, 5 (8), 3215–3223.
- (170) Puckett, S. D.; Taylor, E.; Raimondo, T.; Webster, T. J. The Relationship between the Nanostructure of Titanium Surfaces and Bacterial Attachment. *Biomaterials* **2010**, 31 (4), 706–713.
- (171) Truong, V. K.; Pham, V. T. H.; Medvedev, A.; Lapovok, R.; Estrin, Y.; Lowe, T. C.; Baulin, V.; Boshkovikj, V.; Fluke, C. J.; Crawford, R. J.; et al. Self-Organised Nanoarchitecture of Titanium Surfaces Influences the Attachment of Staphylococcus Aureus and Pseudomonas Aeruginosa Bacteria. *Appl. Microbiol. Biotechnol.* **2015**, 99 (16), 6831–6840.
- (172) Fialho, L.; Carvalho, S. Applied Surface Science Surface Engineering of Nanostructured Ta Surface with Incorporation of Osteoconductive Elements by Anodization. *Appl. Surf. Sci.* **2019**, 495 (July), 143573.
- (173) Maggs, J.; Wilson, M. The Relative Merits of Cemented and Uncemented Prostheses in Total Hip Arthroplasty. *Indian J. Orthop.* **2017**, 51 (4), 377.
- (174) Mohseni, E.; Zalnezhad, E.; Bushroa, A. R. Comparative Investigation on the Adhesion of Hydroxyapatite Coating on Ti-6Al-4V Implant: A Review Paper. *Int. J. Adhes. Adhes.* **2014**, 48, 238–257.
- (175) Bodén, H.; Salemyr, M.; Sköldenberg, O.; Ahl, T.; Adolphson, P. Total Hip Arthroplasty with an Uncemented Hydroxyapatite-Coated Tapered Titanium Stem: Results at a Minimum of 10 Years' Follow-up in 104 Hips. *J. Orthop. Sci.* **2006**, 11 (2), 175–179.
- (176) Goosen, J. H. M.; Kums, A. J.; Kollen, B. J.; Verheyen, C. C. P. M. Porous-Coated Femoral Components with or without Hydroxyapatite in Primary Uncemented Total Hip Arthroplasty: A Systematic Review of Randomized Controlled Trials. *Arch. Orthop. Trauma Surg.* **2009**, 129 (9), 1165–1169.

- (177) Voigt, J. D.; Mosier, M. Hydroxyapatite (HA) Coating Appears to Be of Benefit for Implant Durability of Tibial Components in Primary Total Knee Arthroplasty. *Acta Orthop.* **2011**, *82* (4), 448–459.
- (178) Lee, J. M.; Lee, C. W. Comparison of Hydroxyapatite-Coated and Non-Hydroxyapatite-Coated Noncemented Total Hip Arthroplasty in Same Patients. *J. Arthroplasty* **2007**, *22* (7), 1019–1023.
- (179) Heimann, R. B. Plasma-Sprayed Hydroxylapatite-Based Coatings: Chemical, Mechanical, Microstructural, and Biomedical Properties. *J. Therm. Spray Technol.* **2016**, *25* (5), 827–850.
- (180) Biesbrock, A. R.; Edgerton, M. Evaluation of the Clinical Predictability of Hydroxyapatite-Coated Endosseous Dental Implants: A Review of the Literature. *Int. J. Oral Maxillofac. Implants* *10* (6), 712–720.
- (181) Kim, Y. H.; Kim, J. S.; Oh, S. H.; Kim, J. M. Comparison of Porous-Coated Titanium Femoral Stems with and without Hydroxyapatite Coating. *J. Bone Jt. Surg. - Ser. A* **2003**, *85* (9), 1682–1688.
- (182) Gandhi, R.; Davey, J. R.; Mahomed, N. N. Hydroxyapatite Coated Femoral Stems in Primary Total Hip Arthroplasty. A Meta-Analysis. *J. Arthroplasty* **2009**, *24* (1), 38–42.
- (183) Lazarinis, S.; Krärholm, J.; Hailer, N. P. Increased Risk of Revision of Acetabular Cups Coated with Hydroxyapatite: A Swedish Hip Arthroplasty Register Study Involving 8,043 Total Hip Replacements. *Acta Orthop.* **2010**, *81* (1), 53–59.
- (184) Vahabzadeh, S.; Roy, M.; Bandyopadhyay, A.; Bose, S. Phase Stability and Biological Property Evaluation of Plasma Sprayed Hydroxyapatite Coatings for Orthopedic and Dental Applications. *Acta Biomater.* **2015**, *17* (3), 47–55.
- (185) Sun, L.; Berndt, C. C.; Khor, K. A.; Cheang, H. N.; Gross, K. A. Surface Characteristics and Dissolution Behavior of Plasma-Sprayed Hydroxyapatite Coating. *J. Biomed. Mater. Res.* **2002**, *62* (2), 228–236.
- (186) Le Guéhenec, L.; Soueidan, A.; Layrolle, P.; Amouriq, Y. Surface Treatments of Titanium Dental Implants for Rapid Osseointegration. *Dent. Mater.* **2007**, *23* (7), 844–854.
- (187) Zhang, B. G. X.; Myers, D. E.; Wallace, G. G.; Brandt, M.; Choong, P. F. M. Bioactive Coatings for Orthopaedic Implants-Recent Trends in Development of Implant Coatings. *Int. J. Mol. Sci.* **2014**, *15* (7), 11878–11921.
- (188) Asri, R. I. M.; Harun, W. S. W.; Hassan, M. A.; Ghani, S. A. C.; Buyong, Z. A Review of Hydroxyapatite-Based Coating Techniques: Sol-Gel and Electrochemical Depositions on Biocompatible Metals. *J. Mech. Behav. Biomed. Mater.* **2016**, *57*, 95–108.
- (189) Wang, D.; Chen, C.; He, T.; Lei, T. Hydroxyapatite Coating on Ti6Al4V Alloy by a Sol-Gel Method. *J. Mater. Sci. Mater. Med.* **2008**, *19* (6), 2281–2286.
- (190) Hsieh, M. F.; Perng, L. H.; Chin, T. S. Hydroxyapatite Coating on Ti6Al4V Alloy Using a Sol-Gel Derived Precursor. *Mater. Chem. Phys.* **2002**, *74* (3), 245–250.

- (191) LL, H. Bioactive Materials for Gene Control. *New Mater. Technol. Healthc.* **2011**, 25–48.
- (192) Jones, J. R. Review of Bioactive Glass: From Hench to Hybrids. *Acta Biomater.* **2015**, 23 (S), S53–S82.
- (193) Li, R.; Clark, A. E.; Hench, L. L. An Investigation of Bioactive Glass Powders by Sol-Gel Processing. *J. Appl. Biomater.* **1991**, 2 (4), 231–239.
- (194) Jones, J. R. Reprint of: Review of Bioactive Glass: From Hench to Hybrids. *Acta Biomater.* **2015**, 23 (S), S53–S82.
- (195) Köseoglu, N. C.; Büyükaksoy, A.; Oral, A. Y.; Aslan, M. H. Hydroxyapatite/Bioactive Glass Films Produced by a Sol-Gel Method: In Vitro Behavior. *Adv. Eng. Mater.* **2009**, 11 (11), 194–199.
- (196) Hamadouche, M.; Meunier, A.; Greenspan, D. C.; Blanchat, C.; Zhong, J. P.; La Torre, G. P.; Sedel, L. Bioactivity of Bioactive Sol-Gel Glasses Coated Alumina Implants. *Key Eng. Mater.* **2001**, 192–195, 413–416.
- (197) Yu, B.; Turdean-Ionescu, C. A.; Martin, R. A.; Newport, R. J.; Hanna, J. V.; Smith, M. E.; Jones, J. R. Effect of Calcium Source on Structure and Properties of Sol-Gel Derived Bioactive Glasses. *Langmuir* **2012**, 28 (50), 17465–17476.
- (198) Lin, S.; Ionescu, C.; Baker, S.; Smith, M. E.; Jones, J. R. Characterisation of the Inhomogeneity of Sol-Gel-Derived SiO₂-CaO Bioactive Glass and a Strategy for Its Improvement. *J. Sol-Gel Sci. Technol.* **2010**, 53 (2), 255–262.
- (199) Blaker, J. J.; Bismarck, A.; Boccaccini, A. R.; Young, A. M.; Nazhat, S. N. Premature Degradation of Poly(Alpha-Hydroxyesters) during Thermal Processing of Bioglass-Containing Composites. *Acta Biomater.* **2010**, 6 (3), 756–762.
- (200) Catauro, M.; Bollino, F.; Papale, F. Surface Modifications of Titanium Implants by Coating with Bioactive and Biocompatible Poly (ε-Caprolactone)/SiO₂ Hybrids Synthesized via Sol–Gel. *Arab. J. Chem.* **2018**, 11 (7), 1126–1133.
- (201) Catauro, M.; Bollino, F.; Papale, F.; Gallicchio, M.; Pacifico, S. Synthesis and Chemical Characterization of New Silica Polyethylene Glycol Hybrid Nanocomposite Materials for Controlled Drug Delivery. *J. Drug Deliv. Sci. Technol.* **2014**, 24 (4), 320–325.
- (202) Catauro, M.; Papale, F.; Piccirillo, G.; Bollino, F. PEG-Based Organic-Inorganic Hybrid Coatings Prepared by the Sol-Gel Dip-Coating Process for Biomedical Applications. *Polym. Eng. Sci.* **2017**, 57 (6), 478–484.
- (203) Pebdeni, A. B.; Sadri, M.; Pebdeni, S. B. Synthesis of Chitosan/PEO/Silica Nanofiber Coating for Controlled Release of Cefepime from Implants. *RSC Adv.* **2016**, 6 (29), 24418–24429.
- (204) Jun, S. H.; Lee, E. J.; Yook, S. W.; Kim, H. E.; Kim, H. W.; Koh, Y. H. A Bioactive Coating of a Silica Xerogel/Chitosan Hybrid on Titanium by a Room Temperature Sol-Gel Process. *Acta Biomater.* **2010**, 6 (1), 302–307.
- (205) Palla-Rubio, B.; Araújo-Gomes, N.; Fernández-Gutiérrez, M.; Rojo, L.; Suay, J.;

- Gurruchaga, M.; Goñi, I. Synthesis and Characterization of Silica-Chitosan Hybrid Materials as Antibacterial Coatings for Titanium Implants. *Carbohydr. Polym.* **2019**, *203* (May 2018), 331–341.
- (206) Shirosaki, Y.; Tsuru, K.; Hayakawa, S.; Osaka, A.; Lopes, M. A.; Santos, J. D.; Fernandes, M. H. In Vitro Cytocompatibility of MG63 Cells on Chitosan-Organosiloxane Hybrid Membranes. *Biomaterials* **2005**, *26* (5), 485–493.
- (207) Shirosaki, Y.; Hirai, M.; Hayakawa, S.; Fujii, E.; Lopes, M. A.; Santos, J. D.; Osaka, A. Preparation and in Vitro Cytocompatibility of Chitosan-Siloxane Hybrid Hydrogels. *J. Biomed. Mater. Res. - Part A* **2015**, *103* (1), 289–299.
- (208) Greenhalgh, R. D.; Ambler, W. S.; Quinn, S. J.; Medeiros, E. S.; Anderson, M.; Gore, B.; Menner, A.; Bismarck, A.; Li, X.; Tirelli, N.; et al. Of Hybrid Sol – Gel Inorganic / Gelatin Porous Fibres via Solution Blow Spinning. **2017**, 9066–9081.
- (209) Mahony, O.; Tsigkou, O.; Ionescu, C.; Minelli, C.; Ling, L.; Hanly, R.; Smith, M. E.; Stevens, M. M.; Jones, J. R. Silica-Gelatin Hybrids with Tailorable Degradation and Mechanical Properties for Tissue Regeneration. *Adv. Funct. Mater.* **2010**, *20* (22), 3835–3845.
- (210) Connell, L. S.; Gabrielli, L.; Mahony, O.; Russo, L.; Cipolla, L.; Jones, J. R. Functionalizing Natural Polymers with Alkoxysilane Coupling Agents: Reacting 3-Glycidoxypropyl Trimethoxysilane with Poly(γ -Glutamic Acid) and Gelatin. *Polym. Chem.* **2017**, *8* (6), 1095–1103.
- (211) Hernández-Escolano, M.; Juan-Díaz, M.; Martínez-Ibáñez, M.; Jimenez-Morales, A.; Goñi, I.; Gurruchaga, M.; Suay, J. The Design and Characterisation of Sol-Gel Coatings for the Controlled-Release of Active Molecules. *J. Sol-Gel Sci. Technol.* **2012**, *64* (2), 442–451.
- (212) Li, A.; Shen, H.; Ren, H.; Wang, C.; Wu, D.; Martin, R. A.; Qiu, D. Bioactive Organic/Inorganic Hybrids with Improved Mechanical Performance. *J. Mater. Chem. B* **2015**, *3* (7), 1379–1390.
- (213) Poologasundarampillai, G.; Yu, B.; Tsigkou, O.; Wang, D.; Romer, F.; Bhakhri, V.; Giuliani, F.; Stevens, M. M.; McPhail, D. S.; Smith, M. E.; et al. Poly(γ -Glutamic Acid)/Silica Hybrids with Calcium Incorporated in the Silica Network by Use of a Calcium Alkoxide Precursor. *Chem. - A Eur. J.* **2014**, *20* (26), 8149–8160.

Chapter 3: Development of robust chitosan–silica class II hybrid coatings with antimicrobial properties for titanium implants*

3.1 Introduction

Titanium and its alloys have been the material of choice for biomedical implants over the past half century. Their low specific weight, high strength to weight ratio and resistance to corrosion are features that make titanium the ideal bulk material for numerous clinical applications¹. These include orthopedic and dental implants where their resistance to chipping and capacity to endure repetitive high loading conditions are an advantage over non-metallic substrates. Furthermore, the titanium dioxide layer that forms on their surfaces is highly inert and biocompatible to the cells and extracellular matrix of surrounding tissues.

However, the bio-inertia of titanium surfaces is accompanied by a lack of any significant antimicrobial properties. While implanted titanium materials are well received by the osseous and connective tissues of their host, microbial contamination of their surfaces and the surgical site can often lead to sustained infections and unfavorable patient outcomes. These implant-associated infections are currently a major cause of orthopedic and dental implant failures. Post-operative infections associated with biomaterial implantation range from 2%–5% for orthopedic procedures and 4%–11.5% for dental and oral surgeries^{2–4}. These infections are often extremely resistant to systemic antibiotics and persist until the implant has been surgically retrieved.

The persistence of implant-associated infections is likely due to the presence of polymicrobial biofilms that have formed on implant surfaces. These biofilms contain bacteria that are encased within a bacterial-excreted polysaccharide matrix, which is highly adherent to biomaterial surfaces and largely resistant to the external environment. Accordingly, the bacteria within biofilms may be up to 1000 times more resistant to antibiotics than bacteria that are suspended in a planktonic state^{3,5}.

Therefore, research has now been directed toward the modification of implant surfaces to prevent initial bacterial adhesion and subsequent biofilm formation. Most antimicrobial strategies have relied on either static antimicrobial activity from direct or indirect surface modifications or they

* A version of this chapter has been published: Z. Gouveia, H. Perinpanayagam, J. Zhu, *Coatings* **2020**, *10*, 1–20

have implemented release-based antimicrobial action using biocides imbedded within material surfaces.

Static antimicrobial strategies involve modifications to implant surface properties which can alter their surface roughness, hydrophilicity and/or surface functional groups⁶⁻⁸. Therefore, such intensive surface modifications can lack selectivity for biomedical applications and may inadvertently reduce favorable surface interactions with mammalian cells. These cellular responses are necessary for cell attachment and adequate osseointegration with surrounding tissues⁹. Furthermore, while static antimicrobial factors may inhibit or retard initial bacterial adhesion and proliferation, they become ineffective once biofilms become established on biomaterial surfaces.

In contrast, release-based antimicrobial strategies typically employ a coating system that enables the release of biocidal components such as antibiotics, cationic molecules or metallic compounds¹⁰⁻¹³. Systems that employ release-based antimicrobial strategies often involve an initial burst release of the imbedded biocidal agents that have short-term effects, which are followed by a subsequent diminution of activity. Additionally, for release-based systems the choice of an antibiotic as a biocidal agent may be contraindicated by the rise in antibiotic-resistant infections from resistant bacterial strains¹⁴.

Therefore, recent interest has focused on the utilization of metallic nanoparticles as antimicrobial agents, due to their broad-spectrum effects^{15,16}. Among these, silver nanoparticles (AgNPs) have garnered significant interest due to their limited cytotoxicity, ease of synthesis, low minimum inhibitory concentrations for many pathogenic bacteria and their antimicrobial efficacies in both static and release-based applications¹⁷⁻¹⁹. AgNPs provide antibacterial efficacy through both the release of silver ions (Ag^+) and through the direct action of metallic AgNPs (Ag^0). The Ag^+ provide antibacterial effects by permeating cell walls, damaging proteins and membranes and causing oxidative stress²⁰. The antibacterial action of Ag^0 is by a similar permeation-based toxicity, as well as through cell surface attachment and disturbances to the permeability and metabolism of bacterial cells^{21,22}.

Currently, surface modifications to titanium implants are limited commercially to surface treatments (physical roughening, anodizing, chemical etching, etc.) and inorganic ceramic coatings that typically incorporate hydroxyapatite (HA) as a bioactive layer. However, the

application of such ceramic coatings has numerous disadvantages such as slow processing (biomimetism), high temperature application (plasma spraying) and overly thick or brittle film deposition, which limit their ability to be loaded with process sensitive antimicrobials^{23–25}. Therefore, there was significant interest in using alternative coating materials containing organic components, which could improve the material properties and processability of coating materials while retaining an adequate level of bioactivity within tissues.

One organic material being considered for coating applications is chitosan, which is a naturally occurring polycationic polymer derived from the shells of crustaceans. Chitosan is both biocompatible, biodegradable and has antibacterial effects. Due to these unique properties, chitosan has already found use in multiple biomedical applications that include drug delivery^{26–28}, tissue engineering^{29–31}, ophthalmology^{32–34} and as medical device coatings^{35–37}. However, chitosan alone has a propensity to degrade and has weak mechanical properties in vivo that would make it a poor choice as a coating for implantable titanium materials.

Therefore, the development of class II organic–inorganic hybrid materials that retain the biologic benefits of polymers such as chitosan, while enhancing their physical properties, has been proposed^{38–40}. By covalently coupling biopolymers to inorganic precursors, hybrid materials could be developed that retain their biocompatibility and have improved mechanical properties. For example, gelatin has been utilized as the organic component in a class II hybrid framework with silica, to develop highly porous scaffolds for bony tissue applications with tunable mechanical and dissolution properties⁴¹. Similarly, chitosan has been shown to be an appropriate biopolymer for covalent coupling with silica networks that are otherwise too brittle^{42–45}. Coupling with inorganic silica networks, in these cases, significantly improves the mechanical properties of chitosan alone for applications as biomaterials. Similar studies have used chitosan as a primary organic network modifier and sole antimicrobial agent in the development of coatings for titanium implant materials^{46,47}. These studies have shown that such materials could promote bone forming ability and provide an antimicrobial effect against clinically relevant pathogens. This study evaluated the robustness of these materials and investigated the inclusion of AgNPs into the coating network to improve antimicrobial efficacy against both static and planktonic pathogens.

Therefore, the purpose of this research was to develop robust and functional chitosan–silica coatings for titanium implants. The objective was to develop robust chitosan–silica class II hybrid coatings that could be loaded with AgNPs for manifest antibacterial properties.

3.2 Materials and Methods

3.2.1 Synthesis of Coating Materials

All chemicals involved in the preparation of coating materials were purchased as laboratory grade reagents from Sigma Aldrich (St. Louis, MO, USA), unless otherwise specified. There were four formulations of chitosan–silica hybrid coating materials prepared (Table 1). Their composition and preparation were identical, except for their organic content that varied from 20% to 80% by weight. The variation in organic content was achieved by modifying the ratio of tetraethoxysilane (TEOS) to chitosan coupled with 3-glycidyloxypropyltrimethoxysilane (Ch-GPTMS).

Table 3.1 Composition of hybrid coatings.

<i>Components</i>	80% Organic Blends		60% Organic Blends		40% Organic Blends		20% Organic Blends	
	80ChSi	80 ChSi-nAg	60ChSi	60ChSi-nAg	40ChSi	40ChSi-nAg	20 ChSi	20 ChSi-nAg
Ch-GPTMS ^a	80	80	60	60	40	40	20	20
TEOS ^b	20	20	40	40	60	60	80	80
AgNPs ^c	–	0.023	–	0.023	–	0.023	–	0.023

^aChitosan coupled with 3-glycidyloxypropyltrimethoxysilane (network wt.%); ^b tetraethoxysilane (network wt.%); ^c silver nanoparticles (total coating wt.%)

A coupling reaction between chitosan and GPTMS was initiated as previously described^{42,45}. Briefly, chitosan (200 kDa, 82% DDA) was dissolved in an acidic solution (HCl, pH 4.0) to a concentration of 18 mg/mL. This chitosan solution was strained through a cotton filter and then GPTMS was added at a 1:1 molar ratio of solubilized chitosan to GPTMS and left to couple over a period of 24 hours at room temperature. Following coupling, an appropriate amount of hydrolyzed TEOS (pH 4.0) was added to the Ch-GPTMS solution to yield hybrids of varying organic content (20, 40, 60 and 80 wt.%). The inorganic component of the hybrid material was controlled independently using TEOS. After the addition of an appropriate amount of TEOS as

the inorganic component in the hybrid material, duplicate preparations of each coating material were loaded with AgNPs (0.023 wt.%) and agitated maximally for 1 h.

The AgNPs were synthesized by a chemical reduction method, as previously described⁴⁸⁻⁵⁰. Initially, a solution of NaBH₄ (2.0×10^{-3} M) was prepared in double distilled water and chilled in an ice bath for 15 min. Concurrently, a solution of AgNO₃ (2.0×10^{-3} M) was prepared in double distilled water. While the solution of NaBH₄ was stirred vigorously, the solution of AgNO₃ was added dropwise with NaBH₄ being in excess (NaBH₄:AgNO₃ 6:1 v/v). Following the addition of AgNO₃, stirring was stopped and the AgNP colloid was stabilized with an appropriate amount of polyvinylpyrrolidone (0.3 wt.% PVP) solution. The PVP stabilized AgNP solutions were then subjected to repeated cycles of ultracentrifugation and freeze-drying to collect concentrated AgNPs.

The synthesized AgNPs were examined by transmission electron microscopy (TEM). Nickel grids (400 mesh) were dipped in aqueous suspensions of AgNPs and allowed to air-dry. Analysis was performed using a Philips 420 TEM at an accelerating voltage of 80 kV equipped with an AMT 4000 digital imaging system.

3.2.2 Deposition of Hybrid Coatings

Commercially available titanium alloy (Ti6Al4V) discs ($9 \times 9 \times 2$ mm) were polished with silicon carbide study up to 1200 grit, then rinsed with acetone and washed by ultrasonication in deionized water. Some discs were then immersed in a solution of HCl and H₂SO₄ in double distilled water (2:2:1 v/v) at 65 °C for 20 min. Following this etching process, these discs were neutralized with a NaHCO₃ solution (0.5 M), washed by ultrasonication in deionized water and ethanol and dried at 40 °C.

The polished and acid-etched Ti6Al4V discs were used as substrates for the application of chitosan–silica class II hybrid coatings in a standard dip-coating protocol⁵¹. Briefly, the discs were immersed in freshly prepared chitosan–silica sol using a dip and withdrawal speed of 100 mm/min. Following dip coating, the discs were dried in a vacuum oven at 80 °C for 3 h and then stored at room temperature.

3.2.3 Characterization of Coating Surfaces

The hybrid coating surfaces were carefully analyzed for their chemical structure, composition and microtopographies. The presence of covalent coupling between chitosan and GPTMS was identified by solid-state nuclear magnetic resonance (NMR). ^{13}C Magic-angle spinning (MAS) NMR spectra were acquired at natural abundance on a 14.1 T Inova I600 NMR Spectrometer (Varian Inc., Palo Alto, CA, USA) operating at 79.4 MHz. Hybrid coating samples were spun at 13 kHz using a 3.2 mm MAS HXY probe. In addition, the degree of covalent coupling was measured with a ninhydrin assay as follows^{52,53}. Briefly, a ninhydrin solution was added to solid suspensions of the coating samples at 80 °C for 20 min. Solid suspensions were prepared by grinding dried coating materials with a mortar and pestle and suspending the fine powder in double distilled water. The absorbance of prepared suspensions was measured at 570 nm using a spectrophotometer (G1103A, Agilent Technologies, Santa Barbara, CA, USA) and compared to a standard curve prepared from the chitosan batch used in this study. Using the standard curve, the percentage of free (uncoupled) amino groups present in the coating samples was calculated.

The surface morphologies and microtopographies of the hybrid coatings were examined by scanning electron microscopy (SEM), using a Hitachi SU8230 Regulus Ultra High-Resolution Field Emission SEM (Hitachi, Tokyo, Japan). The coated Ti6Al4V discs were secured to metal stubs with carbon tape and sputter coated with 10 nm gold nanoparticles prior to analysis. Additionally, elemental distribution maps of the coating surfaces were obtained by energy-dispersive X-ray spectroscopy (EDX) using a Bruker X-Flash FQ5060 Annular Quad EDX detector (Bruker, Billerica, MA, USA).

The chemical structure of the coatings and the presence of key functional groups were analyzed using attenuated total reflectance Fourier transform infrared spectroscopy (ATR-FTIR). Hybrid coating samples were analyzed using a Bruker Tensor II system with a Platinum ATR (unit A225) equipped with a 2×2 mm diamond crystal (Bruker, Billerica, MA, USA). Spectra were acquired in the range of $4000\text{--}400\text{ cm}^{-1}$, at a resolution of 4 cm^{-1} and taken as an average of 32 scans. All spectra were analyzed using OPUS spectroscopy software.

3.2.4 Evaluation of Mechanical Properties

The mechanical properties of the hybrid coatings and their interface with underlying titanium substrates were carefully evaluated. Their surface energies were analyzed by measuring the water contact angle for double distilled water. The water contact angles were measured by the DataPhysics OCA 30 (DataPhysics, Filderstadt, Germany) using the sessile drop method. Drop volume was maintained at 10 μ L and replicate ($n = 5$) measurements were obtained.

Overall, adhesion of the hybrid coatings to their titanium substrates was evaluated qualitatively using an abbreviated cross hatch adhesion protocol (ASTM D3359⁵⁴). Briefly, the coatings were scored using a cross hatch cutter (Elcometer, Manchester, United Kingdom) with standardized blade spacing (11 \times 1 mm). There were two perpendicular cuts (20 mm) that were made with a steady motion and force to penetrate the coating layer and create a lattice pattern. ASTM standard tape was then placed over the center of the grid, smoothed with a pencil eraser and then withdrawn in a steady motion at an angle of 180° from the substrate. Resultant defects in the coating layer were examined using a brightfield microscope at a magnification of 50 \times (Mitutoyo, Kanagawa, Japan).

Quantitative assessments of the coatings' adhesion to titanium substrates and risks of delamination were obtained through a tensile adhesion protocol as follows (Figure 3.1)⁵⁵. The coated Ti6Al4V discs were fixed to aluminum dolly specimens with T-88 epoxy resin (System Three Resins, Inc., Lacey, WA, USA). The affixed samples were secured to a tension adapter in an Adelaide TCC universal testing machine (Adelaide Testing Machines, Toronto, ON, Canada), and forced apart at a speed of 3 mm/min. Each coating and treated titanium substrate were tested in triplicate ($n = 3$). Following separation, the site of delamination was carefully examined, with the coating adhesive strength calculated as:

$$\text{Adhesive Strength (MPa)} = \frac{\text{Load at Failure (N)}}{\text{Coated Area (m}^2\text{)}} \quad (1)$$

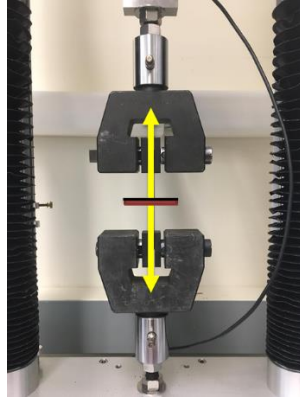


Figure 3.1 Adhesive tensile testing of hybrid coatings on titanium (Ti6Al4V) substrates. The coating (black line) and Ti6Al4V substrate (red line) are forced apart (yellow arrows) in an Adelaide TCC universal testing machine

3.2.5 Evaluation of Antimicrobial Properties

The antimicrobial properties of the hybrid coatings were evaluated against common Gram-positive and -negative bacterial pathogens. Their antimicrobial efficacies were assessed quantitatively against *Escherichia coli* (Gram-negative, ATCC[®] 25922) and *Staphylococcus aureus* (Gram-positive, ATCC[®] 25923) suspended in planktonic bacterial cultures and on their formation of adherent biofilms. Separate *E. coli* and *S. aureus* monocultures suspended in Luria Bertani (LB) medium were prepared from inoculum.

The coated discs were disinfected and sterilized in preparation for bacterial cultures. They were rinsed twice with ethanol (70% v/v), washed thrice with phosphate buffered saline (PBS), then placed in a tissue culture hood and exposed to UV light for 30 minutes to ensure sterility. Replicate coated discs ($n = 3/\text{coating}$) were submerged in each bacterial suspension of 10^5 CFU/mL and incubated at 37 °C under aerobic conditions. At predetermined times (1, 2, 4, ..., 24 h), samples of the bacterial suspension were withdrawn and their absorbance (OD₆₀₀) measured using a spectrophotometer (Agilent Technologies, Santa Barbara, CA, USA). Viable cells from the samples of bacterial suspension were counted by serial dilution and the spread plate method using 100 × 15 mm LB Agar plates.

Additional sterile coated discs ($n = 3/\text{coating}$) were submerged in each bacterial suspension of 10^5 CFU/mL and incubated at 37 °C under aerobic conditions for a period of 24 h. Following incubation, the coated discs were gently rinsed thrice with sterile PBS, transferred to sterile culture tubes containing 2 mL of fresh LB medium and subjected to ultrasonication for 5 min.

Viable bacteria were harvested from the sonicated samples and counted by serial dilution and the spread plate method using 100 × 15 mm LB Agar plates. The inhibition of bacterial biofilm formation was calculated with CFU_{control} representing colonies on uncoated control (Ti6Al4V) surfaces and CFU_{coating} being the colonies on each coating as:

$$\text{Bacterial Inhibition (\%)} = \frac{\text{CFU}_{\text{Control}} - \text{CFU}_{\text{Coating}}}{\text{CFU}_{\text{Control}}} \times 100 \quad (2)$$

3.2.6 Statistical Analysis

The data in this study were analyzed using GraphPad Prism software (V 6.01). All data are expressed as mean ± standard deviation. One-way ANOVA analyses were used to make comparisons among multiple groups. Group differences were specified using Tukey's post hoc tests with the differences considered statistically significant when $p < 0.05$.

3.3 Results and Discussion

3.3.1 Characterization of Coating Materials

The first step in this research was to successfully synthesize class II hybrid coating materials. Class II hybrids have been shown to display synergistic properties that complement the advantages of both organic and inorganic polymers⁵⁶. In this study, class II hybrid materials were developed using chitosan as an organic polymer component, GPTMS as a silane coupling agent and TEOS as an independent inorganic network agent. Initially, covalent coupling occurred between the epoxide functional group of GPTMS and the primary amine group of chitosan (Figure 3.2(A)). Concurrently, the acidic conditions of the reaction catalyzed the hydrolysis of ethoxysilane bonds to form Si–OH pendants. Following coupling, pre-hydrolyzed TEOS was added to the solution of functionalized chitosan, and polycondensation of the network proceeded to occur through the formation of Si–O–Si linkages. After the addition of hydrolyzed TEOS, some of the materials had aqueous suspensions of AgNPs added to their blend to create antimicrobial coatings.

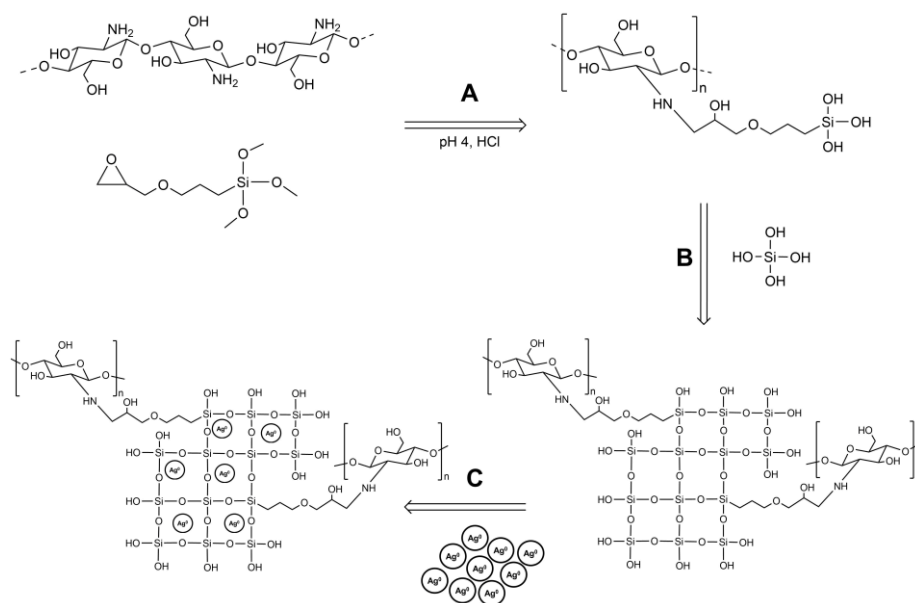


Figure 3.2 Chemical synthesis of chitosan–silica Class II hybrids and imbedding of silver nanoparticles (AgNPs). **(A)** Coupling of chitosan and 3-glycidyloxypropyltrimethoxysilane (GPTMS) in mildly acidic conditions; **(B)** polycondensation of coupled chitosan and hydrolyzed tetraethoxysilane (TEOS); **(C)** imbedding AgNPs into the hybrid sol network.

To verify that these coating materials were indeed class II hybrids, it was essential to confirm that there was covalent coupling between the organic and inorganic components. In this study, the coupling of chitosan using its primary amine functionality to GPTMS was evaluated, because the epoxide functional group of GPTMS is known to form covalent bonds with nucleophilic functional groups such as amines under acidic conditions⁵⁷. To observe these reactions between GPTMS and chitosan, ¹³C MAS-NMR spectroscopy was used. The coupling reaction could be followed by identifying the peak assignments previously described (Figure 3.3)⁴³. The ¹³C resonance labeled ‘6’ (associated with the carbon in the epoxide ring) at $\delta \sim 47$ ppm, showed that some of the epoxide rings of GPTMS had been opened by a nucleophilic attack of the primary amine of chitosan to form a secondary amine. There were no other reactions between chitosan and GPTMS identified, which indicated that the coupling occurred exclusively between the primary amine of chitosan and the epoxide of GPTMS. Indeed, these findings are consistent with what has been reported by others for the coupling of chitosan and GPTMS under similar conditions^{43,45}.

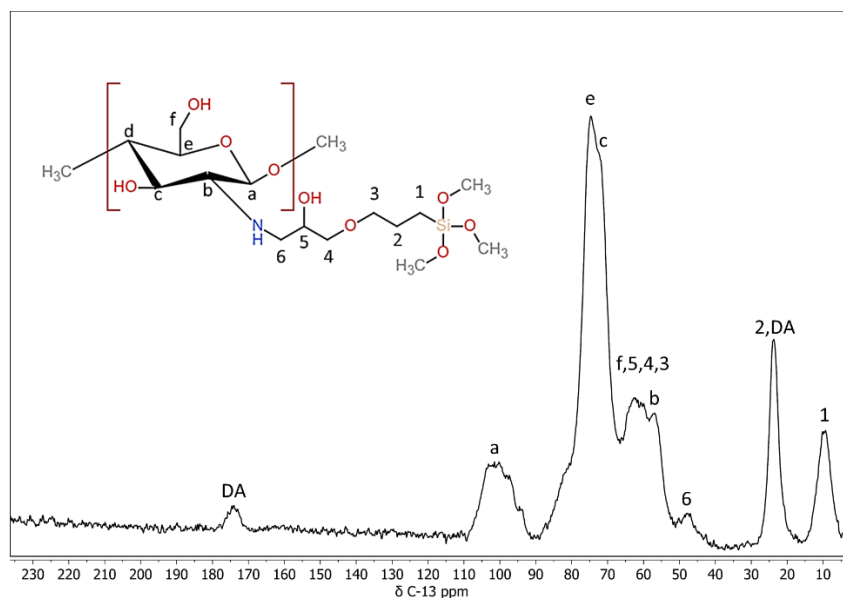


Figure 3.3 Characterization of covalent coupling in hybrid materials. ^{13}C Magic-angle spinning nuclear magnetic resonance (MAS-NMR) spectra of the hybrid material. Covalent coupling was confirmed by peak “6”, which was from a nucleophilic attack of the primary amine in chitosan on the epoxide of 3-glycidyloxypropyltrimethoxysilane (GPTMS). The absence of other peaks associated with coupling of these species indicated that the amine in chitosan was the sole site of coupling.

As a method to conveniently measure the degree of covalent coupling between chitosan and GPTMS, a ninhydrin assay was utilized (Figure 3.4). This assay enabled the detection of primary amine groups that may have remained uncoupled during the development of the hybrid materials. Through this colorimetric assay, the transformation of primary amines in the deacetylated units of chitosan to secondary amines upon coupling with the epoxide functional group of GPTMS, could be monitored.

A standard curve was established with the batch of chitosan used in this study, which had an 82% degree of deacetylation. It was compared to the chitosan coupled with GPTMS and showed that a 91% degree of crosslinking between chitosan and GPTMS was achieved. This high degree of coupling was closely monitored and maintained throughout the study, as variations in covalent coupling can yield large variations in the mechanical and thermomechanical properties of the resulting hybrid materials⁵⁸.

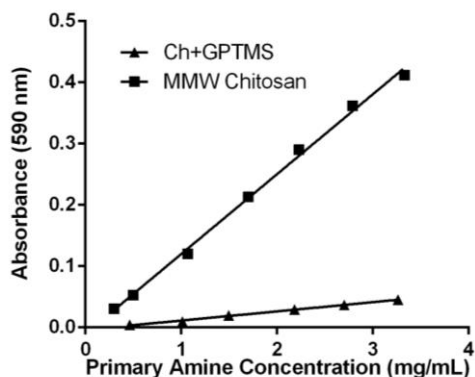


Figure 3.4 Quantitative analysis of covalent coupling between chitosan and 3-glycidyloxypropyltrimethoxysilane (GPTMS) by ninhydrin assay. In finely ground aqueous suspensions of coupled material (Ch+GPTMS) and uncoupled chitosan (MMW Chitosan), ninhydrin reagents selectivity for primary amines was measured by optical absorbance at 590 nm. The degree of covalent coupling between chitosan and GPTMS was measured to be 91% and maintained throughout the study.

SEM was utilized to examine the roughened surface morphologies and microtopographies of the hybrid coating films (Figure 3.5A). A common standardized acid-etching protocol was applied to bare titanium to achieve a roughened substrate topography. To coat these roughened Ti6Al4V substrates, a dip coating protocol was utilized that has been shown to effectively deposit thin films from hybrid sols⁵⁹⁻⁶¹. The thinness of the hybrid coating films ensured that there was a degree of roughness attributed to their acid-etched substrates. The coated surfaces retained a degree of microscale roughness that has been shown to provide a positive topographical stimulus for cell interactions and bone apposition⁶²⁻⁶⁴.

The accompanying EDX analyses and elemental mapping of silicon, oxygen, nitrogen, carbon and silver (Figure 3.5B–F)) showed their distribution across the coated surfaces. All elements were found to be homogeneously distributed throughout the coating matrix for all samples. The distribution of silicon (Figure 3.5B) confirmed the presence of silanol and siloxane networks in the hybrid coatings and their homogenous nature throughout the matrix. The distribution of nitrogen (Figure 3.5D) and carbon (Figure 3.5E) confirmed the presence of an organic chitosan network that was homogeneously integrated throughout the coatings. Additionally, the detection of silver (Figure 3.5F) confirmed the successful incorporation and homogenous distribution of antimicrobial AgNPs throughout the coating matrix.

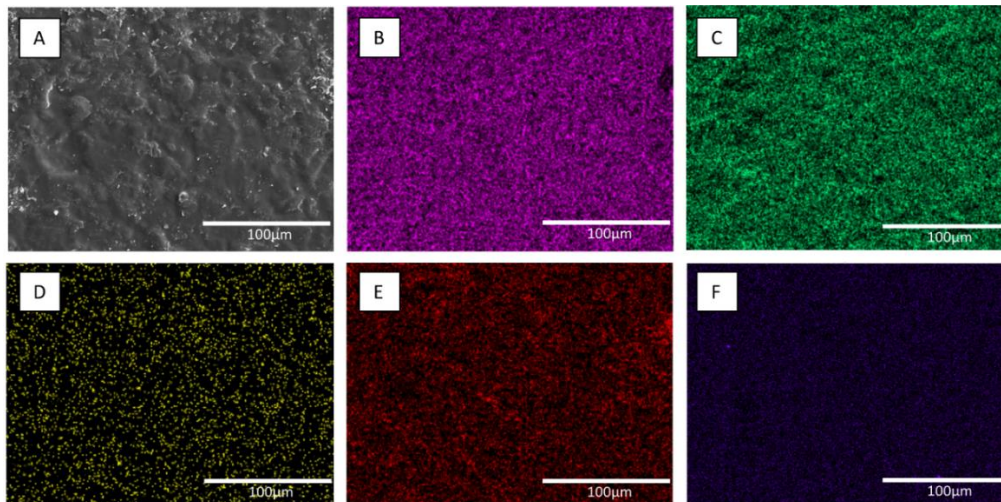


Figure 3.5 Scanning electron microscopy (SEM) and elemental (EDX) analysis of the 40% ChSi-nAg hybrid coating. SEM showed smooth undulating contours and microtopographies (A). EDX mapping detected a homogenous distribution of silicon (B), oxygen (C), nitrogen (D), carbon (E) and silver (F). The SEM/EDX analyses were representative and consistent across all coatings. Scale bar: 100 μm .

The AgNPs was synthesized through supplementary procedures. Their nanoscale dimensions were confirmed by transmission electron microscopy (TEM). Micrographs (Figure 3.6A) showed that all synthesized nanoparticles were under 100 nm in size and UV spectroscopy (Figure 3.6B) confirmed the consistency of their colloidal suspensions. The PVP-capped nanoparticles synthesized in this study, were maintained within 10–20 nm and exhibited long-term colloidal stability in aqueous solutions, before being incorporated into the chitosan–silica hybrid sol–gel system for coating.

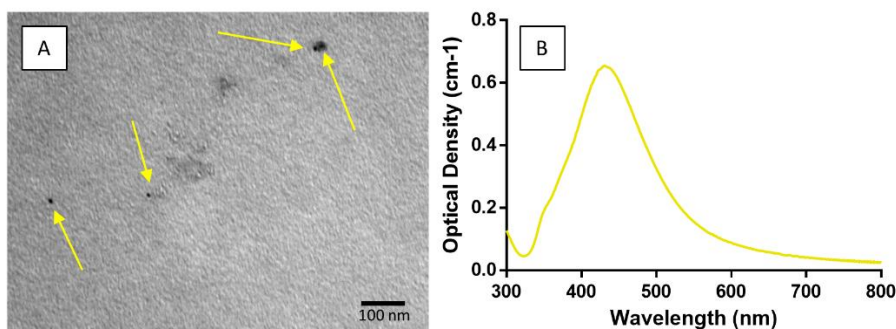


Figure 3.6 Evaluation of synthesized AgNPs. (A) Transmission electron microscopy (TEM) confirmed nanoscale particle sizes. (B) UV spectroscopy of AgNP suspensions verified their consistency.

Through the utilization of class II covalent coupling reactions, highly homogenous hybrid coatings were created. The homogenous coating matrices are consistent with enhanced mechanical properties. In contrast, coating materials that lack homogeneity have been shown to have inconsistent mechanical properties and result in areas across coating surfaces that have inconsistent resorption properties^{65,66}. Indeed, a lack of homogeneity in the HA coating materials that are currently available has limited their clinical usage and success. They have been shown to suffer from phase inconsistency and resultant discrepancies in their mechanical properties^{67,68}.

ATR-FTIR analyses were used to compare the variation in chemical properties between different coating blends (Figure 3.7). For pure chitosan, the peaks associated with the stretching of the primary and secondary amines were identified at 1526 cm⁻¹ and 1635 cm⁻¹, respectively. As expected, these peaks decreased in intensity as the organic content of the hybrid coating blends decreased (80%, 60%, 40% and 20% ChSi), and were completely absent for the purely inorganic TEOS-based material. When comparing the intensity of these peaks for pure chitosan and the coupled chitosan samples (Ch+GPTMS), there was a decrease observed in the relative intensities for the primary amine in chitosan and no change for the secondary amine. This showed that the coupling reaction had only occurred between the primary amine in chitosan and GPTMS, confirming the findings of ¹³C MAS-NMR and the ninhydrin assay.

Additionally, the incorporation of GPTMS into these hybrid materials was detected by the bond stretching associated with the epoxide group identified at 910 cm⁻¹ (Figure 3.7). This epoxide peak was observed in pure coupled samples (Ch+GPTMS) and faintly in the more highly organic

blends (80% and 60% ChSi). As the inorganic fraction increased, this peak was progressively eclipsed by the consequent stretching of the silanol species at 935 cm^{-1} . The incorporation of silane species into the hybrid coatings was observed as peaks from the stretching of the Si–OH bond at 774 cm^{-1} and 935 cm^{-1} in the hydrolyzed material and the stretching of the Si–O–Si bonds at 1065 cm^{-1} from condensed siloxane. As expected, the presence of these peaks became more prevalent as the organic content decreased in the hybrid coating blends.

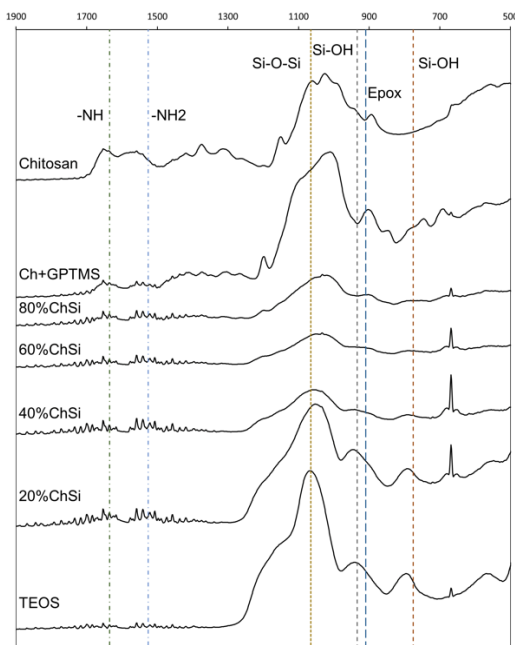


Figure 3.7 Infrared analyses of chemical structures in hybrid materials. Total reflectance Fourier transform infrared (ATR-FTIR) spectra of chitosan, chitosan coupled with 3-glycidyloxypropyltrimethoxysilane (Ch+GPTMS), hybrid materials (80%–20% ChSi) and pure inorganic siloxane (condensed TEOS). There were more peaks attributed to chitosan and GPTMS (-NH, -NH₂, Epox) for hybrid materials with higher organic content. Their chemical characteristics were more similar to a purely inorganic siloxane network (Si–O–Si, Si–OH), as the organic fraction decreased.

3.3.2 Material Properties

For all biomaterials, surface interactions with surrounding physiological fluids that may include the adsorption of serum proteins, are an important determinant of subsequent cellular responses and the ingrowth of host tissues⁶⁹. To predict these interactions, the measurement of water contact angles on the biomaterial surfaces are an effective metric. Surfaces with contact angles

between 60° and 85° are intermediate in hydrophilicity, and have been shown to facilitate the most favorable interactions with host tissues through enhanced cell growth and proliferation^{59,70,71}.

All hybrid coatings that were developed in this study had an intermediate degree of hydrophilicity (Figure 3.8). The coating blend with the least organic content (20% ChSi) had the largest water contact angle and was a little more hydrophobic than the 60% ChSi blend, which had the smallest contact angle and was the most hydrophilic. However, these differences between the blends were small and not statistically significant ($p > 0.05$). However, all coatings had contact angles that were larger than their uncoated acid-etched Ti6Al4V substrate and these differences were statistically significant ($p < 0.05$). Although the coating blends contained many hydrophilic chemistries due to their chitosan content and the remaining silanol linkages, the bare acid-etched Ti6Al4V substrates had a high degree of surface roughness, which enhanced their wettability. For such wettable surfaces (contact angles $< 90^\circ$), an increase in surface roughness has been reported to enhance their hydrophilicity⁷². The acid-etching of Ti6Al4V substrates created numerous pits and valleys ranging in size from 10–40 μm (Figure 3.9), which enhanced their surface roughness and thereby their hydrophilicity. The deposition of coatings on these substrates partially filled these pits and valleys, which reduced their surface roughness and increased water contact angles.

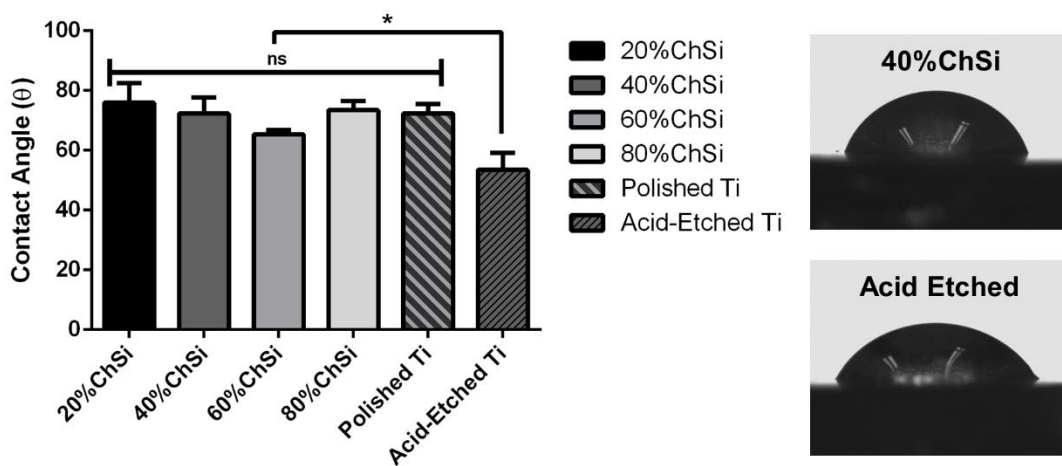


Figure 3.8 Water contact angles for coatings and titanium (Ti6Al4V) substrates. Static water contact angles ($n = 5/\text{surface}$) for all coatings and polished Ti6Al4V were similar with an

intermediate degree of hydrophilicity. Contact angles for acid-etched Ti6Al4V were significantly ($p < 0.05$) lower and more hydrophilic. ns—not significantly different; *—statistically significant difference.

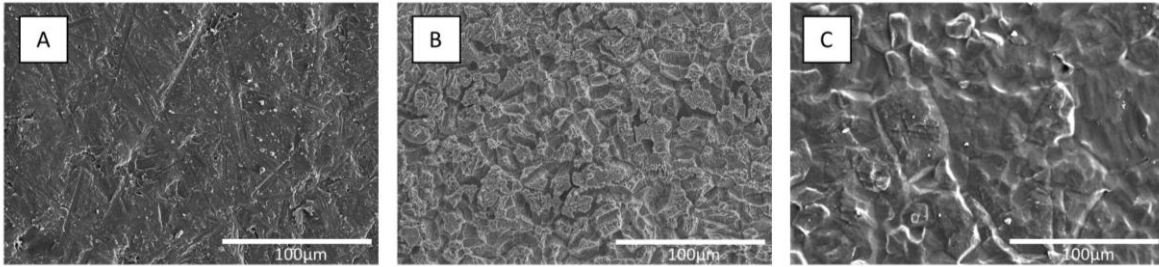


Figure 3.9 Scanning electron microscopy (SEM) of titanium (Ti6Al4V) substrates and coated surfaces. (A) Polished Ti6Al4V was flat with smoothly scalloped surfaces; (B) acid-etched Ti6Al4V had extensive surface fissures that created microscale roughness; (C) hybrid coating (60% ChSi) films on acid-etched Ti6Al4V substrates retained microtopographical features and surface roughness. SEM analyses were representative and consistent across all coatings.

Biomaterial coatings also require adequate adhesive bond strength to their underlying substrates, which is an important parameter that is often overlooked in many studies. Poor adhesive strength may lead to delamination of the coating, which then causes inflammation, bone resorption, loosening of the fixtures and eventually the failure of intraosseous implants^{73,74}.

Initially, the adhesion of the hybrid coatings to Ti6Al4V substrates was evaluated by a cross-hatch delamination protocol as described in ASTM D3359. This method provided a coarse assessment of overall coating adhesion. Additionally, the scoring of the coating materials imparted stresses within their structure, which manifest as extensive cracks and fissures across the surfaces of the purely inorganic controls (Figure 3.10C,D). The purely inorganic coatings were brittle, and cross-hatch testing had led to a widespread cracking of their thin films. In clinical applications, the impact of sharp bony protrusions and/or surgical instruments could lead to a premature failure of such coatings *in vivo*⁷⁵. In contrast, all hybrid coatings exhibited highly robust, intact and integrated surfaces, despite the surface scoring (Figure 3.10A–B).

Additionally, more rigorous and quantitative evaluations of coating adhesion and risk of delamination were performed by adhesive tensile tests based on established protocols^{55,76}. All coatings were assessed for their adhesion to both polished and acid-etched Ti6Al4V substrates (Figure 3.11). All hybrid coatings were significantly ($p < 0.05$) more adherent to acid-etched

Ti6Al4V substrates than to polished titanium. Furthermore, all coating blends that contained AgNPs exhibited identical adhesion characteristics to those without these antimicrobial additives (excluded from figure to ensure clarity). As expected, acid-etching like other surface roughening pretreatments, enhances adherence to the modified substrate⁷⁷⁻⁷⁹. This has been attributed to the increase in bonding area by roughening pretreatments, which thereby enhance the mechanical adhesion of coatings to their substrates. However, purely organic chitosan control coatings showed only a small, statistically insignificant ($p > 0.05$) increase in adhesion to the acid-etched substrate compared to polished Ti6Al4V. This may have been due to the high viscosity of pure chitosan, which led to poor wetting of Ti6Al4V substrates, and lower overall mechanical adhesion compared to that of hybrid coating blends⁷⁹.

Among implant coating materials that are commercially available, plasma sprayed hydroxyapatite (HA) surfaces remain a gold standard for intraosseous applications. However, their preparations involve high temperatures and variable cooling cycles, which retain residual stresses that contribute to failures from adhesive forces of less than 10 MPa⁸⁰⁻⁸². Therefore, the robust adhesion (16–18 MPa) for all hybrid coatings deposited on acid-etched Ti6Al4V that were developed in this research, warrant further study.

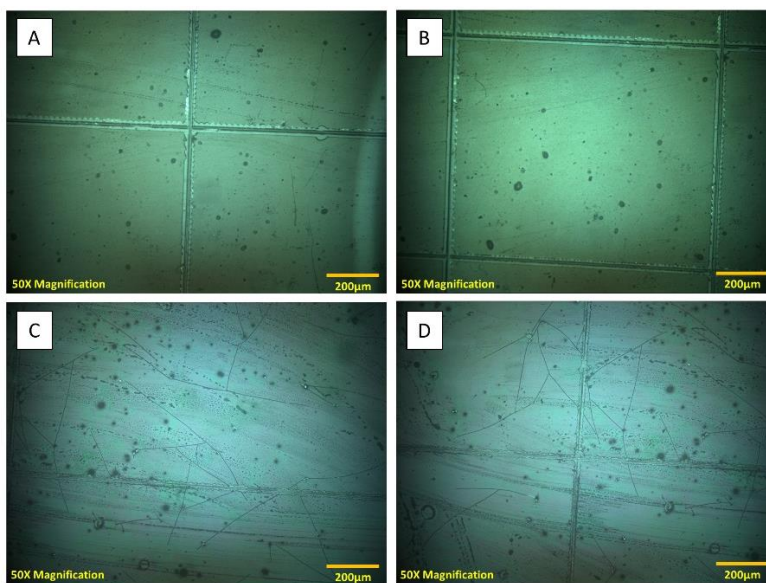


Figure 3.10 Microscopic examination of coatings in cross-hatch tests of adhesion. (A,B) Coating (60% ChSi) surfaces were unblemished by full-depth incisions in the standardized cross-

hatch adhesion protocol; (C,D) inorganic siloxane material (control) developed extensive arrays of surface cracks and fissures from the same cross-hatch testing protocol. Adhesion of the 60% ChSi coating blend was representative and consistent across all hybrid coatings.

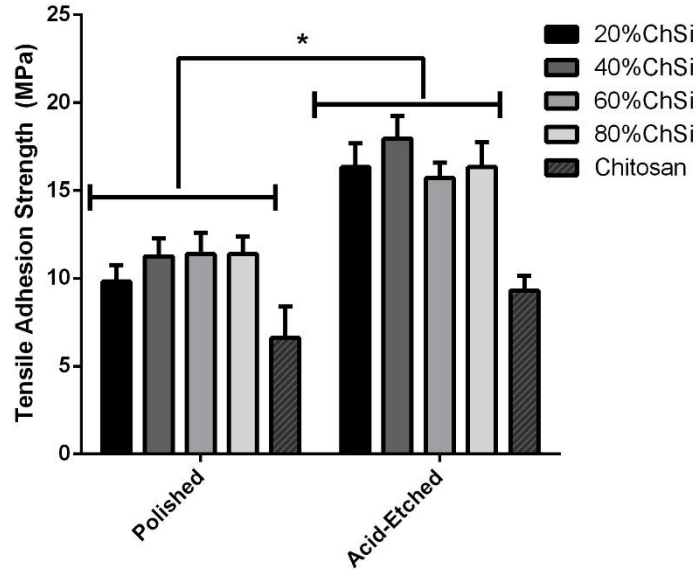


Figure 3.11 Adhesive tensile strengths of coatings and chitosan on titanium (Ti6Al4V) substrates. All hybrid coatings (n = 3/surface) had significantly ($p < 0.05$) more adhesion to acid-etched than to polished Ti6Al4V substrates. All hybrid coatings were more adhesive than pure chitosan to both polished and acid-etched Ti6Al4V. *—statistically significant difference

3.3.3 Antimicrobial Properties

As bacterial infections are the most common cause of implant failure⁷⁻⁹, the application of antimicrobial surface coatings may afford a valuable feature for implantable materials.

Therefore, the coatings in this study were prepared with chitosan as the main organic constituent, which naturally displays some antimicrobial activity. Additionally, some of these coatings were loaded with AgNPs as additives that could further enhance their antimicrobial effects.

Antimicrobial efficacies were evaluated on *S. aureus* and *E. coli* cultures, which are common Gram-positive and Gram-negative bacterial pathogens, respectively, associated with various bodily infections.

Interestingly, the *S. aureus* and *E. coli* cultures were only minimally affected by the base coatings that had not been loaded with AgNPs (Figure 3.12). However, *E. coli* growth was markedly reduced over 24 h, and *S. aureus* growth was completely suppressed for 24 h, with all coatings that contained AgNPs.

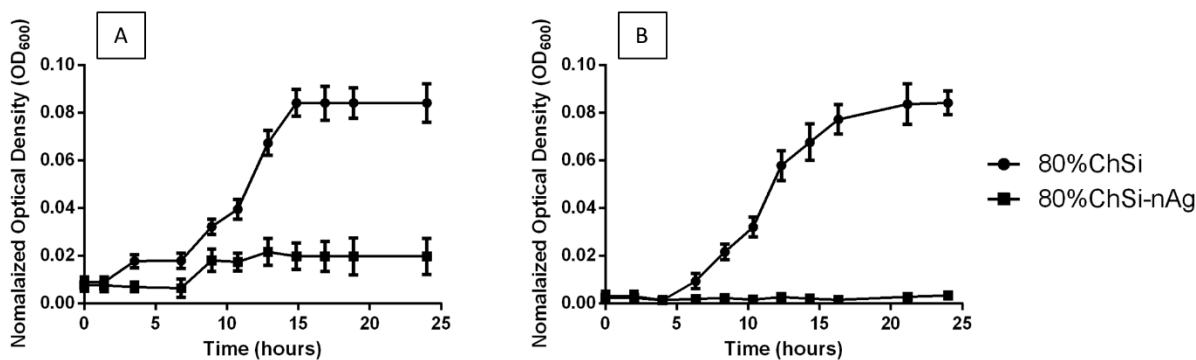


Figure 3.12 Inhibition of bacterial growth in planktonic cultures. There was a (A) marked reduction in *E. coli* growth and (B) complete inhibition of *S. aureus* grown in the presence of 80% ChSi-nAg compared to 80% ChSi. This inhibition of bacterial growth by 80% ChSi-nAg was representative and consistent for all hybrid coatings that contained AgNPs.

The quantitative assessments of these bacterial cultures following 24 h incubations with hybrid coatings showed that there had been some inhibition by all coatings, when compared to uncoated titanium controls (Figure 3.13). The planktonic *E. coli* and *S. aureus* cultures were almost completely inhibited (80%–100% and 75%–77%, respectively) by the presence of coatings that had been loaded with AgNPs. Indeed, coatings loaded with AgNPs were significantly ($p < 0.05$) more effective than base coatings without AgNPs, which had only minimal antibacterial effects (<30%). These results indicated that release-based mechanisms were involved in the antimicrobial properties of the hybrid coatings. They were bacteriostatic and/or bactericidal effects on some of the most common bacterial pathogens that cause opportunistic infections.

Additionally, coatings loaded with AgNPs appeared to have been more effective against *E. coli* cultures, than *S. aureus*. This difference may have been due to the release-based antimicrobial action of AgNPs through the different cell wall structures of these bacteria. Unlike Gram-negative *E. coli* planktonic cells, Gram-positive bacteria such as *S. aureus* are protected from their external environment by much thicker peptidoglycan layers within their cell walls⁸³. These

cell walls may have partially limited the internalization of AgNPs and retarded their release-based action. Similarly, previous studies have reported that Gram-negative bacteria experienced more membrane damage and oxidative stress in response to the release-based action of AgNPs, than Gram-positive bacteria^{84–86}.

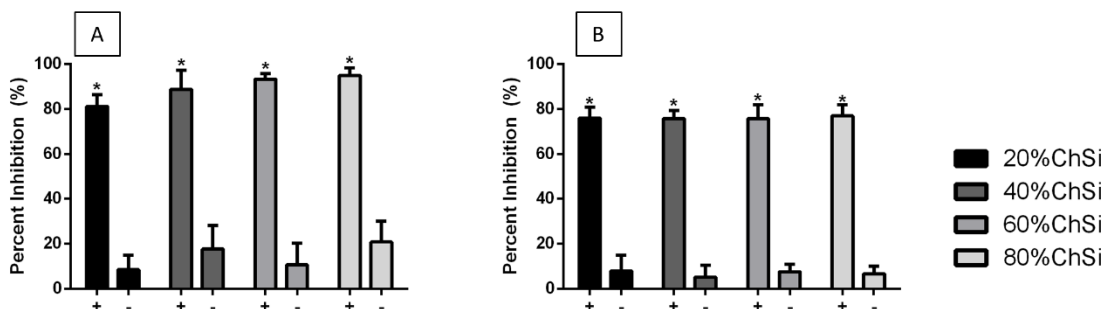


Figure 3.13 Inhibition of bacterial cultures by hybrid coatings with (+) and without (-) AgNPs. (A) *E. coli* and (B) *S. aureus* cultures were inhibited by incubation (24 hours) with all hybrid coatings, compared to uncoated titanium (Ti6Al4V) controls. There was little inhibition from base coatings without AgNPs, but significantly ($p < 0.05$) more and almost total inhibition for coatings loaded with AgNPs.

In addition to the virulence of planktonic cells within bacterial cultures, these pathogens can be particularly pernicious due to their formation of highly adherent biofilms on biomaterial surfaces. In contrast to cells suspended in culture, bacteria encased within biofilms are highly resistant to mechanical dislodgement and antibiotic treatment^{8,10}. Therefore, *E. coli* and *S. aureus* biofilm formation on coatings were carefully compared to uncoated Ti6Al4V controls for inhibitory effects.

Indeed, both *E. coli* and *S. aureus* were clearly inhibited for at least 24 h in their formation of biofilms on all hybrid coatings, compared to uncoated Ti6Al4V controls (Figure 3.14). Base coatings alone were moderately effective at inhibiting *E. coli* biofilm formation on their surfaces (31%–50%) and were even more effective against *S. aureus* (38%–80%). However, the coatings loaded with AgNPs were markedly more effective at inhibiting *E. coli* biofilm formation (60%–95%), and almost completely effective against *S. aureus* (90%–95%). The coatings with AgNPs were significantly ($p < 0.05$) more effective than their unloaded controls for all blends, except those that had a high organic chitosan content. This accompanied the positive trend of greater antimicrobial activity with increasing chitosan content. As chitosan is a naturally antimicrobial

polysaccharide, its role in the coating network was expected to have had this effect on both the inhibition of biofilm formation and the inhibition of bacterial cultures⁸⁷.

The larger inhibition of *S. aureus* compared to *E. coli* biofilms contrasted with the reduced susceptibility of *S. aureus* than *E. coli* cells in culture. This may have been due to differences in their development of extracellular polymeric substances (EPS). Mainly composed of polysaccharides and proteins, the EPS produced by sessile colonies of bacteria has been shown to be a key component in their resistance to antibiofilm agents such as cationic peptides and metal ions⁸⁸. Additionally, the EPS production of sessile colonies has been shown to be enhanced when colonies adhere to toxic surfaces⁸⁹. Therefore, the sessile colonies of *E. coli* may have provided some resistance to the coatings by producing more EPS during biofilm formation. Indeed, prior studies have reported that *E. coli* exhibit rapid EPS formation when compared to their Gram-positive counterparts, leading to a more effective resistance in their sessile state^{84,90}.

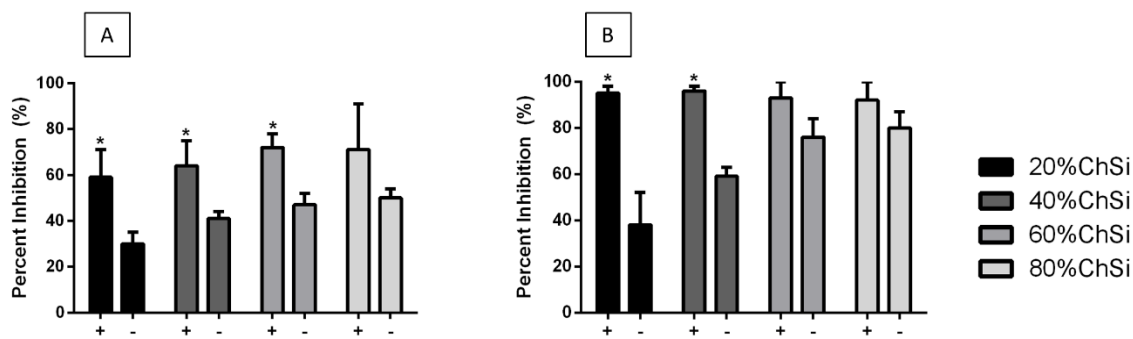


Figure 3.14 Inhibition of bacterial biofilm formation on hybrid coatings with (+) and without (-) AgNPs. (A) *E. coli* and (B) *S. aureus* biofilm formation (24 h) were inhibited on all hybrid coatings, compared to uncoated titanium (Ti6Al4V) controls. Inhibition of biofilm formation was greater on coatings that contained AgNPs and was generally more on coatings with higher organic content. There was near complete inhibition of *S. aureus* biofilms on all hybrid coatings that contained AgNPs.

3.4 Conclusions

In this study, chitosan–silica class II hybrid materials were developed as thin film coatings for implantable Ti6Al4V surfaces. Additionally, the hybrid coatings were effectively loaded with AgNPs for antimicrobial applications. Their chemical structures and composition were

confirmed by MAS-NMR, FTIR and EDX analyses. Surface microtopographies, mechanical properties and wettability were evaluated by SEM, adhesive tensile testing and water contact angles. Antimicrobial properties were assessed in *E. coli* and *S. aureus* cultures and on their biofilm formation.

The hybrid coatings demonstrated strong covalent linkages between their organic chitosan backbone and the silica inorganic network. There was a homogenous dispersion of elements, including AgNP additives, across their surfaces. Hybrid coatings demonstrated a robust resistance to fracture and dislodgement and were highly adherent to acid-etched Ti6Al4V substrates, especially when compared to purely organic or inorganic materials. They exhibited moderate levels of roughness, microtopography and wettability when compared with uncoated Ti6Al4V surfaces. All hybrid coatings displayed some antimicrobial effects and greater organic chitosan content was associated with increased bacterial inhibition. Additionally, coatings loaded with AgNPs showed marked inhibition of planktonic bacteria and their biofilms, with near complete inhibition of *E. coli* cultures and of *S. aureus* biofilm formation. These robust, retentive and antimicrobial coatings for implantable titanium materials were based on rudimentary chitosan–silica coupling processes, which may afford a novel strategy for biomaterial applications.

3.5 References

- (1) Greger, M.; Widomská, M.; Snášel, V. Structure and Properties of Dental Implants. In *METAL 2012 - Conference Proceedings, 21st International Conference on Metallurgy and Materials*; 2012; Vol. 120, pp 434–439.
- (2) Darouiche, R. O. Treatment of Infections Associated with Surgical Implants. *Infect. Dis. Clin. Pract.* **2004**, *12* (4), 258–259.
- (3) Chouirfa, H.; Bouloussa, H.; Migonney, V.; Falentin-daudré, C. Review of Titanium Surface Modification Techniques and Coatings for Antibacterial Applications. *Acta Biomater.* **2018**.
- (4) Camps-Font, O.; Figueiredo, R.; Valmaseda-Castellón, E.; Gay-Escoda, C. Postoperative Infections after Dental Implant Placement: Prevalence, Clinical Features, and Treatment. *Implant Dent.* **2015**, *24* (6), 713–719.
- (5) Mah, T. F.; Pitts, B.; Pellock, B.; Walker, G. C.; Stewart, P. S.; O’Toole, G. A. A Genetic Basis for Pseudomonas Aeruginosa Biofilm Antibiotic Resistance. *Nature* **2003**, *426* (6964), 306–310.
- (6) Yoda, I.; Koseki, H.; Tomita, M.; Shida, T.; Horiuchi, H.; Sakoda, H.; Osaki, M. Effect of Surface Roughness of Biomaterials on Staphylococcus Epidermidis Adhesion. *BMC*

- Microbiol.* **2014**, *14* (1), 1–7.
- (7) Privett, B. J.; Youn, J.; Hong, S. A.; Lee, J.; Han, J.; Shin, J. H.; Schoenfisch, M. H. Antibacterial Fluorinated Silica Colloid Superhydrophobic Surfaces. *Langmuir* **2011**, *27* (15), 9597–9601.
 - (8) Yu, K.; Lo, J. C. Y.; Yan, M.; Yang, X.; Brooks, D. E.; Hancock, R. E. W.; Lange, D.; Kizhakkedathu, J. N. Anti-Adhesive Antimicrobial Peptide Coating Prevents Catheter Associated Infection in a Mouse Urinary Infection Model. *Biomaterials* **2017**, *116*, 69–81.
 - (9) Swartjes, J. J. T. M.; Sharma, P. K.; Kooten, T. G.; Mei, H. C.; Mahmoudi, M.; Busscher, H. J.; Rochford, E. T. J. Current Developments in Antimicrobial Surface Coatings for Biomedical Applications. *Curr. Med. Chem.* **2014**, *22* (18), 2116–2129.
 - (10) Radin, S.; Ducheyne, P. Controlled Release of Vancomycin from Thin Sol-Gel Films on Titanium Alloy Fracture Plate Material. *Biomaterials* **2007**, *28* (9), 1721–1729.
 - (11) Bračić, M.; Fras-Zemljič, L.; Pérez, L.; Kogej, K.; Stana-Kleinschek, K.; Kargl, R.; Mohan, T. Protein-Repellent and Antimicrobial Nanoparticle Coatings from Hyaluronic Acid and a Lysine-Derived Biocompatible Surfactant. *J. Mater. Chem. B* **2017**, *5* (21), 3888–3897.
 - (12) Zhang, X.; Chaimayo, W.; Yang, C.; Yao, J.; Miller, B. L.; Yates, M. Z. Silver-Hydroxyapatite Composite Coatings with Enhanced Antimicrobial Activities through Heat Treatment. *Surf. Coatings Technol.* **2017**, *325*, 39–45.
 - (13) Tabesh, E.; Salimijazi, H.; Kharaziha, M.; Hejazi, M. Antibacterial Chitosan-Copper Nanocomposite Coatings for Biomedical Applications. *Mater. Today Proc.* **2018**, *5* (7), 15806–15812.
 - (14) Stewart, P. S.; William Costerton, J. Antibiotic Resistance of Bacteria in Biofilms. *Lancet* **2001**, *358* (9276), 135–138.
 - (15) Jones, N.; Ray, B.; Ranjit, K. T.; Manna, A. C. Antibacterial Activity of ZnO Nanoparticle Suspensions on a Broad Spectrum of Microorganisms. *FEMS Microbiol. Lett.* **2008**, *279* (1), 71–76.
 - (16) Rai, M.; Kon, K.; Ingle, A.; Duran, N.; Galdiero, S.; Galdiero, M. Broad-Spectrum Bioactivities of Silver Nanoparticles: The Emerging Trends and Future Prospects. *Appl. Microbiol. Biotechnol.* **2014**, *98* (5), 1951–1961.
 - (17) Kim, J. S.; Kuk, E.; Yu, K. N.; Kim, J. H.; Park, S. J.; Lee, H. J.; Kim, S. H.; Park, Y. K.; Park, Y. H.; Hwang, C. Y.; et al. Antimicrobial Effects of Silver Nanoparticles. *Nanomedicine Nanotechnology, Biol. Med.* **2007**, *3* (1), 95–101.
 - (18) Lara, H. H.; Ayala-Núñez, N. V.; del Turrent, L. C. I.; Padilla, C. R. Bactericidal Effect of Silver Nanoparticles against Multidrug-Resistant Bacteria. *World J. Microbiol. Biotechnol.* **2010**, *26* (4), 615–621.
 - (19) Zhao, L.; Wang, H.; Huo, K.; Cui, L.; Zhang, W.; Ni, H.; Zhang, Y.; Wu, Z.; Chu, P. K. Antibacterial Nano-Structured Titania Coating Incorporated with Silver Nanoparticles. *Biomaterials* **2011**, *32* (24), 5706–5716.

- (20) Woo, K. J.; Hye, C. K.; Ki, W. K.; Shin, S.; So, H. K.; Yong, H. P. Antibacterial Activity and Mechanism of Action of the Silver Ion in Staphylococcus Aureus and Escherichia Coli. *Appl. Environ. Microbiol.* **2008**, *74* (7), 2171–2178.
- (21) Kvítek, L.; Panáček, A.; Soukupová, J.; Kolář, M.; Večeřová, R.; Pucek, R.; Holecová, M.; Zbořil, R. Effect of Surfactants and Polymers on Stability and Antibacterial Activity of Silver Nanoparticles (NPs). *J. Phys. Chem. C* **2008**, *112* (15), 5825–5834.
- (22) Sotiriou, G. A.; Pratsinis, S. E. Antibacterial Activity of Nanosilver Ions and Particles. *Environ. Sci. Technol.* **2010**, *44* (14), 5649–5654.
- (23) Ong, J. L.; Lucas, L. C. Post-Deposition Heat Treatments for Ion Beam Sputter Deposited Calcium Phosphate Coatings. *Biomaterials* **1994**, *15* (5), 337–341.
- (24) Li, T.; Lee, J.; Kobayashi, T.; Aoki, H. Hydroxyapatite Coating by Dipping Method, and Bone Bonding Strength. *J. Mater. Sci. Mater. Med.* **1996**, *7* (6), 355–357.
- (25) Wang, B. C.; Lee, T. M.; Chang, E.; Yang, C. Y. The Shear Strength and the Failure Mode of Plasma-Sprayed Hydroxyapatite Coating to Bone: The Effect of Coating Thickness. *J. Biomed. Mater. Res.* **1993**, *27* (10), 1315–1327.
- (26) Hamed, H.; Moradi, S.; Hudson, S. M.; Tonelli, A. E. Chitosan Based Hydrogels and Their Applications for Drug Delivery in Wound Dressings: A Review. *Carbohydr. Polym.* **2018**, *199* (June), 445–460.
- (27) Quiñones, J. P.; Peniche, H.; Peniche, C. Chitosan Based Self-Assembled Nanoparticles in Drug Delivery. *Polymers (Basel)*. **2018**, *10* (3), 1–32.
- (28) Wang, T.; Hou, J.; Su, C.; Zhao, L.; Shi, Y. Hyaluronic Acid-Coated Chitosan Nanoparticles Induce ROS-Mediated Tumor Cell Apoptosis and Enhance Antitumor Efficiency by Targeted Drug Delivery via CD44. *J. Nanobiotechnology* **2017**, *15* (1), 1–12.
- (29) Oryan, A.; Sahviah, S. Effectiveness of Chitosan Scaffold in Skin, Bone and Cartilage Healing. *Int. J. Biol. Macromol.* **2017**, *104*, 1003–1011.
- (30) Zhang, J.; Lu, X.; Feng, G.; Gu, Z.; Sun, Y.; Bao, G.; Xu, G.; Lu, Y.; Chen, J.; Xu, L.; et al. Chitosan Scaffolds Induce Human Dental Pulp Stem Cells to Neural Differentiation: Potential Roles for Spinal Cord Injury Therapy. *Cell Tissue Res.* **2016**, *366* (1), 129–142.
- (31) Saravanan, S.; Sareen, N.; Abu-El-Rub, E.; Ashour, H.; Sequiera, G. L.; Ammar, H. I.; Gopinath, V.; Shamaa, A. A.; Sayed, S. S. E.; Moudgil, M.; et al. Graphene Oxide-Gold Nanosheets Containing Chitosan Scaffold Improves Ventricular Contractility and Function After Implantation into Infarcted Heart. *Sci. Rep.* **2018**, *8* (1), 1–13.
- (32) Vil’Danova, R. R.; Sigaeva, N. N.; Kukovinets, O. S.; Volodina, V. P.; Spirikhin, L. V.; Zaidullin, I. S.; Kolesov, S. V. Modification of Hyaluronic Acid and Chitosan, Aimed at Developing Hydrogels for Ophthalmology. *Russ. J. Appl. Chem.* **2014**, *87* (10), 1547–1557.
- (33) De Oliveira Fulgêncio, G.; Viana, F. A. B.; Silva, R. O. S.; Lobato, F. C. F.; Ribeiro, R. R.; Fanca, J. R.; Byrro, R. M. D.; Faraco, A. A. G.; da Silva Cunha-Júnior, A.

- Mucoadhesive Chitosan Films as a Potential Ocular Delivery System for Ofloxacin: Preliminary in Vitro Studies. *Vet. Ophthalmol.* **2014**, *17* (2), 150–155.
- (34) Zhu, X.; Xu, D.; Zhu, X.; Li, L.; Li, H.; Guo, F.; Chen, X.; Tan, Y.; Xie, L. Evaluation of Chitosan/Aptamer Targeting TGF- β Receptor II Thermo-Sensitive Gel for Scarring in Rat Glaucoma Filtration Surgery. *Investig. Ophthalmol. Vis. Sci.* **2015**, *56* (9), 5465–5476.
- (35) Avcu, E.; Baştan, F. E.; Abdullah, H. Z.; Rehman, M. A. U.; Avcu, Y. Y.; Boccaccini, A. R. Electrophoretic Deposition of Chitosan-Based Composite Coatings for Biomedical Applications: A Review. *Prog. Mater. Sci.* **2019**, *103* (January), 69–108.
- (36) Neto, A. I.; Cibrão, A. C.; Correia, C. R.; Carvalho, R. R.; Luz, G. M.; Ferrer, G. G.; Botelho, G.; Picart, C.; Alves, N. M.; Mano, J. F. Nanostructured Polymeric Coatings Based on Chitosan and Dopamine-Modified Hyaluronic Acid for Biomedical Applications. *Small* **2014**, *10* (12), 2459–2469.
- (37) Tang, J.; Liu, Y.; Zhu, B.; Su, Y.; Zhu, X. Preparation of Paclitaxel/Chitosan Co-Assembled Core-Shell Nanofibers for Drug-Eluting Stent. *Appl. Surf. Sci.* **2017**, *393*, 299–308.
- (38) Tian, D.; Dubois, P.; Jérôme, R. Biodegradable and Biocompatible Inorganic-Organic Hybrid Materials. I. Synthesis and Characterization. *J. Polym. Sci. Part A Polym. Chem.* **1997**, *35* (11), 2295–2309.
- (39) Valliant, E. M.; Jones, J. R. Softening Bioactive Glass for Bone Regeneration: Sol-Gel Hybrid Materials. *Soft Matter* **2011**, *7* (11), 5083–5095.
- (40) Sachot, N.; Castaño, O.; Mateos-Timoneda, M. A.; Engel, E.; Planell, J. A. Hierarchically Engineered Fibrous Scaffolds for Bone Regeneration. *J. R. Soc. Interface* **2013**, *10* (88), 2–6.
- (41) Mahony, O.; Tsigkou, O.; Ionescu, C.; Minelli, C.; Ling, L.; Hanly, R.; Smith, M. E.; Stevens, M. M.; Jones, J. R. Silica-Gelatin Hybrids with Tailorable Degradation and Mechanical Properties for Tissue Regeneration. *Adv. Funct. Mater.* **2010**, *20* (22), 3835–3845.
- (42) Shirosaki, Y.; Tsuru, K.; Hayakawa, S.; Osaka, A.; Lopes, M. A.; Santos, J. D.; Fernandes, M. H. In Vitro Cytocompatibility of MG63 Cells on Chitosan-Organosiloxane Hybrid Membranes. *Biomaterials* **2005**, *26* (5), 485–493.
- (43) Wang, D.; Romer, F.; Connell, L.; Walter, C.; Saiz, E.; Yue, S.; Lee, P. D.; McPhail, D. S.; Hanna, J. V.; Jones, J. R. Highly Flexible Silica/Chitosan Hybrid Scaffolds with Oriented Pores for Tissue Regeneration. *J. Mater. Chem. B* **2015**, *3* (38), 7560–7576.
- (44) Shirosaki, Y.; Okamoto, K.; Hayakawa, S.; Osaka, A.; Asano, T. Preparation of Porous Chitosan-Siloxane Hybrids Coated with Hydroxyapatite Particles. *Biomed Res. Int.* **2015**, *2015*.
- (45) Connell, L. S.; Romer, F.; Suárez, M.; Valliant, E. M.; Zhang, Z.; Lee, P. D.; Smith, M. E.; Hanna, J. V.; Jones, J. R. Chemical Characterisation and Fabrication of Chitosan-Silica Hybrid Scaffolds with 3-Glycidopropyl Trimethoxysilane. *J. Mater. Chem. B* **2014**, *2* (6), 668–680.

- (46) Palla-Rubio, B.; Araújo-Gomes, N.; Fernández-Gutiérrez, M.; Rojo, L.; Suay, J.; Gurruchaga, M.; Goñi, I. Synthesis and Characterization of Silica-Chitosan Hybrid Materials as Antibacterial Coatings for Titanium Implants. *Carbohydr. Polym.* **2019**, *203* (May 2018), 331–341.
- (47) Jun, S. H.; Lee, E. J.; Yook, S. W.; Kim, H. E.; Kim, H. W.; Koh, Y. H. A Bioactive Coating of a Silica Xerogel/Chitosan Hybrid on Titanium by a Room Temperature Sol-Gel Process. *Acta Biomater.* **2010**, *6* (1), 302–307.
- (48) Malina, D.; Sobczak-Kupiec, A.; Wzorek, Z.; Kowalski, Z. Silver Nanoparticles Synthesis with Different Concentrations of Polyvinylpyrrolidone. *Dig. J. Nanomater. Biostructures* **2012**, *7* (4), 1527–1534.
- (49) Zahra, Q.; Fraz, A.; Anwar, A.; Awais, M.; Abbas, M. A Mini Review on the Synthesis of Ag-Nanoparticles by Chemical Reduction Method and Their Biomedical Applications. **2016**, *9* (1), 1–7.
- (50) Gakiya-teruya, M.; Palomino-marcelo, L.; Rodriguez-reyes, J. C. F. Synthesis of Highly Concentrated Suspensions of Silver Nanoparticles by Two Versions of the Chemical Reduction Method. **2019**, 5–9.
- (51) Brinker, C. J.; Frye, G. C.; Hurd, A. J.; Ashley, C. S. Fundamentals of Sol-Gel Dip Coating. *Thin Solid Films* **1991**, *201* (1), 97–108.
- (52) Prochazkova, S.; Vårum, K. M.; Ostgaard, K. Quantitative Determination of Chitosans by Ninhydrin. *Carbohydr. Polym.* **1999**, *38* (2), 115–122.
- (53) Shirosaki, Y.; Tsuru, K.; Hayakawa, S.; Osaka, A.; Lopes, M. A.; Santos, J. D.; Costa, M. A.; Fernandes, M. H. Physical, Chemical and in Vitro Biological Profile of Chitosan Hybrid Membrane as a Function of Organosiloxane Concentration. *Acta Biomater.* **2009**, *5* (1), 346–355.
- (54) Coatings, C.; Products, R. C.; Applica-, E.; Tape, S.; Paint, T.; Materials, R. *Standard Test Methods for Measuring Adhesion by Tape Test 1*; 2012; pp 1–8.
- (55) Piveteau, L. D.; Gasser, B.; Schlapbach, L. Evaluating Mechanical Adhesion of Sol-Gel Titanium Dioxide Coatings Containing Calcium Phosphate for Metal Implant Application. *Biomaterials* **2000**, *21* (21), 2193–2201.
- (56) Haas, K.-H. Hybrid Inorganic-Organic Polymers Based on Organically Modified Si-Alkoxides. *Adv. Eng. Mater.* **2000**, *2* (9), 571–582.
- (57) Tonda-Turo, C.; Cipriani, E.; Gnani, S.; Chiono, V.; Mattu, C.; Gentile, P.; Perroteau, I.; Zanetti, M.; Ciardelli, G. Crosslinked Gelatin Nanofibres: Preparation, Characterisation and in Vitro Studies Using Glial-like Cells. *Mater. Sci. Eng. C* **2013**, *33* (5), 2723–2735.
- (58) S, A.; Erra, X. R. Epoxy Sol-Gel Hybrid Thermosets. *Coatings* **2016**, 1–19.
- (59) Zolkov, C.; Avnir, D.; Armon, R. Tissue-Derived Cell Growth on Hybrid Sol-Gel Films. *J. Mater. Chem.* **2004**, *14* (14), 2200–2205.
- (60) Spirk, S.; Findenig, G.; Doliska, A.; Reichel, V. E.; Swanson, N. L.; Kargl, R.; Ribitsch,

- V.; Stana-Kleinschek, K. Chitosan-Silane Sol-Gel Hybrid Thin Films with Controllable Layer Thickness and Morphology. *Carbohydr. Polym.* **2013**, *93* (1), 285–290.
- (61) Catauro, M.; Papale, F.; Bollino, F. Characterization and Biological Properties of TiO₂/PCL Hybrid Layers Prepared via Sol-Gel Dip Coating for Surface Modification of Titanium Implants. *J. Non. Cryst. Solids* **2015**, *415*, 9–15.
- (62) Feller, L.; Jadwat, Y.; Khammissa, R. A. G.; Meyerov, R.; Schechter, I.; Lemmer, J. Cellular Responses Evoked by Different Surface Characteristics of Intraosseous Titanium Implants. **2015**, *2015*.
- (63) Tan, G.; Tan, Y.; Ni, G.; Lan, G. Controlled Oxidative Nanopatterning of Microrough Titanium Surfaces for Improving Osteogenic Activity. **2014**, 1875–1884.
- (64) Schwartz, Z.; Boyan, B. D. Underlying Mechanisms at the Bone-Biomaterial Interface. **1994**, *347* (1 994), 340–347.
- (65) Liu, D. M.; Chou, H. M.; Wu, J. D. Plasma-Sprayed Hydroxyapatite Coating: Effect of Different Calcium Phosphate Ceramics. *J. Mater. Sci. Mater. Med.* **1994**, *5* (3), 147–153.
- (66) Wu, V. M.; Uskoković, V. Is There a Relationship between Solubility and Resorbability of Different Calcium Phosphate Phases in Vitro? *Biochim. Biophys. Acta - Gen. Subj.* **2016**, *1860* (10), 2157–2168.
- (67) Usinskas, P.; Stankeviciute, Z.; Beganskiene, A.; Kareiva, A. Sol-Gel Derived Porous and Hydrophilic Calcium Hydroxyapatite Coating on Modified Titanium Substrate. *Surf. Coatings Technol.* **2016**, *307*, 935–940.
- (68) Yang, Y.; Chang, E. Measurements of Residual Stresses in Plasma-Sprayed Hydroxyapatite Coatings on Titanium Alloy. **2005**, *190*, 122–131.
- (69) Rupp, F.; Gittens, R. A.; Scheideler, L.; Marmur, A.; Boyan, B. D.; Schwartz, Z.; Geis-Gerstorfer, J. A Review on the Wettability of Dental Implant Surfaces I: Theoretical and Experimental Aspects. *Acta Biomater.* **2014**, *10* (7), 2894–2906.
- (70) Dowling, D. P.; Miller, I. S.; Ardhaoui, M.; Gallagher, W. M. Effect of Surface Wettability and Topography on the Adhesion of Osteosarcoma Cells on Plasma-Modified Polystyrene. *J. Biomater. Appl.* **2011**, *26* (3), 327–347.
- (71) Hou, N.; Perinpanayagam, H.; Mozumder, M.; Zhu, J. Novel Development of Biocompatible Coatings for Bone Implants. *Coatings* **2015**, *5* (4), 737–757.
- (72) Wenzel, R. N. Resistance of Solid Surfaces to Wetting by Water. *Ind. Eng. Chem.* **1936**, *28* (8), 988–994.
- (73) Sundfeldt, M.; Carlsson, L. V.; Johansson, C. B.; Thomsen, P.; Gretzer, C. Aseptic Loosening, Not Only a Question of Wear: A Review of Different Theories. *Acta Orthop.* **2006**, *77* (2), 177–197.
- (74) Banaszkiwicz, P. A. Periprosthetic Bone Loss in Total Hip Arthroplasty: Polyethylene Wear Debris and the Concept of the Effective Joint Space. *Class. Pap. Orthop.* **2014**, *74* (6), 85–87.

- (75) Bhattacharya, P.; Neogi, S. Techniques for Deposition of Coatings with Enhanced Adhesion to Bio-Implants. In *Adhesion in Pharmaceutical, Biomedical, and Dental Fields*; 2017; pp 235–254.
- (76) Chen, J.; Bull, S. J. Approaches to Investigate Delamination and Interfacial Toughness in Coated Systems: An Overview. *J. Phys. D. Appl. Phys.* **2011**, *44* (3).
- (77) van Dam, J. P. B.; Abrahami, S. T.; Yilmaz, A.; Gonzalez-Garcia, Y.; Terryn, H.; Mol, J. M. C. Effect of Surface Roughness and Chemistry on the Adhesion and Durability of a Steel-Epoxy Adhesive Interface. *Int. J. Adhes. Adhes.* **2020**, *96* (June 2019), 102450.
- (78) He, Y.; Zhang, X.; Hooton, R. D.; Zhang, X. Effects of Interface Roughness and Interface Adhesion on New-to-Old Concrete Bonding. *Constr. Build. Mater.* **2017**, *151*, 582–590.
- (79) Jarka, T. G. S. Injection Molding of Multimaterial Systems. In *Specialized Injection Molding Techniques*; 2016; pp 165–210.
- (80) S. R. Brown, I. G. T. & H. R. Residual Stress Measurement in Thermal Sprayed Hydroxyapatite Coatings. *J. Mater. Sci. Mater. Med.* **1994**, *5*, 756–759.
- (81) Yang, Y. C.; Chang, E. Influence of Residual Stress on Bonding Strength and Fracture of Plasma-Sprayed Hydroxyapatite Coatings on Ti-6Al-4V Substrate. *Biomaterials* **2001**, *22* (13), 1827–1836.
- (82) Zhang, Z.; Dunn, M. F.; Xiao, T. D.; Tomsia, A. P.; Saiz, E. M. *Nanostructured Hydroxyapatite Coatings for Improved Adhesion and Corrosion Resistance for Medical Implants*; 2001; Vol. 703.
- (83) Shockman, G. D.; Barren, J. F. Structure, Function, and Assembly of Cell Walls of Gram-Positive Bacteria. *Annu. Rev. Microbiol.* **1983**, *37* (1), 501–527.
- (84) Gholizadeh, P.; Ghotaslou, R. The in Vitro Effects of Silver Nanoparticles on Bacterial Biofilms. *J. Microbiol. Biotechnol. Food Sci.* **2017**, *6* (4), 1077–1080.
- (85) Flores, C. Y.; Min, A. G.; Grillo, C. A.; Salvarezza, R. C.; Vericat, C.; Schilardi, P. L. Citrate-Capped Silver Nanoparticles Showing Good Bactericidal Effect against Both Planktonic and Sessile Bacteria and a Low Cytotoxicity to Osteoblastic Cells. **2013**.
- (86) Hwang, E. T.; Lee, J. H.; Chae, Y. J.; Kim, Y. S.; Kim, B. C.; Sang, B. I.; Gu, M. B. Analysis of the Toxic Mode of Action of Silver Nanoparticles Using Stress-Specific Bioluminescent Bacteria. *Small* **2008**, *4* (6), 746–750.
- (87) Hosseinejad, M.; Jafari, S. M. Evaluation of Different Factors Affecting Antimicrobial Properties of Chitosan. *Int. J. Biol. Macromol.* **2016**, *85*, 467–475.
- (88) Flemming, H. C.; Neu, T. R.; Wozniak, D. J. The EPS Matrix: The “House of Biofilm Cells.” *J. Bacteriol.* **2007**, *189* (22), 7945–7947.
- (89) Díaz, C.; Schilardi, P.; De Mele, M. F. L. Influence of Surface Sub-Micropattern on the Adhesion of Pioneer Bacteria on Metals. *Artif. Organs* **2008**, *32* (4), 292–298.
- (90) Kumar, P.; Senthamilselvi, S.; Lakshmipraba, A.; Premkumar, K.; Muthukumaran, R.; Visvanathan, P.; Ganeshkumar, R. S.; Govindaraju, M. Efficacy of Bio-Synthesized Silver

Nanoparticles Using Acanthophora Spicifera to Encumber Biofilm Formation. *Dig. J. Nanomater. Biostructures* **2012**, 7 (2), 511–522.

Chapter 4: Development of multifunctional bioactive implant coatings using a novel calcium precursor to improve osseointegration and antimicrobial effectiveness

4.1 Introduction

Over the past half century, titanium (Ti) and its alloys have become ubiquitous within implantology as materials of choice for augmenting and restoring function to human tissues^{1,2}. They endure conditions of high-loading and/or repetitive cycling while remaining resistant to chipping and fracture, and possess the appropriate moduli that limit adverse effects from stress shielding seen with other metallic implant materials³⁻⁵. Additionally, the titanium dioxide layer that forms on the surface of these materials resists corrosion and provides a highly inert and biocompatible platform for interactions with surrounding cells and tissues. However, the inherent inertia of titanium surfaces is accompanied by a failure to alleviate two frequent complications in implantology. These are implant associated infections from surface microbes and aseptic loosening from lack of fixation, which pose major challenges to their long-term success and survival in clinical practice.

Despite widespread use of aseptic surgical techniques, implant associated infections continue to pose a threat of complications to their integration and retention within host tissues. Currently, the risk of postoperative infections associated with hard tissue implantations range from 2-5% for orthopaedic procedures, and 4-11.5% for dental and oral surgeries⁶⁻⁸. They can be caused by any bacteria or fungi but are most commonly due to bacterial staphylococci. These include the common pathogen *Staphylococcus aureus* (*S. aureus*) and the ubiquitous *Staphylococcus epidermidis* (*S. epidermidis*)^{9,10} that are prevalent on human skin, and readily form biofilms on implant surfaces¹¹. The biofilms consist of bacterial cells encased within their own polysaccharide matrix, which are highly adherent and resistant on biomaterial surfaces. As the biofilms mature they present a favourable environment for symbiotic microbes such as *Escherichia coli* and *Pseudomonas aeruginosa* to become established within polymicrobial communities¹². These mature polymicrobial biofilms can be up to a thousand times more resistant to antibiotics than bacterial cells that are suspended in a planktonic state^{7,13}. Accordingly, the infections require complex treatments that include complete removal of the implanted protheses and significant debridement of host tissues¹⁴.

Although implant associated infections are the primary cause of implant failures, the aseptic loosening of implants without microbial infections are another complication that occurs. Indeed, aseptic loosening may account for up to 36% of implant failures in joint arthroplasty¹⁵. These implants lack fixation and adequate osseointegration within host tissues¹⁶, and the resultant micromotions of the prosthesis may cause fibrous tissue formation, which exacerbates their loosening. Therefore, current strategies to enhance osseointegration are to promote bone deposition on implant surfaces with ceramic coatings containing calcium phosphates (CaP), hydroxyapatites (HA) and materials containing calcium, silica, phosphorous and magnesium¹⁷⁻²⁰. However, these ceramic coatings are plagued by inconsistent properties from poor processing conditions that risk their delamination under clinical wear^{21,22}.

Therefore, implant surfaces need to both prevent infections and promote bone deposition to ensure success. Immediately following their surgical placement, both host tissue cells and contaminant microbes participate in a “race to the surface” of the biomaterial, where the fate of the implant is determined by which surface colonizers prevail¹². Although current strategies may be effective at either goal, few are proficient in both domains. Therefore, multifunctional surfaces that both promotes bone apposition and prevent microbial colonization are sorely needed for implants.

To develop such multifunctional implant coatings, the application of amorphous ceramic materials by using sol-gel techniques has shown promise. Sol-gel ceramic synthesis involves the hydrolysis and condensation of liquid ceramic precursors under low temperatures. The lower temperatures result in higher porosity and surface area for the materials compared to traditional melt-quench glasses, which promotes cell adhesion and tissue ingrowth²³. Additionally, these solution-based low temperature preparations allow homogeneous loading of process-sensitive antimicrobials. Accordingly, such multifunctional sol-gel materials have been developed as beads/particles, scaffolds, and fibers²⁴⁻²⁶, but their inherent brittleness and poor adhesive tensile strength have limited their application as implant surfaces. Furthermore, the inclusion of calcium to induce apatite formation has not been successfully incorporated into these sol-gel preparations, under low temperatures or non-toxic synthesis conditions.

The sol-gel ceramics mechanical properties can be improved by including organic polymers as composite and hybrid systems. However, simple blending of organic and inorganic networks

creates inhomogeneous sol-gel composites with mismatched degradation rates, which are unstable and deteriorate prematurely^{24,27}. Alternatively, hybrid materials with molecular interactions between their organic and inorganic phases have significantly more stability than composites. Furthermore, hybrids with strong covalent interactions between organic and inorganic components (class II) have advantages over those with weaker molecular forces (class I). These class II hybrids act as single-phase materials exhibiting improved mechanical properties and can be tailored to the needs of a variety of biomedical applications^{26,28-30}.

Sol-gel materials can be further enhanced by including calcium as an osteoconductive factor. Most commonly, calcium salts are added by high temperature processing in order to remove their toxic salt byproducts. However, such processing precludes the use of temperature-sensitive organic polymers and organosilanes such as GPTMS within hybrid sol-gel materials. Therefore, calcium alkoxides are now being investigated as precursors for the inorganic portion of sol-gel hybrid materials. They participate in the same network forming hydrolysis and condensation reactions as traditional silica precursors, which allows simple integration into sol networks at room temperature. However, most calcium alkoxides are highly sensitive to hydrolysis and condensation reactions in the presence of water. Their instability in aqueous systems leads to premature gelation of the inorganic network, which leads to poor and inhomogeneous integration of calcium into materials. Additionally, incompletely hydrolyzed calcium alkoxides can leach toxic by-products such as methanol from calcium methoxide and calcium methoxyethoxide. Accordingly, water-tolerant and non-toxic calcium alkoxides need to be explored.

The purpose of this study was to develop robust multifunctional class II organic-inorganic hybrid coating materials for titanium implants. For the organic phase, PEG-amine was synthesized and coupled to GPTMS. The inorganic phase consisted of silica, and calcium was integrated into the sol-gel network with newly developed calcium 2-ethoxyethoxide (Ca2EE). Ca2EE, was stable in aqueous systems and homogeneously integrated into the hybrid coating network. These coating matrices were loaded with silver nanoparticles (AgNPs) that inhibited bacterial growth and biofilm formation.

4.2 Materials and Methods

All chemicals involved in the preparation of coating materials were purchased as laboratory grade reagents from Sigma Aldrich (St. Louis, MO, USA), unless otherwise specified.

4.2.1 Synthesis of Coating Materials

Synthesis of Ca2EE

Calcium-2-ethoxyethoxide (Ca2EE) was synthesized under similar conditions as other metallic 2-ethoxyethoxides previously described³¹. Dry distilled 2-ethoxyethanol (Caledon Laboratories, Georgetown, ON, Canada) was heated to 80°C under an argon atmosphere. Calcium granules (Alfa Aesar, Tewksbury, MA, USA) were slowly introduced into the heated vessel through a pressure-equalizing funnel with maximal magnetic stirring. After adding metallic calcium, the vessel was heated to 125°C and left to react for 20 hours. Then, Ca2EE was purified by removing excess 2-ethoxyethanol through vacuum drying at 100°C for 6 hours. The Ca2EE structure was confirmed by ¹³C NMR and spectral data agreed with previous reports³².

Functionalization of PEG

Amine functionalized polyethylene glycol (PEG) was prepared for its capacity to covalently couple with inorganic silica networks as follows. PEG ditosylate (2k, 30g) was added to an ammonium hydroxide solution (105 mL, 7.5 M) and stirred at room temperature for 5 days. The resulting solution was washed (5x) with dichloromethane (5 x 100 mL), and the organic phase separated and dried over anhydrous magnesium sulfate, followed by concentration and precipitation with cold diethyl ether. The precipitate (PEG-diamine) was dried by vacuum filtration and collected as a white powder. The PEG-diamine structure was confirmed by ¹H NMR and spectral data agreed with previous reports^{33,34}.

Silane coupling of PEG-NH₂

PEG diamine and 3-glycidyloxypropyltrimethoxysilane (GPTMS) coupling reactions were initiated by methods similar to those previously described³⁵⁻³⁷. PEG-diamine was dissolved in absolute ethanol to a concentration of 40mg/mL. GPTMS was added to this solution at a ratio of 1:2 of PEG-diamine to GPTMS and left to couple under an inert nitrogen atmosphere at room temperature for 24 hours.

Synthesis of AgNPs

Silver nanoparticles (AgNPs) were synthesized by a chemical reduction method previously described³⁸⁻⁴⁰. NaBH₄ solution (2.0 x 10⁻³ M) was prepared in double distilled water and placed in an ice bath for 15 minutes. Chilled NaBH₄ was agitated by rapid magnetic stirring, and

AgNO₃ solution (2.0 x 10⁻³ M) was added dropwise at a ratio of 1:6 (v/v) of AgNO₃ to NaBH₄. Following the addition of AgNO₃, the AgNP suspension was stabilized with polyvinylpyrrolidone solution (0.3wt%). AgNPs were extracted by ultracentrifugation and freeze-drying.

Preparation of hybrid materials

Class II organic-inorganic hybrid materials were synthesized with coupled PEG-NH₂-GPTMS as the organic phase (20wt%) and Si/Ca as the inorganic (80wt%). The molar ratio of Si/Ca (70:30) matched that of traditional bioactive glasses. Tetraethoxysilane (TEOS) and HCl (1N) were added to double distilled water at a ratio of 10:1:3 (v/v) under an inert nitrogen atmosphere and allowed to react for 15 minutes. Si-functionalized PEG-NH₂ was diluted in absolute ethanol and added to the hydrolyzed TEOS solution with stirring for 5 minutes. Then, freshly prepared Ca₂EE was slowly added to the reaction vessel with rapid stirring over 40 minutes. After the addition of Ca₂EE, antibacterial coating blends were loaded with AgNPs (0.023wt%) with rapid stirring for 10 minutes.

Table 4.1 Composition of Si-Ca-PEG based coatings

<i>Components</i>	Inorganic Bioactive Glass		Hybrid Bioactive Glass	
	<i>Si-Ca₂EE</i>	<i>Si-Ca₂EE-nAg</i>	<i>Si-Ca-PEG</i>	<i>Si-Ca-PEG-nAg</i>
TEOS ^a	70	70	56	56
Ca ₂ EE ^b	30	30	24	24
PEG-GPTMS ^c	0	0	20	20
AgNPs ^d	0	0.023	0	0.023

^a tetraethoxysilane (network wt%); ^b calcium-2-ethoxyethoxide (network wt%); ^c PEG-diamine coupled with 3-glycidyloxypropyltrimethoxysilane (network wt%); ^d silver nanoparticles (total coating wt%)

Deposition of Hybrid Coatings

Ti6Al4V (9 x 9 x 2 mm) discs were prepared as substrates for the application of hybrid coatings. All discs were polished with silicon carbide paper up to 1200 grit. They were degreased and cleaned with acetone and deionized water by ultrasonication, and dried at 40°C. Additionally,

some discs were acid-etched by immersion in a HCl and H₂SO₄ solution (2:2:1 v/v) at 65°C for 20 minutes. Following etching, discs were neutralized in a NaHCO₃ solution (0.5 M) and cleaned as detailed above.

Freshly prepared hybrid materials were deposited onto polished and acid-etched Ti6Al4V discs by using a standard dip-coating protocol⁴¹. The discs were dipped and withdrawn from hybrid solutions at a speed of 100 mm/min, dried in a vacuum oven at 80°C for 3 hours, and then stored at room temperature.

4.2.2 Characterization of Coating Materials

Hybrid coating materials were analyzed for their composition, chemical structures, and surface topographies.

Chemical Structures

Chemical structures were analyzed for the presence of bonds and key functional groups by using attenuated total reflectance Fourier transform infrared spectroscopy (ATR-FTIR). Hybrid materials were ground into a fine powder with mortar and pestle, and analyzed in a Bruker Tensor II system with a Platinum ATR (unit A225) equipped with a 2 x 2 mm diamond crystal (Bruker, Billerica, MA, USA). Spectra were acquired in the 4000-400 cm⁻¹ range, at 4 cm⁻¹ resolution, averaged from 32 scans and analyzed using OPUS spectroscopy software.

Surface Properties

Surface morphologies and micro-topographies were examined by scanning electron microscopy (SEM), and elemental distributions were analyzed by energy-dispersive X-ray spectroscopy (EDX). The coated discs were affixed to metal stubs with carbon tape and sputter coated with 10 nm gold nanoparticles. Coatings surface features were visualized using a Hitachi SU8230 Regulus Ultra High-Resolution Field Emission SEM (Hitachi, Tokyo, Japan), and elemental mapping was obtained by from a Bruker X-Flash FQ5060 Annular Quad EDX detector (Bruker, Billerica, MA, USA).

4.2.3 Evaluation of Mechanical Properties

Adhesive Strength

Quantitative assessment of the hybrid coatings adhesion to titanium substrates was further evaluated using an established tensile adhesion protocol⁴². Briefly, coated Ti6Al4V discs were first secured to aluminum dollies using T-88 epoxy resin (System Three Resins, Inc., Lacey, WA, USA). Secured specimens were then seated in a tensile adapter in an Adelaide TCC universal testing machine (Adelaide Testing Machines, Toronto, ON, Canada), and slowly forced apart at a speed of 3 mm/min. Measurements for each coating and titanium surface treatment were tested in triplicate with the method of separation closely examined for the point of delamination. Using the load at failure and contact area of the aluminum dolly with the coated Ti disc, the adhesive strength of coating materials were calculated as:

$$\text{Adhesive Strength (MPa)} = \frac{\text{Load at Failure (N)}}{\text{Coated Area (m}^2\text{)}} \quad (1)$$

4.2.4 Evaluation of Biological Properties

Mineral Bioactivity

Mineral bioactivities were evaluated by immersion of coatings in simulated body fluid (SBF), prepared as previously described by Kokubo et al⁴³. For this preparation, NaCl, NaHCO₃, KCl, K₂HPO₄·3H₂O, MgCl₂·6H₂O, CaCl₂ and Na₂SO₄ were dissolved in double distilled water and buffered to pH 7.4 using tris-(hydroxymethyl)-aminomethane ((CH₂OH)₃CNH₂) and HCl. The resulting simulated body fluid solution had an ionic composition that was similar to that of human blood plasma (Table 2).

Table 4.2 Ionic composition of simulated body fluid and human blood plasma

[mM]	Na ⁺	K ⁺	Mg ²⁺	Ca ²⁺	Cl ⁻	HCO ³⁻	HPO ₄ ²⁻	SO ₄ ²⁻
Body Fluid ⁴³	142	5	1.5	2.5	148.8	4.2	1	0.5
Blood Plasma	142	5	1.5	2.5	103	27	1	0.5

Monoliths (100 mg) of coatings were immersed in 200 mL of simulated body fluid at 37°C for 72 hours. Following immersion, coating monoliths were rinsed with ethanol and double distilled water and dried in a desiccator. Their dried surfaces were analyzed for the presence of crystallized apatite by using scanning electron microscopy (SEM) and energy-dispersive X-ray spectroscopy (EDX).

Antimicrobial Efficacy

The antimicrobial properties of base and AgNP loaded hybrid coatings were evaluated on common Gram-positive and Gram-negative bacterial pathogens. Their antibacterial effects against *Staphylococcus aureus* (Gram-positive, ATCC[®] 25923) and *Escherichia coli* (Gram-negative, ATCC[®] 25922) in monocultures and within single species biofilms were assessed. Separate monocultures of *E. coli* and *S. Aureus* were prepared from inoculum and suspended in Luria Bertani (LB) media for growth.

For these assessments, the coated Ti6Al4V discs were cleaned, disinfected and sterilized as follows. The coated discs were rinsed twice with ethanol (70% v/v), washed thrice with phosphate buffered saline (PBS), then placed in a tissue culture hood and exposed to UV light for 30 minutes to ensure sterility. For each assay, replicate coated discs (n=3/coating) were submerged in each bacterial suspension (10⁵ CFU/mL) and incubated under aerobic conditions at 37°C.

To measure cell growth and survival in the planktonic state, samples of bacterial cultures grown around coatings were withdrawn after 24 hours. Diluted samples were measured for their absorbance (OD₆₀₀) using a spectrophotometer (Agilent Technologies, Santa Barbara, CA). Following 24 hours of incubation, viable cells from bacterial suspensions were counted by serial dilution and the spread plate method using 100 x 15 mm LB Agar plates.

To measure cell formation of biofilms, the coatings submerged within each bacterial suspension were withdrawn following 24 hours incubation. These coated discs were gently rinsed thrice with sterile phosphate buffered saline (PBS) to remove non-adherent cells and transferred to sterile culture tubes containing 2 mL of fresh LB media. They were then ultrasonicated for 5 minutes to dislodge adherent cells from biofilms. Viable bacteria from sonicated samples were harvested and counted by serial dilution and the spread plate method using 100 x 15 mm LB Agar plates.

The inhibition of bacterial growth by each coating for both non-adherent (planktonic) and adherent (biofilm) bacteria was calculated from the plate counts. Using the colonies for uncoated Ti6Al4V discs as the control (CFU_{control}) and the colonies counted for each hybrid coating surface (CFU_{coating}), bacterial inhibition was calculated as:

$$\text{Bacterial Inhibition (\%)} = \frac{CFU_{\text{Control}} - CFU_{\text{Coating}}}{CFU_{\text{Control}}} \times 100 \quad (2)$$

4.2.5 Statistical Analysis

The data in this study were analyzed using GraphPad Prism software (V 6.01). All data are expressed as mean \pm standard deviation. One-way ANOVA analyses were used to make comparisons among multiple groups. Group differences were specified using Tukey's post hoc tests with the differences considered statistically significant when $p < 0.05$.

4.3 Results and Discussion

4.3.1 Characterization of Coating Materials

Hybrid precursor identification and synthesis

The first step in this work was to identify and synthesize an appropriate calcium alkoxide precursor for use within the bioactive glass network. Indeed, the use of calcium alkoxides have been shown to enable successful integration of calcium into silicate networks at low temperatures⁴⁴. Calcium 2-ethoxyethoxide (Ca2EE) was identified as a potential calcium precursor due to its structural stability in aqueous environments and non-toxic degradation by-products. Most previously investigated calcium alkoxide precursors, such as calcium 2-methoxyethoxide (CME), have been unstable in sol-gel systems containing water, which can lead to poor hybridization and premature gelation of network structures⁴⁵⁻⁴⁷. Despite the relative instability of CME, promise exists in the use of similar longer ligand Ca-2-alkoxyalkoxides as they are able to form water-stabilizing chelate cycles enabled through the presence of their secondary ether group³¹. Along with their sensitivity to water, previously used calcium alkoxide precursors have possessed the potential to leach toxic degradation by-products from bioactive

glass materials. For example, calcium precursors such as CME and calcium methoxide (CM) have the potential to leach methanol from bioactive glass materials if their ligands remain uncondensed during network formation which could elicit a degree of cytotoxicity. Ca2EE, if left uncondensed within bioactive glass materials, could instead leach ethanol, mitigating the potential for a developed bioactive glass material to exhibit toxicity *in vivo*.

While this compound has been synthesized in previous works, it has not yet been utilized as a network precursor for bioactive glass materials. One of the primary reasons for this is that traditional methods for synthesizing calcium-2-ethoxyethoxide required the use of a toxic catalyst (mercury (II) chloride), rendering the material unsuitable for biological applications⁴⁸. In this study, Ca2EE was synthesized in the absence of mercury (II) chloride to enable its use within bioactive glass materials. Using ¹³C NMR, the successful synthesis of Ca2EE was confirmed through observation of the pronounced deshielding of the Ca-O adjacent carbon compared to that of the parent alcohol (2-ethoxyethanol) (Figure 4.1). Additionally, the doublets appearing at C-1 and C-3, characteristic of bridging and non-bridging carbon resonances, further confirmed the synthesis of Ca2EE, and were consistent with that of previous work³².

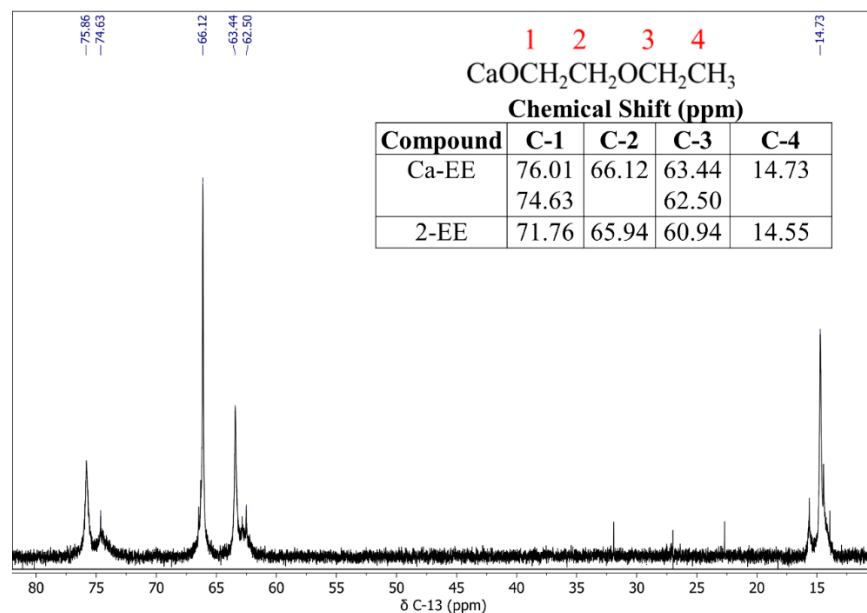


Figure 4.1 ¹³C NMR of synthesized calcium-2-ethoxythoxide (Ca2EE)

The next step in this work was to identify and synthesize an appropriate organic polymer for use within the hybrid bioactive glass network. Hydrophilic organic polymers have often been identified as ideal class II precursors due to their ability to improve the flexibility of hybrid

materials and improve their ability to participate in ion exchange with physiological fluids. For this reason, poly(ethylene) glycol (PEG) was identified as the ideal given its flexible solubility parameters and well established biocompatible and bioresorbable nature^{29,49}. To be successfully integrated into the hybrid network, PEG was amine-functionalized to enable its coupling to a silane precursor. Amine functionalization was selected due to the well-established coupling reaction between amine-bearing polymers through the epoxide of GPTMS^{30,50}. The synthesis of PEG-diamine was confirmed through ¹H-NMR (Figure 4.2).

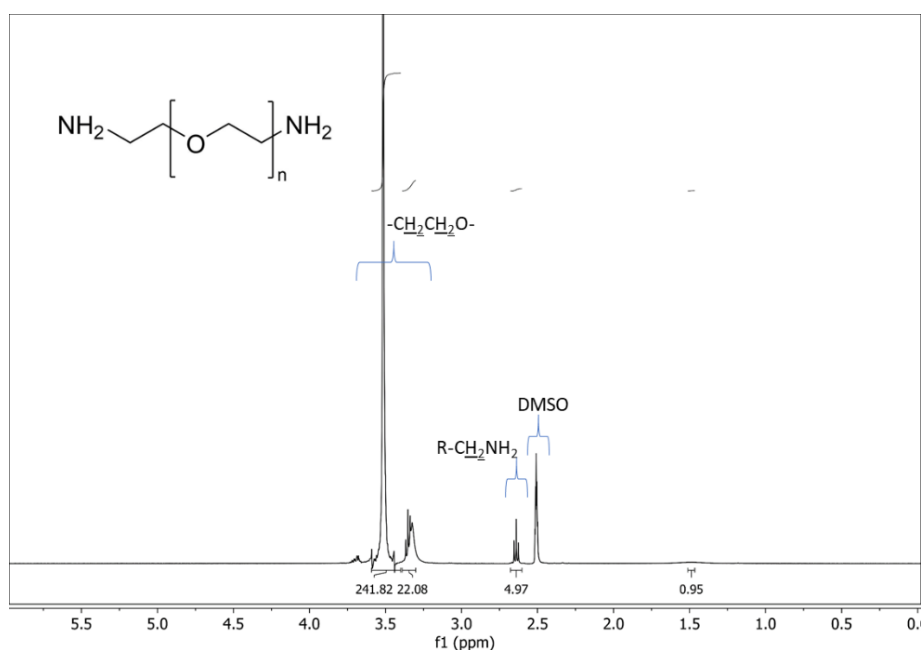


Figure 4.2 ¹H NMR of synthesized PEG-diamine (2K)

Hybrid Bioactive Glass Synthesis

In this study, class II hybrid bioactive glass materials were developed using PEG-diamine as an organic polymer component, GPTMS as a silane coupling agent, Ca2EE as a calcium source, and TEOS as an inorganic silicate networking agent. Initially, covalent coupling occurred between the epoxide functional group of GPTMS and the primary amine groups of PEG-diamine (Figure 4.3(1)). Additionally, during the acidic conditions of this reaction, the ethoxysilane bonds of GPTMS were hydrolyzed to form Si-OH pendants. Following coupling, silane-functionalized PEG-diamine was added to a pre-hydrolyzed solution of TEOS to homogenize. Shortly after the

addition of silane-functionalized PEG-diamine, Ca2EE was added slowly to the reaction vessel to allow for the covalent introduction of calcium and continued polycondensation of the silicate network. Following the reaction of the above-mentioned reagents, antibacterial coating materials were developed through the simple addition of PVP-stabilized AgNPs.

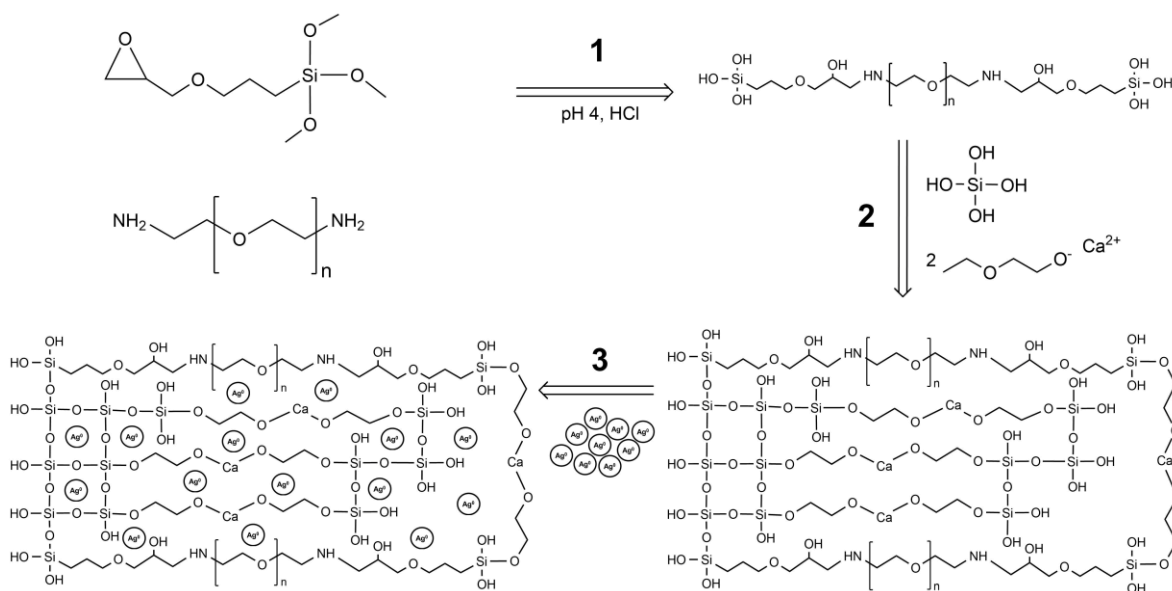


Figure 4.3 Chemical synthesis of PEG–Ca-silica Class II hybrids and imbedding of silver nanoparticles (AgNPs). (1) Coupling of PEG-amine and 3-glycidyloxypropyltrimethoxysilane (GPTMS) in mildly acidic conditions; (2) polycondensation of coupled PEG-amine, calcium 2-ethoxyethoxide, and hydrolyzed tetraethoxysilane (TEOS); (3) imbedding AgNPs into the hybrid sol network.

For synthesized PEG-diamine, it was important to identify the characteristic organic portions of the polymer (Figure 4.4). The primary amines present in the structure were identified at 1570cm^{-1} and the associated -CH backbone bending was identified at 1466cm^{-1} . Upon coupling with GPTMS, the peak attributed to the primary amine of PEG-diamine diminished, as coupling proceeded between the two components to establish secondary amine linkages. Complete organic-inorganic bioactive glass materials composed of coupled PEG-diamine, calcium, and silica sol-gel precursors possessed decreasing characteristics of the organic PEG-diamine. This led to the reduction in both -NH₂ and -CH bending and the broadening of peaks associated to the inorganic network such as Si-OH ($780, 934\text{ cm}^{-1}$) and Si-O-Si (1065 cm^{-1}). As expected, both

completely inorganic materials composed of both bioactive glass and pure silicate networks did not possess any peaks attributed to the inorganic network. Differences between the two networks can be observed through their degree of condensation. The purely silicate network (formed by hydrolyzing and condensing TEOS) had a stronger peak attributed to the condensed silicate species (Si-O-Si). Indeed, this was expected as the calcium alkoxide used in this study (calcium 2-ethoxyethoxide) has fewer terminal sites (2) compared to that of TEOS (4). The integration of Ca2EE was thus expected to decrease the network density, which has been well established to also affect the dissolution rate of the inorganic bioactive glass materials⁴¹.

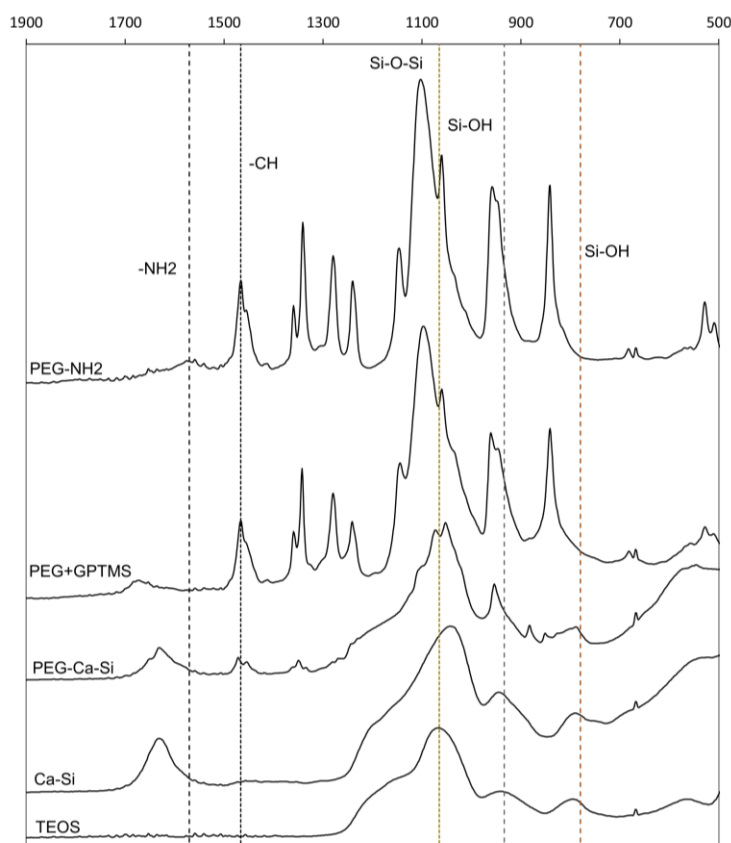


Figure 4.4 Infrared analyses of chemical structures in Si-Ca coating materials. Total reflectance Fourier transform infrared (ATR-FTIR) spectra of PEG-diamine, PEG-diamine coupled with 3-glycidyoxypropyltrimethoxysilane (PEG+GPTMS), hybrid coating material (Si-Ca-PEG), inorganic bioactive glass material (Si-Ca), and pure inorganic siloxane (condensed TEOS). Peaks attributed to PEG-diamine (-NH₂, -CH) were apparent for the hybrid coating material and absent in purely inorganic coating materials. The chemical

characteristics of the inorganic bioactive glass coating materials was similar to that of the pure siloxane network with prominent Si-O-Si and Si-OH peaks.

Coating adhesion is an important factor in determining the clinical translatability of implant coating materials. While overlooked in many studies, poor adhesive strength may lead to delamination of coating materials which can cause inflammation, bone resorption, and to the eventual failure of intraosseous implants *in vivo*^{51,52}.

To quantitatively evaluate the adhesion of the hybrid bioactive glass coatings developed in this study, adhesive tensile tests were performed based on established protocols^{42,53}. Coatings were evaluated for their adhesion to both polished and acid-etched Ti6Al4V substrates (Figure 4.6). Hybrid bioactive glass coatings were significantly ($p < 0.05$) more adherent to acid-etched Ti6Al4V than to polished Ti6Al4V substrates. Indeed, acid-etching, as with other surface roughening pre-treatments, has been well established to increase the adherence of coating materials⁵⁴⁻⁵⁶. This improvement in coating adhesion has been attributed to greater mechanical adhesion due to the increase in bonding area that occurs during roughening pre-treatments.

While plasma-sprayed hydroxyapatite (HA) coating materials remain the gold standard for intraosseous implants, their relative inconsistency and weakness has been the subject of many studies. Their application, which include high temperatures and variable cooling cycles, are known to retain residual stresses within these coating materials which can result in adhesive failures below 10 MPa^{21,57,58}. The robust adhesive characteristics of the developed hybrid bioactive glass coating (15.1 ± 3.3 MPa) developed in this study, therefore, warrants further study.

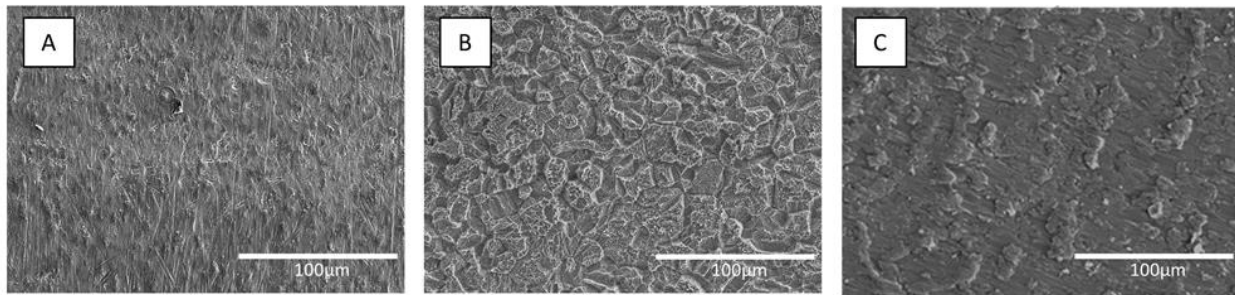


Figure 4.5 Scanning electron microscopy (SEM) of titanium (Ti6Al4V) substrates and coated surfaces. Polished Ti6Al4V was flat with smoothly scalloped surfaces (A). Acid-etched

Ti6Al4V had extensive surface fissures that created micro-scale roughness (B). Hybrid bioactive glass coating (Si-Ca-PEG) films on acid-etched Ti6Al4V substrates retained micro-topographical features and surface roughness (C).

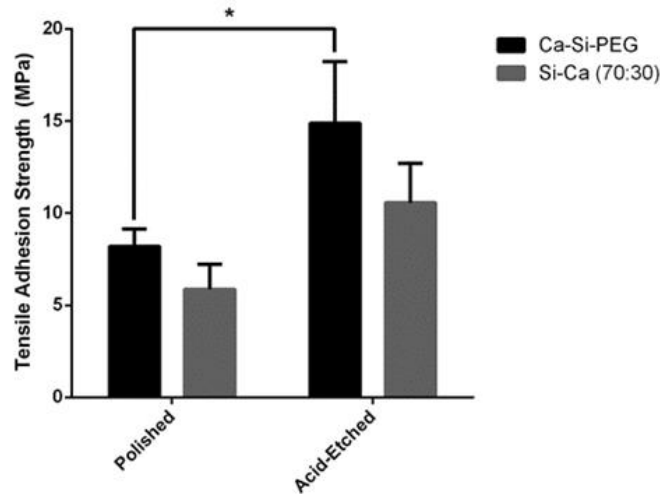


Figure 4.6 Adhesive tensile strengths of coatings and chitosan on titanium (Ti6Al4V) substrates. Hybrid bioactive glass (Si-Ca-PEG) coatings (n=3/surface) were significantly ($p < 0.05$) more adherent to acid-etched Ti6Al4V substrates than they were to polished Ti6Al4V.* - statistically significant difference

4.3.2 In Vitro Bioactivity

The promotion of bone growth is important in ensuring the fixation of metallic implants and preventing events of aseptic loosening. Calcium integration within coating materials has been identified as a key factor in the development of bioactive materials^{21,22}. It was therefore important to determine whether the low temperature integration of Ca₂EE into the hybrid sol-gel coating networks would render the hybrid coatings to be bioactive.

Evaluation of osteoconduction through *in vitro* immersion studies has been well established to be indicative of actual osteoconduction and bone growth *in vivo*^{59,60}. Therefore, in this study, the mineralization of HA on hybrid coating surfaces was evaluated following 72 hours immersion in simulated body fluid (SBF). To evaluate HA mineralization on hybrid coating materials, SEM analysis and EDX maps were used (Figure 4.7). Following 3 days immersion in SBF, characteristic globular HA deposits were found on the surface of hybrid coating materials

(Figure 4.7-a). Indeed, EDX mapping confirmed the composition of globular deposits to be hydroxyapatite through the presence of phosphate on the surface (Figure 4.7 (f)), and, the elemental ratio of Ca/P of 1.6. While the elemental ratio of Ca/P is slightly below the theoretical value of hydroxyapatite (Ca/P = 1.67) it is well within that of common apatite crystallites formed by similar biomimetic processes^{61,62}.

Further, EDX analysis confirmed the retention and homogeneous distribution of coating network elements and imbedded AgNPs (Figure 4.7 b-e). Following 72 hours immersion, AgNPs remained imbedded within the coating network and were not lost to dissolution.

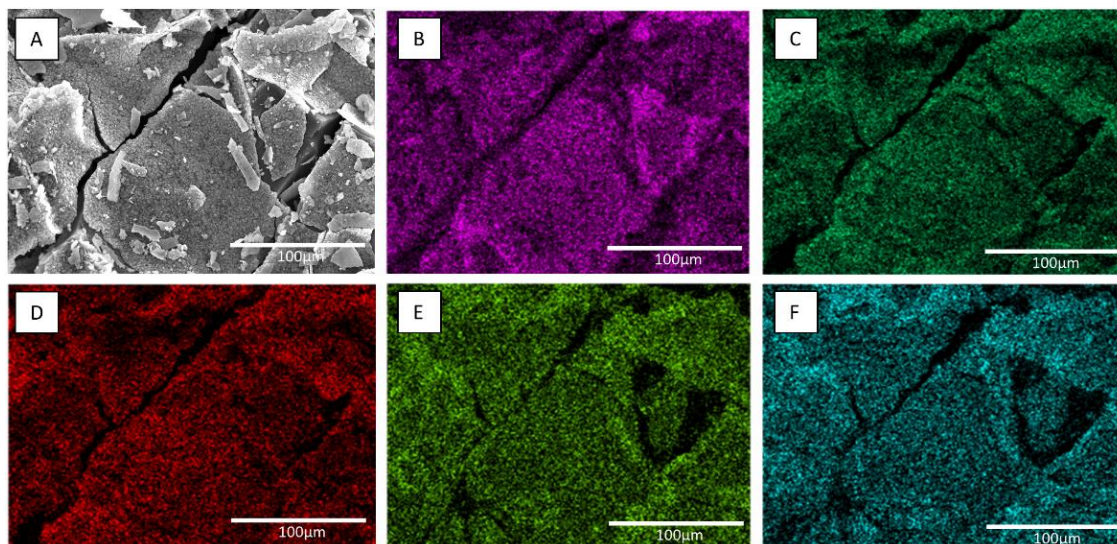


Figure 4.7 Elemental EDX mapping analysis of the hybrid coating material (Si-Ca-PEG) after 72 hours immersion in SBF: (a) selected microscopic SEM field; (b) Si; (c) C; (d) Ag; (e) Ca, and (f) P. SEM micrographs display the presence of apatite globules on the surface of Si-Ca-PEG monoliths following immersion in SBF. Elemental analysis confirms the presence of apatite. Scale bar: 100 μm .

4.3.3 Antimicrobial Properties

Infections due to microbial colonization on implant surfaces currently pose the highest risk to the success of implantable prostheses⁶⁻⁸. Therefore, the application of antimicrobial coatings on implant materials presents an effective strategy in mitigation IAIs.

Further, the utilization of AgNPs within antimicrobial materials has garnered significant interest due to their broad-spectrum effects, limited cytotoxicity, and ease of synthesis^{63,64}. AgNPs possess particular advantages as coating-loaded antimicrobial agents as they have shown efficacy in mitigating the growth of bacteria in both static and planktonic cultures⁶⁵⁻⁶⁷.

Therefore, in this study, hybrid coatings were afforded with antimicrobial properties by imbedding AgNPs within the hybrid coating networks. *S. aureus* and *E. coli*, clinically relevant pathogenic bacteria, were selected as model bacterium to evaluate the antimicrobial efficacy of developed coatings. The efficacy of such antimicrobial coatings was evaluated in both culture and biofilm states.

In planktonic assays, hybrid coatings loaded with AgNPs showed effective inhibition of both bacterial cultures compared to uncoated titanium controls (Figure 4.8). Both planktonic cultures of *E. coli* and *S. aureus* were almost completely inhibited (90% and 82%, respectively) by hybrid coating materials loaded with AgNPs and were significantly ($p < 0.05$) more effective in mitigating microbial growth than base coatings (< 6%). Given the suspended nature of the culture, these results indicated that imbedded AgNPs participated in release-based antimicrobial action against both pathogenic bacteria.

Coating materials loaded with AgNPs, while effective at mitigating the growth of both model bacteria in planktonic cultures, displayed greater efficacy against *E. coli* than *S. aureus*. The differences in antimicrobial efficacy against both pathogenic bacteria can be owed to the differences between Gram-negative and Gram-positive cell wall structures. Gram-positive bacteria, such as *S. aureus*, possess much thicker peptidoglycan layers within their cell walls compared to Gram-negative bacteria such as *E. coli*⁶⁸. The thicker cell walls of Gram-positive bacteria have been shown to limit the internalization of antimicrobial nanoparticles, and, have shown a reported similar resistance to such antimicrobials compared to Gram-negative bacteria⁶⁹⁻⁷¹.

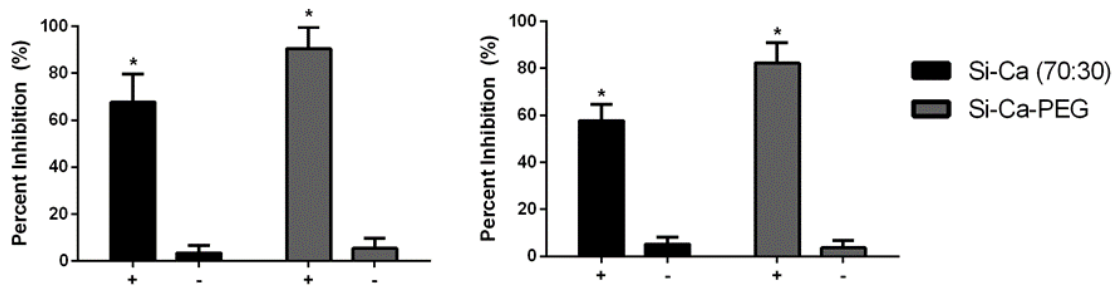


Figure 4.8 Inhibition of bacterial cultures by Si-Ca-PEG coatings with (+) and without (-) AgNPs. *E. coli* and *S. aureus* cultures were inhibited by incubation (24 hours) with AgNP-loaded hybrid coatings, compared to uncoated titanium (Ti6Al4V) controls. There was little inhibition from base coatings without AgNPs, but significantly ($p < 0.05$) more and almost total inhibition for coatings loaded with AgNPs.

Due to the highly resistant nature of biofilms, their treatments remain minimally effective in the clinic. For this reason, antimicrobial coatings are continuously sought to enable the localized dislodgement or inhibition of biofilms on implant surfaces. Therefore, in addition to their efficacy against suspended bacteria, hybrid coatings were assessed for their ability to mitigate the formation of *E. coli* and *S. aureus* biofilms.

Both *E. coli* and *S. aureus* cultures were effectively inhibited by hybrid coatings containing AgNPs compared to their uncoated Ti6Al4V controls (Figure 4.9). The biofilms formed by *E. coli* and *S. aureus* were markedly inhibited (80% and 89%, respectively) by hybrid coatings materials loaded with AgNPs and were significantly ($p < 0.05$) more effective at preventing biofilm formation compared to base coatings ($< 25\%$). Such results indicate the contact-active and anti-adhesive nature of hybrid AgNP-loaded coatings against model sessile bacteria colonies.

In contrast to planktonic susceptibility, *E. coli* was less susceptible than *S. aureus* to antimicrobial coating blends during biofilm assays. While these differences were insignificant ($p > 0.05$) in our study, similar works have also found *E. coli* to be more resistant than other Gram-positive bacteria to antimicrobial coatings in biofilm assays^{69,72}. Such differences have been owed to the rapid extracellular polymeric substance (EPS) formation of *E. coli* in their sessile state, which has shown to be effective in resisting antibiofilm agents such as metal ions⁷³.

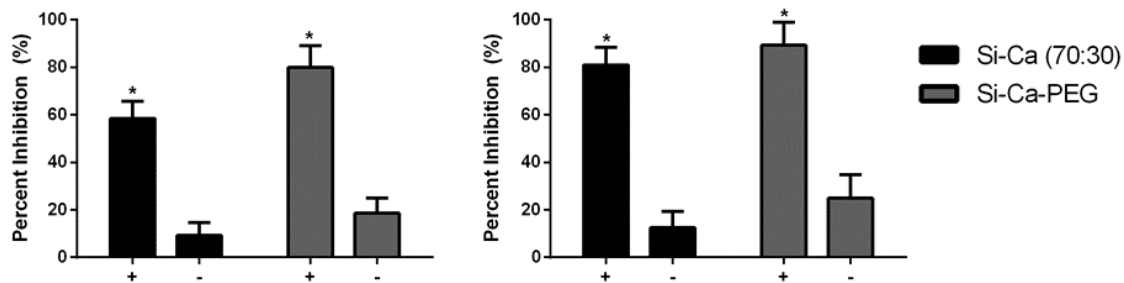


Figure 4.9 Inhibition of bacterial biofilm formation on hybrid coatings with (+) and without (-) AgNPs. *E. coli* and *S. aureus* biofilm formation (24 hours) were inhibited on hybrid coatings, compared to uncoated titanium (Ti6Al4V) controls. Inhibition of biofilm formation was significantly greater ($p < 0.05$) on coatings that contained AgNPs. Hybrid bioactive glass coatings were generally more effective than purely inorganic bioactive glass coatings at inhibiting the formation of biofilms. The highest degree of biofilm inhibition was observed for *S. aureus* biofilms on for both coatings that contained AgNPs.

4.4 Conclusions

In this study, Si-Ca-PEG class II hybrid materials were developed as coating materials for implantable Ti6Al4V substrates. To manifest antimicrobial properties, developed coatings were loaded with AgNPs. Using ^{13}C and ^1H NMR, the synthesis of new precursor components was confirmed. The chemical structure and topographies of developed coating materials was evaluated using FTIR, SEM and EDX analysis. To evaluate the robustness of developed hybrid coatings materials, adhesive tensile testing was performed. The *in vitro* bioactivity of hybrid coatings was assessed through their immersion in SBF and ability to induce the nucleation of HA. The antimicrobial properties of developed coatings were evaluated in planktonic and biofilm cultures of *E. coli* and *S. aureus*.

Coating precursors, including Ca₂EE and PEG-diamine, were introduced into a hybrid bioactive glass network for the first time. Their synthesis was confirmed using through the analysis of relevant NMR data and consistency with relevant literature. Hybrid bioactive glass coatings demonstrated robust resistance to delamination and were highly adherent to Ti6Al4V substrates. Ti6Al4V substrates that were acid-etched demonstrated retained microtopographical roughness and increased resistance to hybrid coating delamination. Hybrid coatings were able to promote apatite mineralization *in vitro*, indicative of their potential to rapidly promote new bone

regeneration and fixation *in vivo*. Additionally, hybrid coating materials loaded with AgNPs showed significant inhibition of *E. coli* and *S. aureus* in both planktonic and biofilm states. The highly adherent and multifunctional hybrid coating materials developed in this study affords a novel strategy in mitigating the risks associate with implantable titanium materials.

4.5 References

- (1) Saini, M. Implant Biomaterials: A Comprehensive Review. *World J. Clin. Cases* **2015**, *3* (1), 52.
- (2) Van Noort, R. Titanium: The Implant Material of Today. *J. Mater. Sci.* **1987**, *22* (11), 3801–3811.
- (3) Özcan, M.; Hämmerle, C. Titanium as a Reconstruction and Implant Material in Dentistry: Advantages and Pitfalls. *Materials (Basel)*. **2012**, *5* (9), 1528–1545.
- (4) Raigrodski, A. J.; Hillstead, M. B.; Meng, G. K.; Chung, K. H. Survival and Complications of Zirconia-Based Fixed Dental Prostheses: A Systematic Review. *J. Prosthet. Dent.* **2012**, *107* (3), 170–177.
- (5) Geetha, M.; Singh, A. K.; Asokamani, R.; Gogia, A. K. Ti Based Biomaterials, the Ultimate Choice for Orthopaedic Implants - A Review. *Prog. Mater. Sci.* **2009**, *54* (3), 397–425.
- (6) Darouiche, R. O. Treatment of Infections Associated with Surgical Implants. *Infect. Dis. Clin. Pract.* **2004**, *12* (4), 258–259.
- (7) Chouirfa, H.; Bouloussa, H.; Migonney, V.; Falentin-daudré, C. Review of Titanium Surface Modification Techniques and Coatings for Antibacterial Applications. *Acta Biomater.* **2018**.
- (8) Camps-Font, O.; Figueiredo, R.; Valmaseda-Castellón, E.; Gay-Escoda, C. Postoperative Infections after Dental Implant Placement: Prevalence, Clinical Features, and Treatment. *Implant Dent.* **2015**, *24* (6), 713–719.
- (9) Ribeiro, M.; Monteiro, F. J.; Ferraz, M. P. Infection of Orthopedic Implants with Emphasis on Bacterial Adhesion Process and Techniques Used in Studying Bacterial-Material Interactions. *Biomatter* **2012**, *2* (4), 176–194.
- (10) Encyclopedia. *Biofilm Infections*; Bjarnsholt, T., Jensen, P. Ø., Moser, C., Høiby, N., Eds.; Springer New York: New York, NY, 2011; Vol. 53.
- (11) Cogen, A. L.; Nizet, V.; Gallo, R. L. Skin Microbiota: A Source of Disease or Defence? *Br. J. Dermatol.* **2008**, *158* (3), 442–455.
- (12) Gristina, A. Biomaterial-Centered Infection: Microbial Adhesion versus Tissue Integration. *Science (80-.)*. **1987**, *237* (4822), 1588–1595.
- (13) Mah, T. F.; Pitts, B.; Pellock, B.; Walker, G. C.; Stewart, P. S.; O’Toole, G. A. A Genetic Basis for *Pseudomonas Aeruginosa* Biofilm Antibiotic Resistance. *Nature* **2003**, *426*

- (6964), 306–310.
- (14) Mirza, S. B.; Dunlop, D. G.; Panesar, S. S.; Naqvi, S. G.; Gangoo, S.; Salih, S. Basic Science Considerations in Primary Total Hip Replacement Arthroplasty. *Open Orthop. J.* **2010**, *4* (1), 169–180.
 - (15) van Der List, J. P.; Zuiderbaan, H. A.; Pearle, A. D. Why Do Medial Unicompartmental Knee Arthroplasties Fail Today? *J. Arthroplasty* **2016**, *31* (5), 1016–1021.
 - (16) Wooley, P. H.; Schwarz, E. M. Aseptic Loosening. *Gene Ther.* **2004**, *11* (4), 402–407.
 - (17) Albrektsson, T.; Johansson, C. Osteoinduction, Osteoconduction and Osseointegration. *Eur. Spine J.* **2001**, *10*, S96–S101.
 - (18) Albrektsson, T.; Chrcanovic, B.; Jacobsson, M.; Wennerberg, A. Osseointegration of Implants – A Biological and Clinical Overview. *JSM Dent Surg* **2017**, *2* (3), 1022.
 - (19) Fialho, L.; Carvalho, S. Applied Surface Science Surface Engineering of Nanostructured Ta Surface with Incorporation of Osteoconductive Elements by Anodization. *Appl. Surf. Sci.* **2019**, *495* (July), 143573.
 - (20) Oliveira, F. G.; Ribeiro, A. R.; Perez, G.; Archanjo, B. S.; Gouvea, C. P.; Araújo, J. R.; Campos, A. P. C.; Kuznetsov, A.; Almeida, C. M.; Maru, M. M.; et al. Understanding Growth Mechanisms and Tribocorrosion Behaviour of Porous TiO₂ Anodic Films Containing Calcium, Phosphorous and Magnesium. *Appl. Surf. Sci.* **2018**, *341* (2015), 1–12.
 - (21) Yang, Y. C.; Chang, E. Influence of Residual Stress on Bonding Strength and Fracture of Plasma-Sprayed Hydroxyapatite Coatings on Ti-6Al-4V Substrate. *Biomaterials* **2001**, *22* (13), 1827–1836.
 - (22) Mohseni, E.; Zalnezhad, E.; Bushroa, A. R. Comparative Investigation on the Adhesion of Hydroxyapatite Coating on Ti-6Al-4V Implant: A Review Paper. *Int. J. Adhes. Adhes.* **2014**, *48*, 238–257.
 - (23) Jones, J. R. Reprint of: Review of Bioactive Glass: From Hench to Hybrids. *Acta Biomater.* **2015**, *23* (S), S53–S82.
 - (24) Jones, J. R. Review of Bioactive Glass: From Hench to Hybrids. *Acta Biomater.* **2015**, *23* (S), S53–S82.
 - (25) Covarrubias, C.; Mattmann, M.; Von Martens, A.; Caviades, P.; Arriagada, C.; Valenzuela, F.; Rodríguez, J. P.; Corral, C. Osseointegration Properties of Titanium Dental Implants Modified with a Nanostructured Coating Based on Ordered Porous Silica and Bioactive Glass Nanoparticles. *Appl. Surf. Sci.* **2016**, *363*, 286–295.
 - (26) Poologasundarampillai, G.; Yu, B.; Jones, J. R.; Kasuga, T. Electrospun Silica/PLLA Hybrid Materials for Skeletal Regeneration. *Soft Matter* **2011**, *7* (21), 10241–10251.
 - (27) Blaker, J. J.; Bismarck, A.; Boccaccini, A. R.; Young, A. M.; Nazhat, S. N. Premature Degradation of Poly(Alpha-Hydroxyesters) during Thermal Processing of Bioglass-Containing Composites. *Acta Biomater.* **2010**, *6* (3), 756–762.

- (28) Mondal, D.; Dixon, S. J.; Mequanint, K.; Rizkalla, A. S. Bioactivity, Degradation, and Mechanical Properties of Poly(Vinylpyrrolidone-*Co*-Triethoxyvinylsilane)/Tertiary Bioactive Glass Hybrids. *ACS Appl. Bio Mater.* **2018**, *1* (5), 1369–1381.
- (29) Granqvist, B.; Helminen, A.; Vehviläinen, M.; Ääritalo, V.; Seppälä, J.; Lindén, M. Biodegradable and Bioactive Hybrid Organic-Inorganic PEG-Siloxane Fibers. Preparation and Characterization. *Colloid Polym. Sci.* **2004**, *282* (5), 495–501.
- (30) Connell, L. S.; Romer, F.; Suárez, M.; Valliant, E. M.; Zhang, Z.; Lee, P. D.; Smith, M. E.; Hanna, J. V.; Jones, J. R. Chemical Characterisation and Fabrication of Chitosan-Silica Hybrid Scaffolds with 3-Glycidoxypropyl Trimethoxysilane. *J. Mater. Chem. B* **2014**, *2* (6), 668–680.
- (31) Turova, N. Y.; Turevskaya, E. P.; Kessler, V. G.; Yanovskaya, M. I. *The Chemistry of Metal Alkoxides*; Kluwer Academic Publishers: Boston, 2002.
- (32) Micha-Screttas, M. Spectroscopic Electronegativities Correlated with the ¹³C NMR Shifts of Metal (Ia, IIa, IIIa) 2-Ethoxyethoxides. *Magn. Reson. Chem.* **1990**, *28* (June), 952–955.
- (33) Izadi, Z.; Hajizadeh-Saffar, E.; Hadjati, J.; Habibi-Anbouhi, M.; Ghanian, M. H.; Sadeghi-Abandansari, H.; Ashtiani, M. K.; Samsonchi, Z.; Raoufi, M.; Moazenchi, M.; et al. Tolerance Induction by Surface Immobilization of Jagged-1 for Immunoprotection of Pancreatic Islets. *Biomaterials* **2018**, *182* (August), 191–201.
- (34) Mahou, R.; Wandrey, C. Versatile Route to Synthesize Heterobifunctional Poly(Ethylene Glycol) of Variable Functionality for Subsequent Pegylation. *Polymers (Basel)*. **2012**, *4* (1), 561–589.
- (35) Valliant, E. M.; Romer, F.; Wang, D.; McPhail, D. S.; Smith, M. E.; Hanna, J. V.; Jones, J. R. Bioactivity in Silica/Poly(*c*-Glutamic Acid) Sol-Gel Hybrids through Calcium Chelation. *Acta Biomater.* **2013**, *9* (8), 7662–7671.
- (36) Mahony, O.; Tsigkou, O.; Ionescu, C.; Minelli, C.; Ling, L.; Hanly, R.; Smith, M. E.; Stevens, M. M.; Jones, J. R. Silica-Gelatin Hybrids with Tailorable Degradation and Mechanical Properties for Tissue Regeneration. *Adv. Funct. Mater.* **2010**, *20* (22), 3835–3845.
- (37) Wang, D.; Romer, F.; Connell, L.; Walter, C.; Saiz, E.; Yue, S.; Lee, P. D.; McPhail, D. S.; Hanna, J. V.; Jones, J. R. Highly Flexible Silica/Chitosan Hybrid Scaffolds with Oriented Pores for Tissue Regeneration. *J. Mater. Chem. B* **2015**, *3* (38), 7560–7576.
- (38) Malina, D.; Sobczak-Kupiec, A.; Wzorek, Z.; Kowalski, Z. Silver Nanoparticles Synthesis with Different Concentrations of Polyvinylpyrrolidone. *Dig. J. Nanomater. Biostructures* **2012**, *7* (4), 1527–1534.
- (39) Zahra, Q.; Fraz, A.; Anwar, A.; Awais, M.; Abbas, M. A Mini Review on the Synthesis of Ag-Nanoparticles by Chemical Reduction Method and Their Biomedical Applications. **2016**, *9* (1), 1–7.
- (40) Gakiya-teruya, M.; Palomino-marcelo, L.; Rodriguez-reyes, J. C. F. Synthesis of Highly Concentrated Suspensions of Silver Nanoparticles by Two Versions of the Chemical Reduction Method. **2019**, 5–9.

- (41) Brinker, C. J.; Frye, G. C.; Hurd, A. J.; Ashley, C. S. Fundamentals of Sol-Gel Dip Coating. *Thin Solid Films* **1991**, *201* (1), 97–108.
- (42) Piveteau, L. D.; Gasser, B.; Schlapbach, L. Evaluating Mechanical Adhesion of Sol-Gel Titanium Dioxide Coatings Containing Calcium Phosphate for Metal Implant Application. *Biomaterials* **2000**, *21* (21), 2193–2201.
- (43) Kokubo, T.; Kushitani, H.; Sakka, S.; Kitsugi, T.; Yamamuro, T. Solutions Able to Reproduce in Vivo Surface-structure Changes in Bioactive Glass-ceramic A-W3. *J. Biomed. Mater. Res.* **1990**, *24* (6), 721–734.
- (44) Yu, B.; Turdean-Ionescu, C. A.; Martin, R. A.; Newport, R. J.; Hanna, J. V.; Smith, M. E.; Jones, J. R. Effect of Calcium Source on Structure and Properties of Sol-Gel Derived Bioactive Glasses. *Langmuir* **2012**, *28* (50), 17465–17476.
- (45) Pereira, M. M.; Clark, A. E.; Hench, L. L. Calcium Phosphate Formation on Sol-gel-derived Bioactive Glasses in Vitro. *J. Biomed. Mater. Res.* **1994**, *28* (6), 693–698.
- (46) Yu, B.; Poologasundarampillai, G.; Turdean-Ionescu, C.; Smith, M. E.; Jones, J. R. A New Calcium Source for Bioactive Sol-Gel Hybrids. *Bioceram. Dev. Appl.* **2011**, *1* (January), 1–3.
- (47) Poologasundarampillai, G.; Yu, B.; Tsigkou, O.; Wang, D.; Romer, F.; Bhakhri, V.; Giuliani, F.; Stevens, M. M.; McPhail, D. S.; Smith, M. E.; et al. Poly(γ -Glutamic Acid)/Silica Hybrids with Calcium Incorporated in the Silica Network by Use of a Calcium Alkoxide Precursor. *Chem. - A Eur. J.* **2014**, *20* (26), 8149–8160.
- (48) Screttas, C. G.; Micha-Screttas, M. Hydrocarbon-Soluble Organoalkali-Metal Reagents. Preparation of Aryl Derivatives. *Organometallics* **1984**, *3* (6), 904–907.
- (49) Li, A.; Shen, H.; Ren, H.; Wang, C.; Wu, D.; Martin, R. A.; Qiu, D. Bioactive Organic/Inorganic Hybrids with Improved Mechanical Performance. *J. Mater. Chem. B* **2015**, *3* (7), 1379–1390.
- (50) Liu, Y. L.; Su, Y. H.; Lai, J. Y. In Situ Crosslinking of Chitosan and Formation of Chitosan-Silica Hybrid Membranes with Using γ -Glycidoxypropyltrimethoxysilane as a Crosslinking Agent. *Polymer (Guildf)*. **2004**, *45* (20), 6831–6837.
- (51) Sundfeldt, M.; Carlsson, L. V.; Johansson, C. B.; Thomsen, P.; Gretzer, C. Aseptic Loosening, Not Only a Question of Wear: A Review of Different Theories. *Acta Orthop.* **2006**, *77* (2), 177–197.
- (52) Banaszkiwicz, P. A. Periprosthetic Bone Loss in Total Hip Arthroplasty: Polyethylene Wear Debris and the Concept of the Effective Joint Space. *Class. Pap. Orthop.* **2014**, *74* (6), 85–87.
- (53) Chen, J.; Bull, S. J. Approaches to Investigate Delamination and Interfacial Toughness in Coated Systems: An Overview. *J. Phys. D. Appl. Phys.* **2011**, *44* (3).
- (54) van Dam, J. P. B.; Abrahami, S. T.; Yilmaz, A.; Gonzalez-Garcia, Y.; Terryn, H.; Mol, J. M. C. Effect of Surface Roughness and Chemistry on the Adhesion and Durability of a Steel-Epoxy Adhesive Interface. *Int. J. Adhes. Adhes.* **2020**, *96* (June 2019), 102450.

- (55) He, Y.; Zhang, X.; Hooton, R. D.; Zhang, X. Effects of Interface Roughness and Interface Adhesion on New-to-Old Concrete Bonding. *Constr. Build. Mater.* **2017**, *151*, 582–590.
- (56) Jarka, T. G. S. Injection Molding of Multimaterial Systems. In *Specialized Injection Molding Techniques*; 2016; pp 165–210.
- (57) S. R. Brown, I. G. T. & H. R. Residual Stress Measurement in Thermal Sprayed Hydroxyapatite Coatings. *J. Mater. Sci. Mater. Med.* **1994**, *5*, 756–759.
- (58) Zhang, Z.; Dunn, M. F.; Xiao, T. D.; Tomsia, A. P.; Saiz, E. M. *Nanostructured Hydroxyapatite Coatings for Improved Adhesion and Corrosion Resistance for Medical Implants*; 2001; Vol. 703.
- (59) Æ, T. K.; Takadama, H. How Useful Is SBF in Predicting in Vivo Bone Bioactivity? *J. Biomed. Mater. Res. Part B: Appl. Biomater.* **2006**, *27*, 2907–2915.
- (60) Pishbin, F.; Mouriño, V.; Gilchrist, J. B.; McComb, D. W.; Kreppel, S.; Salih, V.; Ryan, M. P.; Boccaccini, A. R. Single-Step Electrochemical Deposition of Antimicrobial Orthopaedic Coatings Based on a Bioactive Glass/Chitosan/Nano-Silver Composite System. *Acta Biomater.* **2013**, *9* (7), 7469–7479.
- (61) Ye, X.; Leeflang, S.; Wu, C.; Chang, J.; Zhou, J.; Huan, Z. Mesoporous Bioactive Glass Functionalized 3D Ti-6Al-4V Scaffolds with Improved Surface Bioactivity. *Materials (Basel)*. **2017**, *10* (11), 1244.
- (62) Pipattanawarothai, A.; Suksai, C.; Srisook, K.; Trakulsujaritchok, T. Non-Cytotoxic Hybrid Bioscaffolds of Chitosan-Silica: Sol-Gel Synthesis, Characterization and Proposed Application. *Carbohydr. Polym.* **2017**, *178* (September), 190–199.
- (63) Jones, N.; Ray, B.; Ranjit, K. T.; Manna, A. C. Antibacterial Activity of ZnO Nanoparticle Suspensions on a Broad Spectrum of Microorganisms. *FEMS Microbiol. Lett.* **2008**, *279* (1), 71–76.
- (64) Rai, M.; Kon, K.; Ingle, A.; Duran, N.; Galdiero, S.; Galdiero, M. Broad-Spectrum Bioactivities of Silver Nanoparticles: The Emerging Trends and Future Prospects. *Appl. Microbiol. Biotechnol.* **2014**, *98* (5), 1951–1961.
- (65) Kim, J. S.; Kuk, E.; Yu, K. N.; Kim, J. H.; Park, S. J.; Lee, H. J.; Kim, S. H.; Park, Y. K.; Park, Y. H.; Hwang, C. Y.; et al. Antimicrobial Effects of Silver Nanoparticles. *Nanomedicine Nanotechnology, Biol. Med.* **2007**, *3* (1), 95–101.
- (66) Lara, H. H.; Ayala-Núñez, N. V.; del Turrent, L. C. I.; Padilla, C. R. Bactericidal Effect of Silver Nanoparticles against Multidrug-Resistant Bacteria. *World J. Microbiol. Biotechnol.* **2010**, *26* (4), 615–621.
- (67) Zhao, L.; Wang, H.; Huo, K.; Cui, L.; Zhang, W.; Ni, H.; Zhang, Y.; Wu, Z.; Chu, P. K. Antibacterial Nano-Structured Titania Coating Incorporated with Silver Nanoparticles. *Biomaterials* **2011**, *32* (24), 5706–5716.
- (68) Shockman, G. D.; Barren, J. F. Structure, Function, and Assembly of Cell Walls of Gram-Positive Bacteria. *Annu. Rev. Microbiol.* **1983**, *37* (1), 501–527.

- (69) Gholizadeh, P.; Ghotaslou, R. The in Vitro Effects of Silver Nanoparticles on Bacterial Biofilms. *J. Microbiol. Biotechnol. Food Sci.* **2017**, *6* (4), 1077–1080.
- (70) Flores, C. Y.; Min, A. G.; Grillo, C. A.; Salvarezza, R. C.; Vericat, C.; Schilardi, P. L. Citrate-Capped Silver Nanoparticles Showing Good Bactericidal Effect against Both Planktonic and Sessile Bacteria and a Low Cytotoxicity to Osteoblastic Cells. **2013**.
- (71) Hwang, E. T.; Lee, J. H.; Chae, Y. J.; Kim, Y. S.; Kim, B. C.; Sang, B. I.; Gu, M. B. Analysis of the Toxic Mode of Action of Silver Nanoparticles Using Stress-Specific Bioluminescent Bacteria. *Small* **2008**, *4* (6), 746–750.
- (72) Kumar, P.; Senthamilselvi, S.; Lakshmipraba, A.; Premkumar, K.; Muthukumar, R.; Visvanathan, P.; Ganeshkumar, R. S.; Govindaraju, M. Efficacy of Bio-Synthesized Silver Nanoparticles Using *Acanthophora Spicifera* to Encumber Biofilm Formation. *Dig. J. Nanomater. Biostructures* **2012**, *7* (2), 511–522.
- (73) Flemming, H. C.; Neu, T. R.; Wozniak, D. J. The EPS Matrix: The “House of Biofilm Cells.” *J. Bacteriol.* **2007**, *189* (22), 7945–7947.

Chapter 5: General Discussion

5.1 Summary

The main objective of this study was to develop bioactive and biocompatible covalently coupled (class-II) hybrid coating materials to mitigate the complications associated with titanium implants. In this thesis, the synthesis and evaluation of two coatings systems were discussed.

First, in chapter 3, the synthesis of chitosan-silica hybrid coatings prepared through sol-gel processing were presented. In this study, the inorganic network was composed exclusively of silica and the organic network materials were comprised 3-glycidoxypropyl trimethoxysilane (GPTMS) and chitosan. Developed hybrid coatings possessed improved robustness to control inorganic silica coatings which have previously been shown to be brittle when cured at low temperatures. Additionally, upon acid-etching Ti6Al4V substrates, all hybrid coatings possessed improved adhesive properties and outperformed some clinically available hydroxyapatite-based implant coating materials. By loading these hybrid materials with silver nanoparticles, coated substrates were able to provide an effective resistance against both *E. coli* and *S. aureus* in culture and adherent states.

In chapter 4, the synthesis of novel polyethylene glycol-diamine-calcium-silica coatings prepared through sol-gel processing were presented. In this study, the inorganic network was composed of silica and newly synthesized calcium-2-ethoxyethoxide (Ca2EE) to afford the material with greater bone-bioactivity. Here, the organic network was comprised of 3-glycidoxypropyl trimethoxysilane (GPTMS) and PEG-diamine (2K). In this work, we provided a non-toxic synthesis method for developing Ca2EE which has not yet seen use in the development of other bioactive glass materials. The room temperature addition of calcium into the hybrid coating network was successfully achieved using this new calcium alkoxide and promoted apatite mineralization *in vitro* after only 3 days immersion in simulated body fluid (SBF). Developed hybrid coatings were highly adherent to acid-etched Ti6Al4V substrates and outperformed that of some clinically available hydroxyapatite-based implant coating materials described in other studies. By loading these hybrid materials with silver nanoparticles, coated substrates were able to provide effective antimicrobial action against both *E. coli* and *S. aureus* in both culture and adherent states.

5.2 Contributions to current knowledge

For metallic implants, the synergistic risks of loosening and infection have been well established since the 1980s¹. Despite this, aseptic loosening and implant associated infections continue to plague hard tissue implants and limit their success in the clinic. In this thesis work, we provide two feasible coating systems which can be utilized to improve the success of metallic implants.

In the study of both coating materials, delamination protocols were followed to better evaluate the robustness of the developed hybrid coating materials. Such tensile adhesion pull-tests have not yet been performed on similar hybrid materials to the ones described in this work. These results can provide a much-needed baseline to assess the robustness of other such coatings which may be used for metallic implant materials.

This study also evaluated the contact and release-based antimicrobial action of silver nanoparticles imbedded within hybrid coating materials. While other studies typically assess the antimicrobial action of such coatings through either release-based (Kirby-Bauer) or contact-based (biofilm) assays, we evaluated the antimicrobial action of our coating in both domains.

These results will ideally emphasize the importance of both antimicrobial strategies in the development of effective antibacterial implant coatings.

Lastly, in chapter 4, the novel non-toxic synthesis of calcium-2-ethoxyethoxide (Ca₂EE) is proposed, and, for the first time, used in the synthesis a bioactive glass material. In this work, synthesized Ca₂EE displayed stability in water-containing sol-gel systems and was able to be homogeneously introduced into hybrid coating material networks at low temperatures. By providing the synthesis and network integration protocol for Ca₂EE, other researchers may use this sol precursor to develop other bioactive materials that can be cured at low temperatures, enabling the inclusion of temperature sensitive components.

5.3 Limitations and Suggestions for Future Work

Through this work, sol-gel derived hybrid coatings on Ti6Al4V substrates were preliminarily examined. While the materials developed in this study displayed favourable results in improving the lifetime of metallic implants, more experimental works are suggested before this coating technology could be transferred to the clinic. Therefore, the following limitations of this study are discussed below, with appropriate recommendations for future works.

While coated substrates displayed a high degree of robustness and resistance to delamination, more detailed experimentation could be conducted to further evaluate the physical properties of coating materials. For example, the thickness of the coating materials could be further evaluated using advanced SEM/TEM techniques to better evaluate the effect of dipping speed, the adherence characteristics of modified coatings, and the effect of relevant substrate pre-treatments. Additionally, as roughness and porosity are important parameters in determining the cellular response to biomaterials, quantitative measurements to evaluate coating topographies (such as atomic force microscopy) should be used in place of the qualitative SEM descriptions provided in this work. Lastly, while the robustness of developed coating materials was evaluated in a quantitative manner, additional clinically relevant assessments could be performed. For example, the resistance of coating materials to fracture or delamination in a more clinical setting could be evaluated by coating titanium dental screws and performing pseudo-implantation and removal in a model bone material².

Another limitation to this study is the absence of release and degradation-based data of developed coating materials. For future works it is recommended that elemental release data be collected (using inductively coupled plasma mass spectroscopy) in relevant solutions (preferably simulated body fluid). This data could be used to better evaluate how the hybrid coating materials degrade, and, assess if there is any inhomogeneous degradation of coating components. Additionally, using ICP-MS, the mineralization of apatite on hybrid coating surfaces could be quantified over time which could be used to compare the *in vitro* bioactivity of a variety of modified and control surfaces.

Lastly, one major limitation to this study is that cell culture or *in vivo* studies were not performed on developed coating materials. Although developed coatings displayed favourable signs for cell viability (microroughness, hydrophilicity, etc.), relevant cytotoxicity and proliferation assays should be performed to better assess their *in vivo* compatibility. In general, cell attachment and proliferation studies are necessary to determine the cellular metabolic activity and osteoinductive of developed hybrid coatings to ensure that they are indeed biocompatible³.

5.4 References

- (1) Gristina, A. Biomaterial-Centered Infection: Microbial Adhesion versus Tissue Integration. *Science (80-.)*. **1987**, 237 (4822), 1588–1595.
- (2) Xia, W.; Grandfield, K.; Hoess, A.; Ballo, A.; Cai, Y.; Engqvist, H. Mesoporous Titanium Dioxide Coating for Metallic Implants. *J. Biomed. Mater. Res. Part B Appl. Biomater.* **2012**, 100B (1), 82–93.
- (3) Kim, H.-W.; Kim, H.-E.; Salih, V.; Knowles, J. C. Hydroxyapatite and Titania Sol-Gel Composite Coatings on Titanium for Hard Tissue Implants; Mechanical Andin Vitro Biological Performance. *J. Biomed. Mater. Res.* **2005**, 72B (1), 1–8.

5.5 Curriculum Vitae

Zach Gouveia

Academic Information

MESc. Biomedical Engineering (Biomaterials)

Sept 2020

Western University, London ON

Thesis Title: Multifunctional hybrid sol-gel implant coatings on anodized titanium substrates to improve osseointegration and antimicrobial effectiveness

BESc. Biochemical/Chemical Engineering

April 2018

Western University, London ON

Thesis Title: Applications of ultrasound in process monitoring: Characterization of suspensions of nano to micron size particles & particle size determinations

CAPSTONE Title: Industrial production of penicillin G: Chemical plant design

Research Experience



Western

Graduate Research Assistant

Sept 2018 – Present

Dr. Jesse Zhu, Western University, London ON

- Developed multifunctional implant coatings for dental applications
- Synthesized a Class II hybrid organic-inorganic materials
- Evaluated antimicrobial efficacy and mechanical suitability of developed materials



Summer Research Assistant

May – Aug 2018

Dr. Victor Yang, Zhejiang University of Technology, Hangzhou CN

- Assisted in the mechanical evaluation of chitosan microneedle (MN) arrays
- Using COMSOL Multiphysics, developed a finite element model to assess stress and buckling forces on MN arrays
- Tuned material properties to manipulate dissolution time *in vitro*



Western

Undergraduate Research Assistant

Sept – April 2018

Dr. Anand Prakash, Western University, London ON

- Investigated suspensions of nano to micron-sized particles in aqueous suspensions
- Using ultrasound, measured suspension properties using correlations related to pulse attenuation and time of flight
- Using MatLab's Artificial Neural Network (ANN) tool, developed a predictive model to solve for the particle size and concentration, based on system variable and pulse parameters

Appointed/Elected Positions



President & Founder – CBS Southwestern Ontario Student Chapter

Oct 2019 – Present

Role: The chapter was inspired by the quality of research in the field of biomaterials at Western University, McMaster University, and the University of Waterloo. My role is to manage the operations and affairs of the chapter across southwestern Ontario.



EIT Volunteer – Professional Engineers Ontario (PEO) London Chapter

April 2018 – Present

Role: Assisted with event initiatives for the London PEO membership. Hosted London Chapter Mathletics competition (2 years) where I planned and developed challenging math questions for grade 7 and 8 students at Western University



Event Coordinator – Big Brothers Big Sisters London

Sept 2017 – Sept 2018

Role: In coordination with Western University, I planned events for Bigs and Littles in London to participate in healthy lifestyle activities on and off campus.

Awards and Accomplishments

CAMBR Travel Award

January 2020

Value of \$1500 awarded for travel to an international conference

1st Place – CBS 2019 Poster Showcase (Scientific Quality)

May 2019

1st Place – CBS 2019 Poster Showcase (Scientific Communication)

May 2019

Mitacs Globalink Research Award

May 2018

Value of \$6000 awarded for international research initiatives

2nd Place – Engineering CAPSTONE Project

April 2018

Value of \$1000 awarded to 2nd place project in specialty chemicals category

Dean's List

2014 – 2018

Awarded based on academic excellence

Presentations

CBS 2019 (Poster)

May 2019

Topic: Development of multifunctional hybrid sol-gel implant coatings to promote osseointegration and antimicrobial effectiveness

CAMBR Day (Poster)

April 2019

Topic: Development of multifunctional hybrid sol-gel implant coatings to improve osseointegration and antimicrobial effectiveness

Undergraduate Thesis (Poster)

April 2018

Topic: Applications of ultrasound in process monitoring: Characterization of suspensions of nano to micron size particles & particle size determinations

Engineering CAPSTONE Project Presentation

March 2018

Topic: Industrial Scale Production of Benzylpenicillin